



UNIWERSYTET ŚLĄSKI
INSTYTUT FIZYKI
IM. AUGUSTA CHEŁKOWSKIEGO

Instytut Fizyki

Praca doktorska:

Poprawa rozpuszczalności w wodzie oraz fizycznej stabilności
bikalutamidu w formie amorficznej – wykonanie stałych
rozproszeń w matrycach polimerowych.

mgr Justyna Pacuł

Promotor:

prof. dr hab. Marian Paluch

Promotor pomocniczy:

dr Marzena Rams-Baron

Chorzów 2020

*Serdecznie dziękuję mojemu Promotorowi Panu
Profesorowi Marianowi Paluchowi za możliwość
poszerzenia swoich horyzontów naukowych, życzliwość
i ogromne wsparcie merytoryczne, które pozwoliło na
zrealizowanie niniejszej pracy doktorskiej.*

*Dziękuję Promotorowi Pomocniczemu
dr Marzenie Rams-Baron za cierpliwość, okazaną
życzliwość i wsparcie merytoryczne.*

*Pragnę również podziękować Koleżankom i Kolegom
z laboratorium dielektrycznego za miłą,
pełną uśmiechu atmosferę pracy.*

Spis treści

1. Wstęp.....	4
2. Omówienie osiągniętych wyników	8
2.1 Badanie dynamiki molekularnej i rozpuszczalności w wodzie amorficznego bikalutamidu oraz jego stabilizacja z wykorzystaniem poliwinylpirolidonu.	8
2.2 Wpływ długości łańcucha polimerowego na stabilność fizyczną amorficznych mieszanin lek-polimer.	12
2.3 Jak poprawić fizyczną stabilność amorficznego układu bikalutamid – flutamid? Badania trójskładnikowych amorficzne stałych rozproszeń.....	13
3. Wykaz publikacji stanowiących podstawę rozprawy doktorskiej wraz z oświadczeniami współautorów	16
4. Podsumowanie.....	68
5. Bibliografia.....	70

1. Wstęp

Drugą najczęściej diagnozowaną chorobą nowotworową wśród mężczyzn jest rak gruczołu krokowego. Według Światowej Organizacji Zdrowia (WHO – *World Health Organization*) w 2018 roku na tą chorobę zmarło około 30% zdiagnozowanych mężczyzn na całym świecie. Jedną z możliwości leczenia wspomnianej choroby jest chemioterapia z wykorzystaniem leku o nazwie bikalutamid (BIC). Działa on antagonistycznie na androgeny produkowane przez gonady oraz korę nadnerczy, co powoduje zahamowanie wzrostu nowotworu gruczołu krokowego¹. Bikalutamid jest mieszaniną racemiczną, w której enancjomer *R* wykazuje większą aktywność biologiczną oraz przypisuje się mu działanie antyandrogenowe². Lek ten należy do II klasy systemu klasyfikacji biofarmaceutycznej (ang. *BCS – Biopharmaceutical Classification System*), tzn. charakteryzuje się niską rozpuszczalnością w wodzie (<5mg/L)³ oraz małą biodostępnością. Oznacza to, iż ilość bikalutamidu, która dostaje się do krwioobiegu pacjenta, po podaniu leku, jest niewielka w stosunku do przyjętej dawki. Powoduje to, iż dawka stosowana w kuracji musi być odpowiednio większa, aby uzyskać oczekiwane rezultaty w leczeniu. Ponadto część farmaceutyku, która nie jest metabolizowana może prowadzić do podrażnienia układu pokarmowego lub innych narządów wewnętrznych, wywołując niepożądane skutki uboczne. Ograniczona rozpuszczalność leków jest obecnie dużym problemem, z którym zmagają się rynek farmaceutyczny, dlatego poszukiwane są metody które pozwolą na polepszenie właściwości fizycznych farmaceutyków.

Jedną z efektywniejszych i szeroko dyskutowanych metod pozwalających na poprawę rozpuszczalności leków jest amorfizacja, która polega na przemianie formy krystalicznej badanej substancji w formę szklistą⁴⁻⁸. Powstały materiał charakteryzuje się brakiem uporządkowania dalekozasięgowego w porównaniu do formy krystalicznej⁹, co powoduje zwiększenie rozpuszczalności oraz biodostępności substancji. Jednakże forma szklista charakteryzuje się również wyższą energią swobodną Gibbsa, w porównaniu do formy krystalicznej, co sprawia, iż jest termodynamicznie niestabilna. Innymi słowy, materiał w formie amorficznej zmierzając do minimum energetycznego powraca do formy krystalicznej. Jest to poważny problem w przypadku produktów leczniczych, ponieważ muszą one spełniać szereg wymogów dotyczących stabilności, czyli okresu ważności, zanim zostaną wprowadzone do obrotu. Kryteria, które musi spełnić dany lek opisane są przez Międzynarodową Radę Harmonizacji (ang. *ICH – International Council on Harmonisation*),

która wskazuje m.in. jak wykonać testy stabilności dla badanych produktów oraz jak długi musi być okres przydatności leku^{10,11}. Przyjmuje się, iż minimalny czas, w którym farmaceutyk jest stabilny w temperaturze pokojowej powinien być nie mniejszy niż dwa lata.

Aby uzyskać lek w formie amorficznej, który będzie spełniał powyższe wymagania należy otrzymaną formę szklistą ustabilizować, czyli sprawić, aby badany materiał przez odpowiednio długi czas nie powrócił do formy krystalicznej. Do tego celu opracowano szereg metod, które pozwalają osiągnąć opisany powyżej efekt. Pierwszą możliwością jest sporządzenie układów binarnych substancji czynnej (z ang. *API – Active Pharmaceutical Ingredient*) z dodatkami takimi jak cukry, aminokwasy czy krzemionki^{12–17}. Innym sposobem, który w ostatnich latach cieszy się dużym zainteresowaniem, jest metoda tworzenia układów lek-lek (z ang. *co-amorphous*)^{18–23}. Poza otrzymaniem stabilnej mieszaniny w formie amorficznej, metoda ta pozwala na uzyskanie efektu synergicznego działania zastosowanych leków. W takim przypadku idealnym zestawem dwóch API są farmaceutyki, które stosowane są razem podczas kuracji pacjenta, co skutkuje osiągnięciem wzmocnionego efektu terapeutycznego. Kolejnym przykładem metody stabilizacji leków w postaci amorficznej jest wykonanie tzw. stałych rozprożeń leku w matrycy polimerowej (z ang. *ASD – Amorphous Solid Dispersion*^{24–27}). Jest to nic innego jak mieszanina lek-polimer, w której cząsteczki substancji aktywnej są równomiernie rozproszone w polimerze. Do tego celu zazwyczaj wykorzystywany jest polimer charakteryzujący się wyższą temperaturą przejścia szklistego niż jest to w przypadku stabilizowanego API. Zastosowanie takiej substancji powoduje obniżenie objętości swobodnej substancji aktywnej, zwiększenie jej lepkości oraz spowolnienie jej dynamiki molekularnej, a co za tym idzie podwyższenie temperatury przejścia szklistego. W konsekwencji zazwyczaj otrzymywana jest stabilna mieszanina amorficzna. Mechanizm ten nazywany jest efektem antyplastyfikującym. Układ lek-polimer może być również stabilizowany poprzez obecność specyficznych oddziaływań pomiędzy cząsteczkami, takimi jak np. wiązania wodorowe^{28,29} lub przez ograniczenie przez polimer możliwości tworzenia się specyficznych wiązań pomiędzy cząsteczkami leku.

Obecnie stałe rozprożenia leków w matrycach polimerowych są intensywnie dyskutowane na łamach wielu publikacji naukowych. Rozważane jest dodawanie różnego rodzaju polimerów do amorficznych substancji aktywnych w celu ich stabilizacji. Co więcej, coraz częściej zwraca się uwagę również na to, iż wybierany polimer powinien charakteryzować się odpowiednimi właściwościami fizycznymi dla otrzymania stabilnego układu binarnego. Jednak temat ten pozostaje wciąż niedostatecznie zgłębiany, dlatego

w niniejszej rozprawie doktorskiej skupiono się na przeanalizowaniu amorficznych stałych rozproszeń w matrycach polimerowych, mając na celu przybliżenie tego ważnego aspektu.

Celem pracy doktorskiej pt. „*Poprawa rozpuszczalności w wodzie oraz fizycznej stabilności bicalutamidu w formie amorficznej - stałe rozproszenia w matrycach polimerowych.*” było:

- poprawa rozpuszczalności bicalutamidu poprzez konwersję do formy amorficznej a następnie ustabilizowanie formy szklistej tworząc stałe rozproszenia w matrycy polimerowej,
- zbadanie wpływu długości łańcucha polimerowego na stabilność fizyczną układu lek-polimer,
- poprawa stabilności amorficznej formy bicalutamidu przez stworzenie mieszaniny binarnej z innym lekiem przeciwnowotworowym flutamidem, a następnie zmieszania powstałego układu z polimerem.

Wyniki prowadzonych badań zostały opublikowane jako ciąg tematycznie spójnych artykułów, w prestiżowych czasopismach naukowych: *Molecular Pharmaceutics* oraz *European Journal of Pharmaceutics Sciences*, których współczynniki oddziaływania (z ang. *Impact Factor*) wynosiły w roku publikacji odpowiednio: 4.556, 4.396 i 3.352.

- A1. J. Szczurek, M. Rams-Baron, J. Knapik-Kowalczyk, A. Antosik, J. Szafraniec, W. Jamróz, M. Dulski, R. Jachowicz, M. Paluch, *Molecular Dynamics, Recrystallization Behavior, and Water Solubility of the Amorphous Anticancer Agent Bicalutamide and Its Polyvinylpyrrolidone Mixtures*, *Mol. Pharmaceutics* 14, (2017), 1071–1081.
- A2. J. Pacułt (Szczurek), M. Rams-Baron, B. Chrzęszcz, R. Jachowicz, M. Paluch, *Effect of Polymer Chain Length on the Physical Stability of Amorphous Drug–Polymer Blends at Ambient Pressure*, *Mol. Pharmaceutics*, 15, (2018), 2807–2815.
- A3. J. Pacułt (Szczurek), M. Rams-Barona, K. Chmiel, K. Jurkiewicz, A. Antosik, J. Szafraniec, M. Kurek, R. Jachowicz, M. Paluch, *How can we improve the physical stability of co-amorphous system containing flutamide and bicalutamide? The case of ternary amorphous solid dispersions*, *Eur. J. Pharm. Sci.* 136, (2019), 104947.

Poza tematyką pracy doktorskiej pozostają 2 współautorskie artykuły naukowe które, pomimo iż nie zostały włączone do rozprawy, świadczą o mojej aktywności naukowej:

- B1. M. Rams-Baron, J. Pacułt (Szczurek), A. Jędrzejowska, J. Knapik-Kowalczyk, M. Paluch, *Changes in physical stability of supercooled etoricoxib after compression*, Mol. Pharm. 15(9), 2018, 3969-3978.
- B2. J. Knapik-Kowalczyk, K. Chmiel, J. Pacułt (Szczurek), K. Bialek, L. Tajber, M. Paluch, *Enhancement of the Physical Stability of Amorphous Sildenafil in a Binary Mixture, with either a Plasticizing or Antiplasticizing Compound*, Pharmaceutics 12(5), 2020, 460.

Wyniki przeprowadzonych badań były również zaprezentowane na poniżej wymienionych międzynarodowych konferencjach naukowych:

- C1. *Silesian Cross-Border Workshop on Applied Physics* (2016) Ostrawa, Czechy.
- C2. *8th International Discussion Meeting on Relaxations in Complex Systems* (2017) Wisła, Polska
- C3. *1st International Conference on Contemporary Pharmacy Challenges: Amorphous Pharmaceuticals and Biopharmaceuticals* (2018) Wisła, Polska.

Badania przeprowadzone na potrzeby niniejszej pracy doktorskiej były finansowane przez Narodowego Centrum Nauki w ramach programu SYMFONIA 3 pt. *Wpływ procesów fizycznych oraz substancji pomocniczych na charakterystykę właściwości substancji leczniczych trudno rozpuszczalnych w wodzie* o numerze 2015/16/W/NZ7/00404.

2. Omówienie osiągniętych wyników

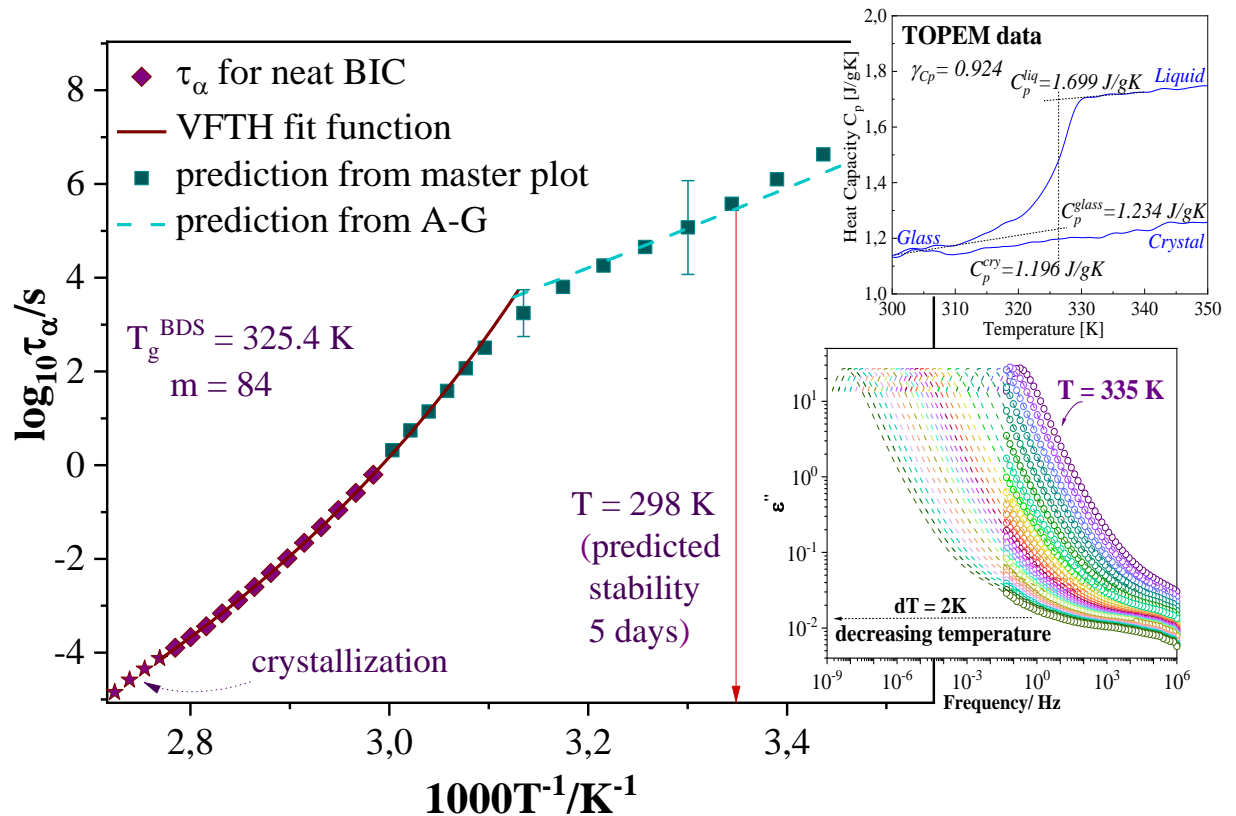
2.1 Badanie dynamiki molekularnej i rozpuszczalności w wodzie amorficznego bikalutamidu oraz jego stabilizacja z wykorzystaniem poliwinylpirolidonu.

Celem niniejszej pracy była poprawa rozpuszczalności w wodzie BIC oraz jego biodostępności. Aby tego dokonać lek został przekonwertowany do formy amorficznej a następnie stabilizowany za pomocą polimeru poliwinylpirolidonu (PVP).

W pierwszym etapie badań scharakteryzowano amorficzną formę bikalutamidu, którą otrzymano stosując metodę witrifikacji, tzn. stopienia substancji krystalicznej i szybkiego jej schłodzenia. Aby wyznaczyć temperaturę topnienia ($T_m = 467$ K) oraz przejścia szklistego ($T_g = 398$ K) BIC, wykonano pomiary przy zastosowaniu techniki różnicowej kalorymetrii skaningowej (ang. *DSC – Differential Scanning Calorimetry*) [A1 rysunek 1]. Następnie aby zbadać tendencję analizowanego materiału do krystalizacji wykonano eksperymenty nieizotermiczne oraz izotermiczne metodą szerokopasmowej spektroskopii dielektrycznej (ang. *BDS – Broadband Dielectric Spectroscopy*) [A1 ryunek 2,3]. Dzięki tej technice można z powodzeniem analizować dynamikę molekularną amorficznych układów w szerokim zakresie częstotliwości oraz temperatur, zarówno poniżej jak i powyżej temperatury zeszklenia. Na zarejestrowanych widmach dielektrycznych w cieczy przechłodzonej [A1 rysunek 2] można zaobserwować pik pochodzący od relaksacji strukturalnej α , charakterystycznej dla ruchów kooperatywnych molekuly. W temperaturze powyżej $T_k = 359$ K zauważono znaczny spadek intensywności krzywej absorpcji, co wskazuje na tzw. zimną krystalizację próbki. Wyznaczony został również czas krystalizacji próbki w cieczy przechłodzonej w $T \approx 306$ K, który wyniósł ~ 16 h.

Na podstawie otrzymanych danych dielektrycznych obliczono temperaturę przejścia szklistego (dla $\tau_\alpha = 100$ s) $T_g \approx 325$ K oraz parametr kruchości (m), mówiący o stopniu odchylenia zależności $\tau_\tau(T)$ od arrheniusowskiego przebiegu liniowego³⁰. Biorąc pod uwagę uzyskaną wartość parametru m możliwe jest podzielenie substancji na tzw. kruche ($m \geq 100$) oraz silne ($m \leq 30$). Ponadto kruchość korelowana jest również z tendencją do krystalizacji substancji, co oznacza, że silny materiał może charakteryzować się mniejszą podatnością na rekrytalizację. Należy jednak zaznaczyć, iż w literaturze znane są również przykłady nie spełniające tej zależności^{31–35}. Uzyskana wartość $m = 84$ wskazuje, iż bikalutamid można

zaliczyć do substancji o umiarkowanej tendencji do tworzenia fazy szklistej. Ponadto porównano kształt krzywej absorpcji w różnych temperaturach poprzez horyzontalne nałożenie widm strat dielektrycznych. Zaobserwowano, że dla bikalutamidu wartość temperatury nie ma wpływu na kształt zarejestrowanej krzywej absorpcji.



Rysunek 1. Temperaturowa zależność czasów relaksacji strukturalnej wyznaczona na podstawie widm dielektrycznych (fioletowe punkty). Zielone punkty oraz przerywana linia prezentują oszacowane wartości τ_α poniżej T_g , otrzymane poprzez zastosowanie metod tzw. „master plot” oraz modelu Adama-Gibbsa. Na dodatkowych panelach przedstawiono termogram z uzyskanymi wartościami ciepła właściwego BIC (górny panel) oraz widma dielektryczne zarejestrowane powyżej T_g (dolny panel). [A1 rysunek 7]

Poniżej temperatury zeszklenia kooperatywny ruch molekuł jest bardzo spowolniony co powoduje, iż proces relaksacji strukturalnej może osiągać rzędy wielkości nawet kilku miesięcy. Z tego względu wyznaczenie czasów relaksacji w fazie szklistej jest kluczowe, ponieważ uważa się, iż można je powiązać z tendencją do krystalizacji. zarejestrowanie go eksperymentalnie jest bardzo trudne bądź niemożliwe. Jednak w literaturze opisano, iż α -proces można powiązać z tendencją materiału do krystalizacji poniżej T_g . Do przybliżenia czasu, w którym materiał pozostanie stabilny w temperaturze pokojowej (poniżej T_g), można

zatem wykorzystać otrzymane eksperymentalnie wartości τ_α . Do tego celu wykorzystano metodę polegającą na horyzontalnym nasuwaniu krzywej absorpcji zarejestrowanej powyżej T_g , na widma strat dielektrycznych, w których zarejestrowane jest jedynie prawe zbocze relaksacji strukturalnej (rys. 1). Metodę tą jednak można zastosować jedynie gdy kształt krzywej absorpcji nie jest wrażliwy na temperaturę, tak jak jest to w przypadku bikalutamidu. Kolejną metodą oszacowania τ_α poniżej temperatury zeszklenia jest zastosowanie zmodyfikowanego modelu Adama-Gibbsa, który został zaproponowany przez Hodgea³⁰ i wyrażony jest następującym równaniem:

$$\tau_\alpha(T, T_f) = \tau_\infty \exp\left(\frac{D}{T(1 - T_0/T_f)}\right) \quad (1)$$

gdzie τ_∞ , D i T_0 to parametry otrzymane z równania Vogel-Fuler-Taman, a T_f to fikcyjna temperatura (ang. *fictive temperature*), definiowana jako:

$$\frac{1}{T_f} = \frac{\gamma_{C_p}}{T_g} + \frac{1 - \gamma_{C_p}}{T} \quad (2)$$

$$\gamma_{C_p} = \frac{C_p^{liq} - C_p^{glass}}{C_p^{liq} - C_p^{cryst}} \Bigg|_{T=T_g} \quad (3)$$

Gdzie C_p^{liq} , C_p^{glass} , C_p^{cryst} , to ciepło właściwe otrzymane dla cieczy, formy szklistej oraz krystalicznej próbki.

Badania modulowanej temperaturowo różnicowej kalorymetrii skaningowej (górny panel rys. 1) pozwoliły na wyznaczenie powyższych wielkości w tym fikcyjną temperaturę, którą wykorzystano do obliczenia teoretycznych wartości czasów relaksacji (równanie nr 1), a następnie temperaturowej zależności τ_α bikalutamidu w fazie szklistej. Z obu przedstawionych metod można wnioskować, iż bikalutamid w formie amorficznej w $T = 298$ K będzie stabilny przez jedynie około 5 dni.

Ze względu na silną tendencję do krystalizacji amorficznej formy BIC, podjęto próbę ustabilizowania go poprzez zmieszanie z polimerem poliwinylpirolidonem. Jest to polimer bardzo często stosowany w przemyśle farmaceutycznym jako spoiwo tabletek. Ponadto w mieszaninach z lekiem wykazuje właściwości, które poprawiają biodostępność oraz rozpuszczalność w wodzie substancji aktywnych poprzez tworzenie wiązań wodorowych. Przygotowane mieszaniny BIC-PVP w stosunkach w wagowych 10-1, 5-1, 2-1, 1-2 zbadano

za pomocą różnicowej kalorymetrii skaningowej. Na otrzymanych termogramach [A1 rysunek 8] można zauważyć schodkowy charakter zmiany ciepła właściwego, który wskazuje na obecność przejścia szklistego w badanych mieszaninach. Brak procesu egzotermicznego oraz endotermicznego w przypadku układów BIC-PVP 2-1 oraz 1-2 wskazuje, iż dodatek około 30% polimeru hamuje krystalizację leku.

Stabilizacja układów binarnych może być wynikiem obecności efektu antyplastyfikującego, oddziaływaniami pomiędzy molekułami leku i polimeru lub sumą obu tych mechanizmów. Aby określić, jaki mechanizm jest odpowiedzialny za poprawę fizycznej stabilności leku w formie amorficznej porównano eksperymentalne wartości temperatury zeszklenia mieszanin z wartościami teoretycznymi otrzymanymi z modelu Gordona – Taylora [A1 rysunek 8] oraz wykonano analizę za pomocą spektroskopii fourierowskiej w podczerwieni (ang. *FT-IR - Fourier Transformer Infrared Spectroscopy*) [A1 rysunek 9]. Ponieważ pierwsza z wymienionych metod nie dała jednoznacznej odpowiedzi czy na stabilizację układu ma wpływ obecność specyficznych oddziaływań, wykonano również pomiary FT-IR. Na zamieszczonych widmach IR [A1 rysunek 9] w zakresie $1400-1800\text{ cm}^{-1}$ można zaobserwować pasmo charakterystyczne dla drgań rozciągających grupy C=O. Wraz ze zwiększającą się ilością PVP w mieszaninie widoczne jest zwiększanie się intensywności pasma przy 1670 cm^{-1} co wskazuje na tworzenie się wiązań wodorowych. Eksperymenty wykazały, iż za stabilizację układu może być odpowiedzialne złożenie dwóch czynników, mianowicie efektu antyplastyfikującego oraz obecności wiązań wodorowych.

W końcowym etapie badań przeprowadzono również analizę rozpuszczalności w wodzie oraz uwalniania mieszanin BIC-PVP. Na podstawie otrzymanych wyników DSC oraz przewidywań stabilności próbek w temperaturze pokojowej, do analiz wybrano mieszaninę BIC-PVP (2-1), która szacunkowo pozostałaby w niezmienniej formie amorficznej przez ponad 100 lat. Otrzymane wyniki potwierdziły, iż układy dwuskładnikowe BIC-PVP charakteryzują się znacznie lepszą kinetyką uwalniania substancji aktywnej oraz 37 razy lepszą rozpuszczalnością w wodzie w stosunku do krystalicznego bikalutamidu.

2.2 Wpływ długości łańcucha polimerowego na stabilność fizyczną amorficznych mieszanin lek-polimer.

W poprzedniej pracy z powodzeniem ustabilizowano bicalutamid w formie amorficznej dzięki zastosowaniu polimeru poliwinylpirolidonu. Wykonywanie mieszanin ASD w matrycy polimerowej jest obecnie chętnie wybieraną metodą stabilizacji farmaceutyków w fazie szklistej. Pomimo dobrze znanej procedury wykonywania układów ASD wciąż wiele aspektów doboru polimeru pozostaje nie zbadane. Okazuje się bowiem, iż wybór optymalnego polimeru do sporządzenia takiej mieszaniny nie jest trywialny. Należy wziąć pod uwagę nie tylko wartość temperatury zeszklenia polimeru, ale również jego strukturę, długość, ułożenie w przestrzeni, a zatem również jego splątanie, obecność specyficznych grup funkcyjnych itp. Z tego względu w niniejszej pracy skupiono się na zbadaniu wpływu długości łańcucha polimerowego na stabilność fizyczną amorficznych mieszanin lek-polimer.

W pierwszym kroku wybrano polimer poliwinylpirolidon, który uprzednio wykazał bardzo dobre właściwości stabilizujące bicalutamid w formie amorficznej. Następnie wybrano trzy różne długości łańcucha polimerowego (w tekście opisane odpowiednio od najkrótszego do najdłuższego jako: K10, K30, K90) i wykonano mieszaniny BIC-PVP 10% (w/w). Do badania dynamiki molekularnej wykonanych układów zastosowano technikę BDS. Na zamieszczonych widmach dielektrycznych [A2 rysunek 1] można zauważyć, iż początek krystalizacji dla każdej z mieszanin znajduje się w tej samej temperaturze $T = 373$ K. Ponadto wykreślenie temperaturowej zależności czasów relaksacji [A2 rysunek 3] pokazuje, iż dynamika molekularna badanych układów jest identyczna dla każdej badanej mieszaniny. Potwierdzają to również otrzymane termogramy, na których można zaobserwować, że próbki BIC-PVP charakteryzują się jednakową temperaturą zeszklenia $T_g = 331$ K [A2 rysunek 5]. Otrzymane wyniki mogły by wskazywać, iż nie istnieje żadna korelacja pomiędzy długością łańcucha polimerowego a stabilnością układów lek-polimer w stanie amorficznym. Brak różnic w dynamice molekularnej badanych układów może wynikać z faktu, iż w mieszaninie BIC-PVP ilość zastosowanego polimeru jest niewielka. Aby finalnie zweryfikować tą tezę, przeprowadzono eksperymenty izotermiczne techniką BDS. Zamieszczone kinetyki krystalizacji na rysunku [A2 rysunek 6] wyraźnie pokazują, iż w zależności od zastosowanej długości polimeru w próbkach BIC-PVP obserwujemy znaczne różnice w tendencji do krystalizacji. Mieszanina API z polimerem o najdłuższym łańcuchu krystalizuje najszybciej,

natomiast najlepiej stabilizuje układ binarny PVP K30. Na podstawie powyższych wyników zapostulowano, że mechanizmem odpowiedzialnym za otrzymane różnice w stabilności fizycznej badanych mieszanin może być ułożenie łańcucha polimerowego w przestrzeni. Z tym aspektem bezpośrednio powiązane jest zagadnienie wolnej objętości (ang. *free volume*), która charakteryzuje obecność wolnych przestrzeni pomiędzy łańcuchami polimerowymi. W przypadku zaproponowanej tezy, wnioskujemy, iż polimer w zależności od długości łańcucha będzie przyjmował różne ułożenie w mieszaninie i w ten sposób będą mogły powstawać mniejsze bądź większe przestrzenie pomiędzy cząsteczkami polimeru i leku, co spowoduje zaobserwowanie różnic w badanej wolnej objętości próbek. Odpowiednią techniką do zbadania tych efektów jest spektroskopia czasów życia pozytonów (ang. *PALS – Positron Annihilation Lifetime Spectroscopy*). Uzyskane wyniki PALS potwierdziły obserwowaną zależność, wynikającą z badań dielektrycznych. Największa wartość wolnej objętości została zarejestrowana dla próbki BIC-PVP K90, która w eksperymentach izotermicznych wykazała największą tendencję do krystalizacji. Sądzymy, iż wynika to z faktu, iż polimer w mieszaninie układa się w taki sposób, że łańcuch polimerowy nie wypełnia wolnych przestrzeni, co ułatwia proces krystalizacji. W przypadku krótszych łańcuchów, tak jak jest to w zastosowanym PVP K10, zwiększa się upakowanie polimeru w mieszaninie, co powoduje stabilizację układu. Co również warte podkreślenia, zaobserwowana zależność nie jest tendencją monotoniczną. Istnieje pewna optymalna długość łańcucha polimerowego, która w najkorzystniejszy sposób będzie polepszać stabilność fizyczną mieszaniny. Otrzymane wyniki wykazały, że polimerem o najlepszych właściwościach stabilizujących układ BIC-PVP jest PVP K30.

Uzyskane rezultaty pokazują jak ważne jest badanie wpływu właściwości fizycznych polimerów na zahamowanie krystalizacji mieszanin amorficznych lek-polimer, aby wybrać najlepszą formę polimeru do wykonania stabilnych układów amorficznych.

2.3 Jak poprawić fizyczną stabilność amorficznego układu bicalutamid – flutamid? Badania trójskładnikowych amorficzne stałych rozproszeń.

W ostatnich latach dużym zainteresowaniem wśród naukowców cieszy się metoda prowadząca do poprawy rozpuszczalności w wodzie oraz fizyczną stabilność układów amorficznych polegająca na zmieszaniu dwóch substancji aktywnych. Wynika to z faktu, że do tej pory najczęstszym podejściem do API charakteryzującej się ograniczoną rozpuszczalnością oraz tendencją do krystalizacji, było zmieszanie jej np. z polimerem.

Koncentrowano się bowiem tylko na jednej konkretnej substancji, aby polepszyć jej właściwości fizyczne. Jednakże zaczęto zastanawiać się nad wykorzystaniem innych substancji aktywnych w procesie stabilizacji, które wykorzystywane są np. razem podczas terapii lub gdy w przypadku leczenia pacjenta przepisany jest mu więcej niż jeden lek. Jest to bardzo interesujący aspekt, ponieważ stosując dwa API jednocześnie możliwe jest otrzymanie efektu synergicznego.

W niniejszej pracy sporządzono amorficzną mieszaninę bikalutamidu i flutamidu (FL), które wykorzystywane są w terapii nowotworu gruczołu krokowego. Ponadto grupa badawcza Joyce³⁶ wykazała, iż możliwe jest zastosowanie obu tych leków w jednej terapii. Pomimo, że obecnie nie jest zarejestrowany lek, który łączył by w sobie wyżej wymienione farmaceutyki, w niniejszej pracy postanowiono sprawdzić czy możliwe jest uzyskanie polepszonej stabilności fizycznej oraz rozpuszczalności obu tych leków poprzez stworzenie z nich układu binarnego, w celu zaproponowania nowego rozwiązania do potencjalnego stosowania w terapii przeciwnowotworowej.

W pierwszej kolejności porównano tendencję do krystalizacji obu materiałów w stanie szklistym oraz w cieczy przechłodzonej. Do tego celu wybrano technikę różnicowej kalorymetrii skaningowej i dyfrakcji rentgenowskiej. Jak można zaobserwować na termogramie otrzymanym z badań kalorymetrycznych [A3 rysunek 1] oba farmaceutyki krystalizują powyżej temperatury zeszklenia. Ponadto badania XRD wykazały, iż bikalutamid jest także niestabilny w fazie szklistej i powraca całkowicie do fazy krystalicznej po około 8 dniach. W przypadku flutamidu T_g jest niższa od temperatury pokojowej, co powoduje, iż zarówno eksperymenty DSC jak i XRD obrazują tendencję farmaceutyku do krystalizacji z cieczy przechłodzonej. W obu przypadkach potwierdzona jest silna tendencja FL do krystalizacji. Wykonane badania wykazują, iż zastosowanie analizowanych API w formie amorficznej w przemyśle farmaceutycznym jest niemożliwe ze względu na ich brak stabilności w temperaturze pokojowej. Z tego powodu sprawdzono możliwość zahamowania procesu krystalizacji leków poprzez sporządzenie układu binarnego zawierającego BIC i FL

W następnym kroku wykonano szereg mieszanin o różnych stosunkach wagowych (FL-BIC 10%, FL-BIC 30%, FL-BIC 50%, FL-BIC 65%) bikalutamidu i flutamidu, aby sprawdzić wpływ obu API na stabilizację takiej mieszaniny. Do tego celu wykorzystano technikę DSC, z której otrzymane termogramy można obserwować na rysunku [A3 rysunek 2]. Jak można zauważyć, w trakcie ogrzewania jedynie próbka FL – BIC 10% krystalizuje powyżej temperatury zeszklenia. Dla potwierdzenia otrzymanych wyników wykonano

również badania dielektryczne za pomocą techniki BDS. W przypadku zarejestrowanej dynamiki molekularnej zaobserwowano, że [różnice wobec wyników kalorymetrycznych, tj.]dopiero próbka FL – BIC 50% charakteryzowała się brakiem tendencji do krystalizacji. Różnice w otrzymanych wynikach dielektrycznych i kalorymetrycznych mogą wynikać z zastosowania różnego tempa grzania próbek podczas wykonywanych eksperymentów. Pomimo to, uzyskana stabilność układu binarnego nie jest satysfakcjonująca ze względu na to, iż stężenie mieszaniny, które wykazuje stabilność, nie znajduje odzwierciedlenia w dawce terapeutycznej. Z tego względu przygotowano również układy trójskładnikowe zawierające BIC i FL w stosunku terapeutycznym wraz z 30% dodatkiem polimeru. Do stworzenia tych mieszanin wybrano dwa polimery często stosowane w przemyśle farmaceutycznym: PVP oraz poli(meta akrylan metylu-co-akrylan etylu) (MMA/EA). Przedstawione na rysunku [A3 rysunek 5] termogramy pokazują, iż mieszanina FL-BIC-MMA/EA nie jest jednorodna, na co wskazuje obecność dwóch przejść szklistych. W przypadku mieszaniny FL-BIC-PVP obserwowana jest tylko jedna $T_g = 307$ K, oraz nie zanotowano procesu krystalizacji powyżej temperatury zeszklenia. Wskazuje to na to, iż mieszanina FL i BIC wraz z polimerem PVP jest jednorodna oraz stabilna. Wobec tego, wykonano badania dyfrakcji rentgenowskiej w temperaturze pokojowej aby sprawdzić tendencję wybranego układu do krystalizacji. W trakcie wykonywanych eksperymentów wykazano, iż mieszanina jest stabilna przez 182 dni. Ponadto przeprowadzono również badania rozpuszczalności oraz uwalniania dla próbki FL-BIC-PVP. Jak można zaobserwować na rysunku [A3 rysunek 6] trójskładnikowa mieszanina charakteryzuje się zdecydowanie lepszą zarówno rozpuszczalnością w wodzie jak i kinetyką uwalniania substancji. W przypadku rozpuszczalności jest to dwukrotna poprawa dla FL i siedmiokrotna dla BIC. Jeśli chodzi zaś o badanie uwalniania to zarejestrowana została dwukrotnie większa ilość uwolnionej substancji dla FL i trzykrotnie wyższa dla BIC niż jest to dla amorficznych form tych leków.

3. Wykaz publikacji stanowiących podstawę rozprawy doktorskiej wraz z oświadczeniami współautorów

A1.J. Szczurek, M. Rams-Baron, J. Knapik-Kowalczyk, A. Antosik, J. Szafranec, W. Jamróz, M. Dulski, R. Jachowicz, M. Paluch, *Molecular Dynamics, Recrystallization Behavior, and Water Solubility of the Amorphous Anticancer Agent Bicalutamide and Its Polyvinylpyrrolidone Mixtures*, *Mol. Pharmaceutics* 14 , (2017), 1071–1081.

Impact Factor czasopisma z roku opublikowania pracy: 4.556

Liczba punktów ministerialnych MNiSW czasopisma z roku opublikowania pracy: 40

DOI: 10.1021/acs.molpharmaceut.6b01007

Mój wkład w wyżej wymienionym artykule polegał na wykonaniu pomiarów dielektrycznych, analizie wszystkich otrzymanych wyników oraz przygotowaniu manuskryptu. Wkład pozostałych współautorów, w formie oświadczeń, zamieszczono na końcu artykułu.

dr Marzena Rams-Baron

Katowice, 16 września 2020 r.

Zakład Biofizyki i Fizyki Molekularnej

Wydział Nauk Ścisłych i Technicznych

Uniwersytet Śląski

ul. Bankowa 12, 40-007 Katowice

OŚWIADCZENIE

Oświadczam, że w pracy:

J. Szczurek, M. Rams-Baron, J. Knapik-Kowalczyk, A. Antosik, J. Szafraniec, W. Jamróz, M. Dulski, R. Jachowicz, M. Paluch, *Molecular Dynamics, Recrystallization Behavior, and Water Solubility of the Amorphous Anticancer Agent Bicalutamide and Its Polyvinylpyrrolidone Mixtures*, Mol. Pharmaceutics 14 , (2017), 1071–1081.

Mój udział polegał na nadzorowaniu wykonanych analiz, dyskusji otrzymanych wyników oraz korekcji manuskryptu.

Marzena Rams-Baron

Podpis

dr inż. Justyna Knapik-Kowalczyk

Katowice, 16.09.2020r.

Zakład Biofizyki i Fizyki Molekularnej

Wydział Nauk Ścisłych i Technicznych

Uniwersytet Śląski

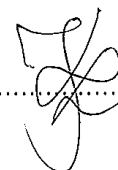
ul. Bankowa 12, 40-007 Katowice

OŚWIADCZENIE

Oświadczam, że w pracy:

J. Szczurek, M. Rams-Baron, J. Knapik-Kowalczyk, A. Antosik, J. Szafraniec, W. Jamróz, M. Dulski, R. Jachowicz, M. Paluch, *Molecular Dynamics, Recrystallization Behavior, and Water Solubility of the Amorphous Anticancer Agent Bicalutamide and Its Polyvinylpyrrolidone Mixtures*, *Mol. Pharmaceutics* 14 , (2017), 1071–1081.

Mój udział polegał na wykonaniu badań kalorymetrycznych.



.....
Podpis

dr Agata Antosik-Rogóż

Kraków, 16.09.2020

Katedra Technologii Postaci Leku i Biofarmacji

Wydział Farmaceutyczny

Uniwersytet Jagielloński

ul. Medyczna 9, 30-688 Kraków

OŚWIADCZENIE

Oświadczam, że w pracy:

J. Szczurek, M. Rams-Baron, J. Knapik-Kowalczyk, A. Antosik, J. Szafraniec, W. Jamróz, M. Dulski, R. Jachowicz, M. Paluch, *Molecular Dynamics, Recrystallization Behavior, and Water Solubility of the Amorphous Anticancer Agent Bicalutamide and Its Polyvinylpyrrolidone Mixtures*, Mol. Pharmaceutics 14 , (2017), 1071–1081.

Mój udział polegał na wykonaniu badań rozpuszczalności.



Podpis

dr Joanna Szafraniec-Szczęśny

Kraków, 16.09.2020

Katedra Technologii Postaci Leku i Biofarmacji

Wydział Farmaceutyczny

Uniwersytet Jagielloński

ul. Medyczna 9, 30-688 Kraków

OŚWIADCZENIE

Oświadczam, że w pracy:

J. Szczurek, M. Rams-Baron, J. Knapik-Kowalczyk, A. Antosik, J. Szafraniec, W. Jamróz, M. Dulski, R. Jachowicz, M. Paluch, *Molecular Dynamics, Recrystallization Behavior, and Water Solubility of the Amorphous Anticancer Agent Bicalutamide and Its Polyvinylpyrrolidone Mixtures*, Mol. Pharmaceutics 14, (2017), 1071–1081.

Mój udział polegał na wykonaniu badań szybkości rozpuszczania substancji leczniczej.



Podpis

dr Witold Jamróz

Kraków, 18.09.2020

Katedra Technologii Postaci Leku i Biofarmacji

Wydział Farmaceutyczny

Uniwersytet Jagielloński

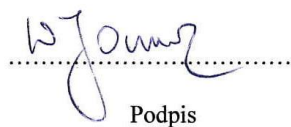
ul. Medyczna 9, 30-688 Kraków

OŚWIADCZENIE

Oświadczam, że w pracy:

J. Szczurek, M. Rams-Baron, J. Knapik-Kowalczyk, A. Antosik, J. Szafraniec, W. Jamróz, M. Dulski, R. Jachowicz, M. Paluch, *Molecular Dynamics, Recrystallization Behavior, and Water Solubility of the Amorphous Anticancer Agent Bicalutamide and Its Polyvinylpyrrolidone Mixtures*, *Mol. Pharmaceutics* 14, (2017), 1071–1081.

Mój udział polegał na dyskusji otrzymanych wyników.



Podpis

dr Mateusz Dulski

Katowice,

Instytut Inżynierii Materiałowej

Wydział Nauk Ścisłych i Technicznych

Uniwersytet Śląski

ul. Bankowa 12, 40-007 Katowice

OŚWIADCZENIE

Oświadczam, że w pracy:

J. Szczurek, M. Rams-Baron, J. Knapik-Kowalczyk, A. Antosik, J. Szafraniec, W. Jamróz, M. Dulski, R. Jachowicz, M. Paluch, *Molecular Dynamics, Recrystallization Behavior, and Water Solubility of the Amorphous Anticancer Agent Bicalutamide and Its Polyvinylpyrrolidone Mixtures*, Mol. Pharmaceutics 14 , (2017), 1071–1081.

Mój udział polegał na wykonaniu pomiarów FT-IR.

Mateusz Dulski

.....
Podpis

Prof. dr hab. Renata Jachowicz
Katedra Technologii Postaci Leku i Biofarmacji
Wydział Farmaceutyczny
Uniwersytet Jagielloński
ul. Medyczna 9, 30-688 Kraków

Kraków 16.09.2020.

OŚWIADCZENIE

Oświadczam, że w pracy:

J. Szczurek, M. Rams-Baron, J. Knapik-Kowalczyk, A. Antosik, J. Szafraniec, W. Jamróz, M. Dulski, R. Jachowicz, M. Paluch, *Molecular Dynamics, Recrystallization Behavior, and Water Solubility of the Amorphous Anticancer Agent Bicalutamide and Its Polyvinylpyrrolidone Mixtures*, *Mol. Pharmaceutics* 14 , (2017), 1071–1081.

Mój udział polegał na udziale w dyskusji otrzymanych wyników.

Kierownik
Katedry i Zakładu Technologii
Postaci Leku i Biofarmacji CM UJ
Renata Jachowicz
Prof. dr hab. Renata Jachowicz

Prof. zw. dr hab. Marian Paluch

Chorzów,

Instytut Fizyki

Uniwersytet Śląski

ul. 75 Pułku Piechoty 1A, 41-500 Chorzów

OŚWIADCZENIE

Oświadczam, że w pracy:

J. Szczurek, M. Rams-Baron, J. Knapik-Kowalczyk, A. Antosik, J. Szafraniec, W. Jamróz, M. Dulski, R. Jachowicz, M. Paluch, *Molecular Dynamics, Recrystallization Behavior, and Water Solubility of the Amorphous Anticancer Agent Bicalutamide and Its Polyvinylpyrrolidone Mixtures*, Mol. Pharmaceutics 14 , (2017), 1071–1081.

Mój udział polegał na udziale w dyskusji otrzymanych wyników oraz korekcji manuskryptu.

.....

Podpis

Molecular Dynamics, Recrystallization Behavior, and Water Solubility of the Amorphous Anticancer Agent Bicalutamide and Its Polyvinylpyrrolidone Mixtures

Justyna Szczurek,^{†,‡} Marzena Rams-Baron,^{*,†,‡,§} Justyna Knapik-Kowalczyk,^{†,‡} Agata Antosik,[§] Joanna Szafraniec,[§] Witold Jamróz,[§] Mateusz Dulski,^{‡,||} Renata Jachowicz,[§] and Marian Paluch^{†,‡}

[†]Institute of Physics, University of Silesia, Uniwersytecka 4, 40-007 Katowice, Poland

[‡]Silesian Center for Education and Interdisciplinary Research, 75 Pulku Piechoty 1A, 41-500 Chorzow, Poland

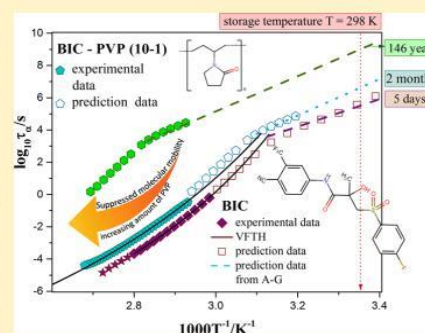
[§]Jagiellonian University, Faculty of Pharmacy, Department of Pharmaceutical Technology and Biopharmaceutics, Medyczna 9, 30-688 Kraków, Poland

^{||}Institute of Materials Science, University of Silesia, 75 Pulku Piechoty 1A, 41-500 Chorzow, Poland

Supporting Information

ABSTRACT: In this paper, we investigated the molecular mobility and physical stability of amorphous bicalutamide, a poorly water-soluble drug widely used in prostate cancer treatment. Our broadband dielectric spectroscopy measurements and differential scanning calorimetry studies revealed that amorphous BIC is a moderately fragile material with a strong tendency to recrystallize from the amorphous state. However, mixing the drug with polymer polyvinylpyrrolidone results in a substantial improvement of physical stability attributed to the antiplasticizing effect governed by the polymer additive. Furthermore, IR study demonstrated the existence of specific interactions between the drug and excipient. We found out that preparation of bicalutamide–polyvinylpyrrolidone mixture in a 2–1 weight ratio completely hinder material recrystallization. Moreover, we determined the time-scale of structural relaxation in the glassy state for investigated materials. Because molecular mobility is considered an important factor governing crystallization behavior, such information was used to approximate the long-term physical stability of an amorphous drug and drug–polymer systems upon their storage at room temperature. Moreover, we found that such systems have distinctly higher water solubility and dissolution rate in comparison to the pure amorphous form, indicating the genuine formulation potential of the proposed approach.

KEYWORDS: amorphous bicalutamide, polyvinylpyrrolidone, molecular dynamic, physical stability, glass transition, crystallization



INTRODUCTION

One of the most common forms of cancer, which occurs among men, is prostate cancer. This tumor causes death in one in three cases.¹ Because its growth is stimulated by androgens, various androgens blockers, such as cyproterone or flutamide, are clinically used. Unfortunately, taking these drugs is not free from side effects, such as loss of libido, thrombosis, or gynecomastia.² This serious problem motivates scientists to search for other drugs suitable for patients with prostate cancer.³ As an alternative choice, free from the mentioned repercussions, bicalutamide (BIC) (Figure 1) was proposed.⁴ BIC is a nonsteroidal antiandrogen inhibiting conversion of testosterone to 5 α -dihydrotestosterone influencing growth of prostate tumors. Despite many advantages, its main limitation is low solubility (<5 mg/L);⁵ thus, the drug is classified as a class II pharmaceutical according to the Biopharmaceutics Classification System (BCS).⁶

Since low aqueous solubility is one of the crucial problems in the pharmaceutical field, many efforts are directed toward

searching for effective methods of improving drug solubility and bioavailability. One such approach, widely described in the literature,^{7–9} includes conversion of crystalline material into the amorphous state.¹⁰ Besides multiply benefits, the amorphous state is characterized by higher free energy than the crystalline state, which consequently leads to its lower stability. This is a serious limitation from the pharmaceutical point of view because amorphous substances can recrystallize during production, storage, and using of the drug.^{7,10} Therefore, a key condition that must be satisfied by an amorphous formulation to be implemented into practice is the resistance to crystallization during the product shelf life.

From a fundamental point of view, crystallization is a two-step process consisting of nucleation and crystal growth. These

Received: November 6, 2016

Revised: January 7, 2017

Accepted: February 23, 2017

Published: February 23, 2017

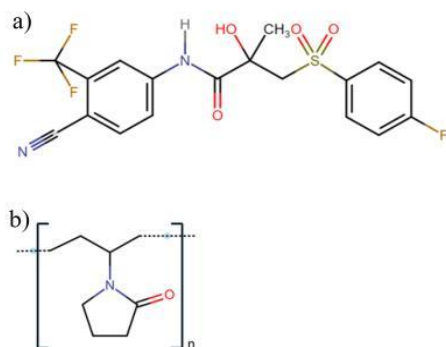


Figure 1. Chemical structures of BIC (a) and PVP (b).

events are described by nucleation rate/growth velocity, which depends on the probability of forming nuclei and diffusion of atoms/molecules across the solid–liquid interface. Their temperature dependencies are bell-shaped and can overlap each other. The degree of their imposing determines the glass forming ability of a material (expected to be better for more separated curves). Thus, such information may be helpful during anticipation of the possible recrystallization tendencies of amorphous pharmaceuticals.^{11–14}

To stabilize the amorphous form of a drug, a variety of excipients can be used (e.g., low-molecular weight materials like sugars,^{15–17} other APIs,^{18–20} and mesoporous silica materials^{21–23}). One of the most promising approaches aimed at stability enhancement includes preparation of a solid dispersion containing amorphous drug dispersed in a matrix formed by polymer with significantly higher T_g . Nowadays, solid dispersion technology has been well recognized and successfully implemented as evidenced by the growing number of solid-dispersion products available on the market (griseofulvin, troglitazone, or ritonavir).²⁴ This success is related to the superior physical stability of drug–polymer formulations, which is attributed to specific interactions between the drug and polymer additive and reduced molecular mobility of such binary systems.^{25,26}

Experimentally, molecular dynamics can be probed using broadband dielectric spectroscopy (BDS). The BDS technique allows investigation of relaxation processes at temperatures lower and higher than the glass transition temperature (T_g). At higher temperatures ($T > T_g$), one can detect a structural α -process which is correlated to the collective motions of a large group of molecules. Below T_g , the movement of the whole group of molecules becomes not as significant as their local mobility. It has been suggested that both processes are associated with devitrification and consequently the stability of amorphous drugs.^{7–9,27} Thus, the utility of the BDS technique to long-term stability prediction of drugs in amorphous form has been thoroughly investigated. This is important because requirements concerning the physical stability of active pharmaceutical ingredients (APIs) are strictly defined, i.e. 2 years at 25 °C and 60% RH.²⁸ At the same time, their experimental verification may be time-consuming. BDS offers the opportunity to predict the stability of an amorphous material by measuring its molecular mobility, and thereby, it can support faster decision making during the process of new formulation development. Since structural relaxation times deep in the glassy state are too long to be experimentally attainable, the reliable methods of their predictions are

necessary. Concurrently, much effort is put into complete understanding of mutual relationships between the time-scales of molecular relaxations and recrystallization from glassy and liquid states. All these attempts are necessary to find a general rule for proper selection of excipients capable of efficiently improving the stability of a drug by modulating its mobility.

In this paper we used BDS and DSC techniques to analyze the molecular dynamics and recrystallization behavior of amorphous BIC. Since our studies revealed that amorphous BIC has a strong tendency to recrystallize, we verified the possibility of its stabilization in a binary bicalutamide–polyvinylpyrrolidone (BIC-PVP) mixture. To approximate the stability of drug and BIC-PVP mixtures in the glassy state, we predicted structural relaxation times below T_g by master plot construction and compared them with those obtained from the Adam and Gibbs (A-G) extended model. Finally, we compared the solubility and dissolution rates of pure drug in crystalline and amorphous form with those obtained for examined BIC-PVP binary systems.

■ MATERIALS AND METHODS

Materials. The crystalline form of BIC ($M_w = 430.37$ g/mol) of 99.8% purity was purchased from Hangzhou Hyper Chemicals Limited. The systematic name of BIC is *N*-[4-cyano-3-(trifluoromethyl)phenyl]-3-[(4-fluorophenyl)sulfonyl]-2-hydroxy-2-methylpropanamide.²⁹ Amorphous samples of pure BIC were prepared by the quench cooling method; that is, crystalline powder was molten on a capacitor plate at $T_m \cong 463$ K and subsequently vitrified on a chilled copper plate. The applied vitrification procedure did not cause glass cracking, which could affect its properties. According to literature reports, BIC is thermally stable, and near to the T_m , it does not decompose.¹⁹ Based on this information, we assumed that the chosen vitrification method is correct for our experiments.

Polyvinylpyrrolidone (PVP) ($M_w = 40\,000$ g/mol, $K = 30$), whose commercial name is Plasdone, was supplied from Sigma-Aldrich. The amount of water in the material was determined as 4% (Carl-Fisher method).

Preparation of binary system. The binary BIC-PVP systems were prepared at different BIC-PVP weight ratios which were assigned as 10–1, 5–1, 2–1, and 1–2. This corresponds to the following weight percentage concentrations of BIC in each sample: 90% (w/w), 83% (w/w), 66% (w/w), and 33% (w/w), respectively. To acquire homogeneous samples in the first step, we mixed compounds with polymer at appropriate ratios in mortar for a few minutes. In order to remove water, we kept the mixtures for 15 min at $T = 373$ K on the capacitor plate lying on a hot plate magnetic stirrer (CAT M. Zipperer GmbH H 17.5D). The mixtures were then melted at $T = 463$ K and vitrified by fast transfer to a previously chilled copper plate. As previously, the applied vitrification procedure did not cause glass cracking, which could affect its properties. The thus made BIC-PVP systems were analyzed immediately after preparation to avoid recrystallization. The water content in the analyzed samples did not exceed 2% (Carl-Fisher method).

Differential scanning calorimetry (DSC). To characterize the thermal properties of neat BIC and BIC-PVP mixtures, we used a Mettler-Toledo DSC 1 STARe System equipped with an HSS8 ceramic sensor having 120 thermocouples and a liquid nitrogen cooling station. The device was calibrated for temperature and enthalpy using zinc and indium standards. Mentioned calibration processes were performed in accordance

with the manufacturer's recommendation.^{32,33} After calibration, about 10 mg of the samples were measured in aluminum crucibles (40 μL) with pin-ME-27331. All measurements were carried out in the range from 300 to 475 K with heating rates being equal to 10 K/min. Crystallization as well as melting points were determined as the onset of the peak, whereas the glass transition temperature was determined as the midpoint of the heat capacity increment. To obtain accurate temperature dependencies of the heat capacity for pure amorphous BIC, a stochastic temperature-modulated differential scanning calorimetry (TOPEM) method implemented by Mettler-Toledo TOPEM was employed. During these experiments the biggest amount of the sample has been used (~ 15 mg). These measurements were performed in the temperature range from $T = 300$ K to $T = 350$ K with a heating rate of 0.5 K/min, period of modulation 15 s, and temperature amplitude of modulation equal to ± 0.25 K.

Broadband dielectric spectroscopy measurements.

Dielectric measurements for pure BIC, PVP, and binary BIC-PVP systems were carried out using a Novo-Control Alpha spectrometer, in the frequency range from 10^{-1} Hz to 10^6 Hz and at various temperatures from 173 to 433 K. Instrument was equipped with a temperature controller Quatro operating with an accuracy of 0.1 K. All samples were analyzed directly after quench-cooling preparation using a capacitor made of stainless steel (diameter 15 mm or 10 mm with 0.1 mm gap providing by Teflon spacers). To analyze the kinetics of crystallization, we performed time-dependent measurements at the temperatures: 341 K, 348 K, 350.5 K, 353 K, and 355.5 K in the frequency range from 10^{-1} Hz to 10^6 Hz. Spectra were collected every 10 min.

Fourier transform infrared spectroscopy (FTIR). Infrared measurements were carried out using a Agilent Cary 640 FTIR spectrometer equipped with a standard source and a DTGS Peltier-cooled detector. The spectra have been collected using a GladiATR diamond accessory (Pike Technologies) and analyzed in the $1400\text{--}1800$ cm^{-1} range, which is characteristic for carbonyl spectral regions. All spectra were accumulated with a spectral resolution of 4 cm^{-1} and recorded by accumulation of 16 scans.

Apparent solubility studies. The equilibrium apparent solubility of BIC in water was determined using the shake-flask method. An excess amount of BIC or binary BCL-PVP systems was added to 25 mL of water in a conical flasks and shaken for 24 h at room temperature using a KS 130 Basic orbital shaker (IKA, Germany). After centrifugation at 3600 rpm for 30 min in the MPW 221 apparatus (MPW, Poland), the samples were filtered through a 0.2 μm PTFE filter (ChemLand, Poland) and diluted with the solvent. The amount of the drug in samples was determined spectrophotometrically at 270 nm using a UV-VIS spectrophotometer UV 1800 (Shimadzu, Japan). All measurements were performed in triplicate.

Dissolution studies. The dissolution of BIC and BIC-PVP mixtures was performed in the automated pharmacopoeial paddle dissolution apparatus using the method recommended by the FDA (Food and Drug Administration) for tablets. The dissolution tests were carried out in 1000 mL of water with 1% SLS at a temperature of 37 ± 0.5 $^{\circ}\text{C}$ in the VisionElite 8 dissolution test station (Hanson Research, USA) connected to VisionG2 Autosampler AutoPlus. The paddle speed was set at 50 rpm. A certain amount of binary mixture and drug alone, equivalent to 50 mg of BIC, were placed into the beakers. The 5 mL of samples were withdrawn from the dissolution vessel

through the polyethylene filter (0.1 μm) at predetermined time intervals 5, 15, 30, 45, and 60 min. The equal volume of fresh dissolution medium was replaced. The amount of dissolved drug was determined spectrophotometrically at 272 nm as described earlier. The amount of drug dissolved over time in percentage as well as standard deviation were calculated.

RESULTS AND DISCUSSION

Thermal properties of pure BIC. Figure 2 presents the DSC thermograms obtained during heating (rate 10 K/min) of

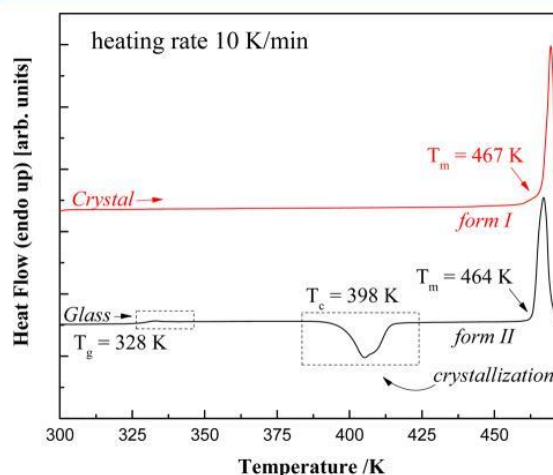


Figure 2. DSC thermograms of the crystalline (red line) and amorphous (black line) forms of BIC (data vertically displaced).

crystalline and amorphous BIC samples. The upper thermogram measured for crystalline BIC exhibits only a well resolved endothermic peak at $T = 467$ K, which corresponds to the melting point of the investigated material. The bottom DSC thermogram, obtained for amorphous BIC, revealed several additional thermal effects. At $T = 328$ K an endothermic event corresponding to the glass transition is visible. One can see that further heating leads to sample recrystallization manifested by the cold crystallization exotherm in the range from 398 to 415 K. Consequently, melting of the recrystallized substance was observed at $T_m = 464$ K. Furthermore, the melting temperatures observed for crystalline and recrystallized samples were different, indicating the presence of distinct polymorphic forms of BIC, which is consistent with literature data.^{30,31} The observed nonisothermal cold crystallization phenomenon clearly indicates that amorphous BIC is physically unstable and tends to recrystallize after heating above T_g .

Molecular dynamics of pure BIC in the supercooled liquid state. There are several factors that can influence a tendency to recrystallize amorphous material. Among them molecular mobility is usually reported.^{34,35} To characterize the molecular dynamics of BIC drug at various temperatures, we applied the BDS technique. Figure 3 presents the dielectric spectra obtained for BIC in the supercooled liquid state.

It can be observed that the maximum of the α -process which corresponds to structural relaxation is moving to higher frequencies when temperature increases. It is correlated to the intensified molecular mobility of the BIC sample. Above $T = 359$ K one can see that the dielectric strength, $\Delta\epsilon$, dramatically decreases. Since the $\Delta\epsilon$ value corresponds to the

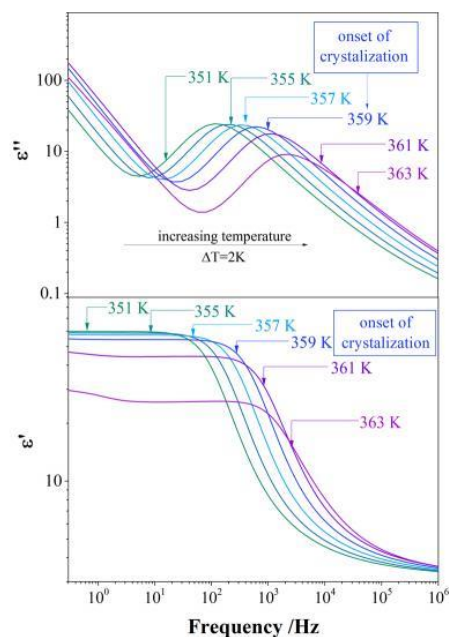


Figure 3. Representative ambient pressure dielectric loss (upper panel) and dispersion (lower panel) spectra of BIC registered above T_g .

number of particles involved in the relaxation process, such a change in peak height indicates the beginning of crystallization. In order to get insight into the mechanism and time-scale of processes responsible for BIC instability, we performed isothermal crystallization studies at ambient pressure conditions. The dielectric spectra registered as a function of time at $T = 350.5$ K are shown in Figure 4. The decrease of spectral intensity with time is visible both at $\epsilon'(f)$ and at $\epsilon''(f)$ spectra. The detailed analysis of crystallization data using the Avrami and Avramov approaches is presented in the Supporting Information section.

To obtain the relaxation time values, we fitted acquired spectra using the Havriliak–Negami function:³⁶

$$\epsilon^*(\omega) = \epsilon_\infty + \frac{\Delta\epsilon}{(1 + (i\omega\tau_{HN})^\alpha)^\beta} \quad (1)$$

where ϵ_∞ denotes the high frequency limit permittivity, $\Delta\epsilon$ is the dielectric strength, and τ_{HN} is a parameter connected to a characteristic relaxation time. The exponents α and β describe the shape of the dielectric loss curves. Information obtained from dielectric data was then used to plot the temperature dependence of the relaxation times τ_ω , as is shown in Figure 5. The relaxation times τ_α were then calculated as follows:

$$\tau_\alpha = \tau_{HN} \left[\sin\left(\frac{\alpha\pi}{2\beta + 2}\right) \right]^{1/\alpha} \left[\sin\left(\frac{\alpha\beta\pi}{2\beta + 2}\right) \right]^{1/\alpha} \quad (2)$$

In a supercooled liquid state, the α -process has non-Arrhenius behavior, which can be well described by the Vogel–Fulcher–Tamman–Hesse (VFTH) equation:^{37–39}

$$\tau_\alpha = \tau_\infty \exp\left(\frac{DT_0}{T - T_0}\right) \quad (3)$$

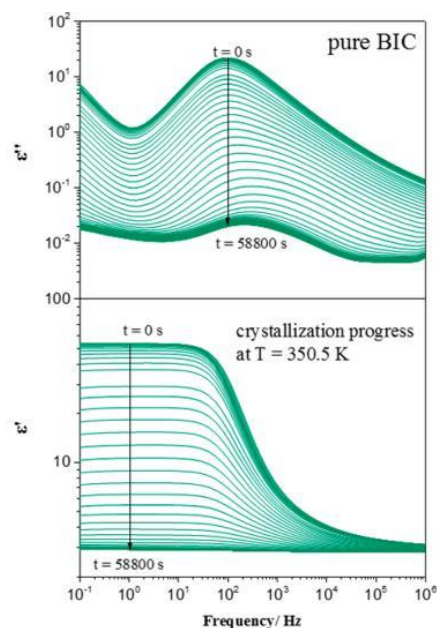


Figure 4. Dielectric spectra of the imaginary (above) and real (below) parts of the complex dielectric permittivity measured under isothermal conditions at $T = 350.5$ K, illustrating the progress of BIC crystallization.

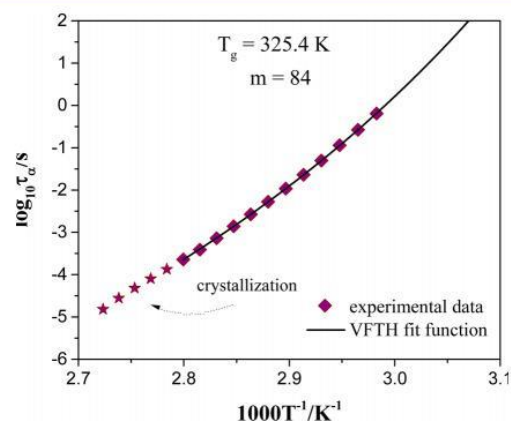


Figure 5. Temperature dependence of structural relaxation times obtained for the BIC sample. Stars indicates the τ_α values determined at temperatures for which the crystallization began to proceed.

where τ_∞ , T_0 , and D denote fitting parameters. Parameter τ_∞ is a pre-exponential factor describing the limiting high-temperature value of τ_α related to the vibrational frequency ($\sim 10^{-11}$ to 10^{-14} s),⁴⁰ parameter D reflects the deviation from the Arrhenius behavior, while T_0 is Vogel temperature, which is related to the state with infinite relaxation time.⁴¹ For neat BIC, the obtained fitting parameters were as follows: $D = 11.4$, $T_0 = 266$ K, $\log \tau_\infty = -16.1$. From the data presented in Figure 5 one can see that the VFTH function fits well the experimental data, but the resultant value of τ_∞ is physically unintelligible. This may indicate that the dynamical behavior of BIC cannot be rightly described by a single set of VFTH parameters. However, due to the narrow range of accessible relaxation

times, the value of the pre-exponential factor being equal to $\sim 10^{-16}$ s was maintained.

Based on these data we calculated T_g and the fragility of the BIC sample. The glass transition temperature, determined as the temperature at which the relaxation time τ_α equals 100 s, was $T_g = 325$ K. This value is in good agreement with T_g obtained from DSC experiments, i.e. 328 K. To acquire information about the fragility of the investigated material, we considered parameter m expressed by the following equation:⁴²

$$m = \left. \frac{d \log \tau_\alpha}{d(T_g/T)} \right|_{T=T_g} = \frac{D(T_0 - T_g)}{(1 - (T_0 - T_g))^2 \ln(10)} \quad (4)$$

The parameter m , known also as the steepness index, is commonly used to classify glass forming materials as “strong” or “fragile”. According to this concept, “strong” glass-formers are characterized by $m \leq 30$ while for “fragile” $m \geq 100$. If the calculated value lies between 30 and 100, we can consider the substance as an intermediate glass-former.⁴³ The value of the m parameter determined for neat BIC equals $m = 84$, which allows classification of this material as an intermediate glass former. In general the term fragility describes the rate with which the molecular dynamics of a material are changing during approaching T_g . Then, the dynamics of fragile samples changes rapidly, whereas the strong ones behave in the opposite way.⁴⁴ Furthermore, the m value reflects the extent of deviation of the $\tau_\alpha(T)$ dependence from Arrhenius-like, which is typical for strong materials. The classification of glass formers as strong and fragile is also relevant in the discussion concerning the possible correlation between the fragility of a material and its recrystallization tendency. Strong materials are usually considered as less susceptible to crystallization. This was explained by Tanaka in the framework of the two-order parameter (TOP) model by their large frustration against crystallization.⁴⁵ On the other hand, the recrystallization behavior of materials with similar fragilities can be distinctly different.⁴⁶ This shows that the tendency to crystallize from the amorphous state is a complex problem, and in some cases, factors other than molecular mobility may govern this effect (e.g., molecular interactions, high specific surface area, crystalline defects, amorphization route).^{47–50}

Usually in the amorphous state the time distribution of molecular relaxation times does not have a simple exponential pattern and observed asymmetry can be well described by the Kohlraush–Williams–Watts equation (KWW):⁵¹

$$\Phi(t) = \exp \left[- \left(\frac{t}{\tau_\alpha} \right)^{\beta_{\text{KWW}}} \right] \quad (5)$$

The value of the stretching parameter β_{KWW} ($0 < \beta_{\text{KWW}} \leq 1$) reflects the deviation of the shape of the α -relaxation process from the Debye-like behavior (then $\beta_{\text{KWW}} = 1$). The β_{KWW} value determined for the spectrum registered at $T = 343$ K for BIC drug was equal to 0.85. Furthermore, when we horizontally shifted the dielectric spectra registered at various temperatures (i.e., 343–357 K) toward the spectrum at $T = 343$ K, we observed that the temperature does not influence the shape of the α -process significantly (see Figure 6). Since the stretching parameter β_{KWW} expresses the distribution of relaxation times, it can also characterize the degree of cooperativity and the length scale of dynamic heterogeneity in the investigated material.⁵² The possible relation between physical stability and broadening

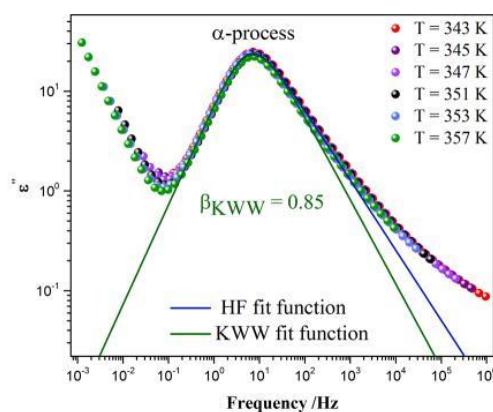


Figure 6. Masterplot constructed for the BIC sample by horizontally shifting of BDS spectra which were measured at various temperatures. The reference spectrum measured at $T = 343$ K is expressed by red circles. The circles represent experimental data points while blue and green solid lines denote HN and KWW fit functions, respectively.

of the α -loss peak was considered by Shamblyn et al.⁵³ The authors suggested that the increasing value of the β_{KWW} parameter correlates with the extended “shelf life” of the amorphous drug. According to this notion, we should be able to predict the stability of a pharmaceutical material from the analysis of the structural relaxation times distribution. Unfortunately, the example of BIC with a large value of the β_{KWW} parameter and a strong recrystallization tendency does not support this claim. The same was reported by Tombari et al.⁵⁴ One can find several other examples of drugs for which the discussed relationship was not satisfied, such as ezetimibe⁹ and sildenafil.⁵⁵

In the literature the value of the β_{KWW} parameter was also discussed in terms of correlation with sample fragility. Böhmer et al. summarized literature data for 70 different samples and found a linear relationship between fragility and the β_{KWW} value.⁴² This relation was expressed by the following equation: $m_{\text{pred}} = 250(\pm 30) - 320\beta_{\text{KWW}}$. However, so far, many exceptions to this correlation have been uncovered. The here investigated BIC is another example of material for which the above role is not valid. The predicted value of the fragility index $m_{\text{pred}} = 22 \pm 30$ was significantly lower than those obtained experimentally.

Prediction of the temperature behavior of BIC structural relaxation times in the glassy state. As was mentioned in previous sections, intensified molecular mobility is often considered as an important factor responsible for the physical instability of different amorphous pharmaceuticals.^{7,56–59} Generally, molecular motions can be divided in terms of their origin into global and local. The α -process observed above T_g describes cooperative intermolecular reorientations, while secondary processes observed below T_g correspond to local motions of intramolecular origin, excluding those classified as Johari–Goldstein relaxation.^{60,61} Despite the considerable work put into explanation of the mutual relationship between mobility and stability of amorphous APIs, an unambiguous opinion of what kind of molecular motions determines the recrystallization behavior at given conditions is still unknown. Currently available results seem to be highly material specific. The stability of different materials in the supercooled liquid state was correlated both with α -

relaxation time^{62–64} as well as with secondary relaxation modes.^{7,35,65} It was also suggested that the α -process can be responsible for sample recrystallization below T_g . In the case of several amorphous APIs, such as celecoxib,⁷ nifedipine,⁶⁶ griseofulvin¹¹ and phenobarbital,⁵⁶ it was shown that the time scale of recrystallization has the same order of magnitude as the value of the structural relaxation time in the glassy state. Thus, τ_α values predicted for the glassy state may help approximate the long-term stability of such amorphous drugs upon storage below T_g .

There are a couple of methods allowed to determine the structural relaxation times deeply in the glassy state. One of them is construction of master curve, where we horizontally shifted the α -loss peak, obtained at a certain temperature higher than T_g , to the glassy region where the α -process is too slow to be experimentally observed. It should be noted that this method can be used only when the shape of the α -process is nearly insensitive to temperature, which actually is true in the case of the investigated sample. Such analysis enables prediction of the temperature behavior of α -relaxation times in the glassy state. Another method frequently applied to estimate α -relaxation times below T_g is the modified Adam and Gibbs model. As was shown by Hodge,⁶⁷ the temperature dependence of structural relaxation times can be predicted from the following formula:

$$\tau_\alpha(T, T_f) = \tau_\infty \exp\left(\frac{D}{T(1 - T_0/T_f)}\right) \quad (6)$$

where τ_∞ , D , and T_0 are parameters obtained from the VFTH equation while T_f is a fictive temperature defined as follows:

$$\frac{1}{T_f} = \frac{\gamma C_p}{T_g} + \frac{1 - \gamma C_p}{T} \quad (7)$$

The fictive temperature was proposed by Tool and Eichlin⁶⁸ as an “equilibrium temperature”. The authors described T_f as a temperature where the nonequilibrium value characterizing the macroscopic property will achieve the equilibrium value.⁶⁷ The γC_p in the above formula is a thermodynamic parameter which can be described as

$$\gamma C_p = \left. \frac{C_p^{liq} - C_p^{glass}}{C_p^{liq} - C_p^{cryst}} \right|_{T=T_g} \quad (8)$$

To determine the heat capacity (C_p) of liquid, glassy, and crystalline BIC, we performed DSC measurements. The inset in Figure 7 shows collected thermograms. The obtained heat capacity values for liquid, glassy, and crystalline samples were $C_p^{liq} = 1.70$ J/gK, $C_p^{glass} = 1.23$ J/gK, and $C_p^{cryst} = 1.20$ J/gK, respectively.

We used both methods to find out theoretical τ_α values and predict the temperature dependence of τ_α for BIC in the glassy state. These results are depicted in Figure 7. One can compare the τ_α values predicted from the A-G model with those obtained from imposed spectra. Based on the assumption presented in our previous papers⁵² that the time scales of structural relaxation and crystallization in the glassy state are related to each other, we can roughly estimate that at $T = 298$ K the BIC sample should be stable for about 4.5 (from the Adam–Gibbs method) to 5 days (from masterplot predictions), depending on the applied prediction method. Such a

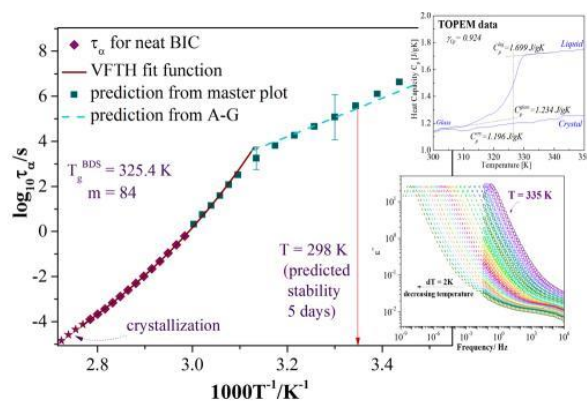


Figure 7. Temperature dependence of structural relaxation times (τ_α) determined from dielectric spectra for the BIC sample (purple squares). The green symbols and blue dashed line represent τ_α values predicted from the so-called master plot method (see bottom inset) and the A-G model, respectively. The upper inset shows the heat capacity obtained from the TOPEM measurements performed near the glass transition temperature for the BIC sample.

result was confirmed by our unaided eye observations performed for the BIC sample stored at room temperature, which indicated that after five and half days the crystallites appear in the investigated material.

Improving stability of BIC by preparation of BIC-PVP mixtures. To overcome one of the longstanding limitations resulting from the application of amorphous pharmaceuticals, i.e. their physical instability and tendency to rapidly convert to the crystalline state, different polymers can be used, for example, polyvinylpyrrolidone (PVP), hydroxypropylmethylcellulose (HPMC), cyclodextrin, etc. A mixture of a drug with a polymer has not only better physical stability but also improved water solubility and bioavailability. Bearing this in mind, we decided to use PVP ($K = 30$) to verify the possibility of improving the physical stability of BIC in the amorphous form.⁶⁹ We prepared mixtures with various BIC-PVP weight ratios, i.e. 10–1, 5–1, 2–1, and 1–2. The DSC thermograms obtained during heating (10 K/min) of pure BIC as well as BIC-PVP mixtures are shown in Figure 8. All prepared samples were characterized by a single T_g which usually refers to homogeneous mixtures. Otherwise, if the components are not miscible with each other, two T_g corresponding to each component should be observed.⁷⁰ For samples mixed in 10–1 and 5–1 BIC-PVP ratios, recrystallization during heating above T_g was still observed, but in the case of samples with higher PVP amount, i.e. mixed in 2–1 and 1–2 ratios, no signs of crystallization were found, indicating that PVP can efficiently improve the stability of the amorphous BIC drug.

The stability enhancement observed for amorphous APIs mixed with various excipients, such as polymers, may be due to the antiplasticizing effect, which can be associated with eventual molecular interactions existing between mixture components or may be the sum of these two effects.^{2,5,26,71–73} The antiplasticizing effect of additive on drug properties relies on slowing down of the dynamics reflected by the higher T_g of the mixture in comparison to pure drug. To predict the T_g of such a binary system, the Gordon–Taylor (GT) equation can be applied:^{74,75}

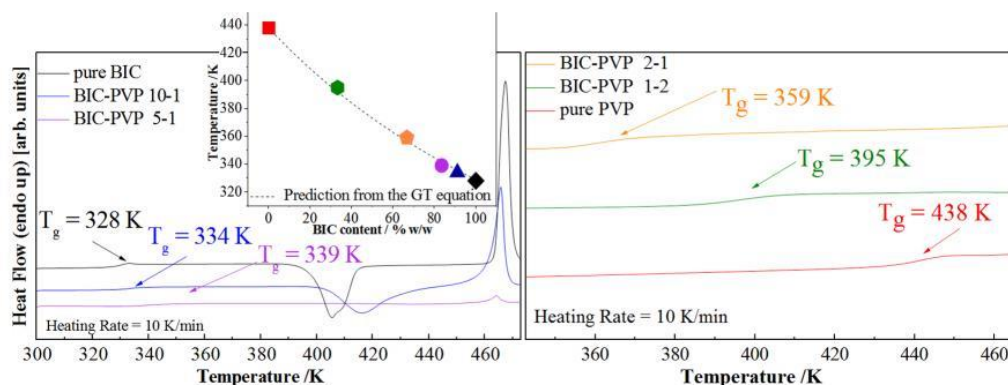


Figure 8. DSC thermograms measured for BIC-PVP mixtures prepared in various weight ratios, i.e. 10–1, 5–1, 2–1, and 1–2, as well as neat mixture components. The inset represents the comparison of theoretical (black dashed line) and experimental T_g values (filled symbols) for all these samples (data vertically displaced).

$$T_g = \frac{w_1 T_{g1} + K w_2 T_{g2}}{w_1 + K w_2} \quad (9)$$

where w_1 and w_2 are component weight ratios, T_{g1} and T_{g2} are glass transition temperatures, and parameter K describes the ratio of changes in heat capacity at a particular T_g .⁷⁶

$$K = \frac{\Delta C_{p2}}{\Delta C_{p1}} \quad (10)$$

To estimate the value of parameter K , we used $\Delta C_p^{BIC} = 0.48$ J/gK for BIC and $\Delta C_p^{PVP} = 0.32$ J/gK for polymer additive. Based on eq 9 and eq 10, we calculated T_g values and compared them to those obtained from experiment. Deviation of experimentally obtained T_g values from those predicted by the GT equation is usually discussed in terms of the strength of the molecular attractions between the solid dispersion components.⁷⁰ The positive deviation of experimental points from the theoretical ones may indicate a strong interaction between both materials. In the case of negative discrepancies, moderate interactions may be involved. When experimental and predicted T_g values are consistent with each other, the presence of interactions or lack of them should be considered.⁷⁷ This is due to the fact that one can find examples of API-polymer systems in which the GT equation predicts well T_g values despite the presence of specific interactions between the mixture components (e.g., nifedipine-PVP, felodipine-PVP, indomethacin-PVP).^{70,78} In the here investigated BIC-PVP system, we observed that the dashed line corresponding to theoretical T_g values coincides well with the experimental data points. Only small deviations within the range 1.5–3 K were found. Thus, to verify the existence of the molecular interactions between sample components, we performed FTIR measurements. We characterized spectra for pure BIC and PVP, and then we analyzed those registered for BIC-PVP mixtures with different drug and polymer content. For amorphous BIC, the following assignments can be done: 3463 cm^{-1} (NH), 3328 cm^{-1} (OH), 1694 cm^{-1} (N–H, C–OH), and 1670 cm^{-1} (C=O). When we look at the structure of PVP and BIC, we can notice that in BIC there are several groups which can act as proton donors or acceptors while PVP can only act as an acceptor through the O or N atoms of the pyrrole ring. However, due to the steric constraints on the nitrogen, the carbonyl group should have a principal role during

the eventual interactions between drug and polymer molecules.⁷⁹ Thus, looking for evidence of molecular attractions between mixture components, we expected shifting of the band corresponding to the stretching vibration of the carbonyl group in the pyrrole ring. Such a characteristic band assigned as $\nu(\text{C}=\text{O})$ is located at 1650 cm^{-1} for pure PVP. Figure 9 (left

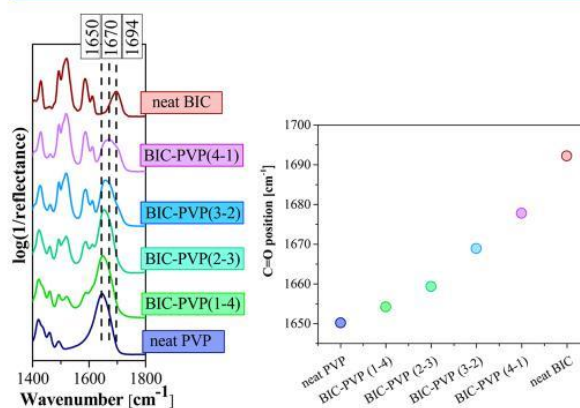


Figure 9. Comparison of carbonyl IR spectral regions (1400–1800 cm^{-1}) for BIC, PVP, and BIC-PVP mixtures with different drug and polymer ratios. On the right side are shown the changes in position of the C=O band for measured samples.

panel) shows the comparison of the carbonyl spectral regions (1400–1800 cm^{-1}) for BIC, PVP, and BIC-PVP mixtures with different drug and polymer ratios. One can see that the addition of PVP leads to a gradual decrease of the band visible at 1694 cm^{-1} for pure BIC and the appearance of a new IR band, clearly indicating the presence of PVP. For samples with lower polymer content, these bands overlapped each other. Consequently, for BIC-PVP (1–2) sample, one can see the broad band with a maximum at 1670 cm^{-1} , with a characteristic shoulder at the higher wavenumber side. With increasing content of polymer, the shoulder becomes less visible while the peak maximum starts shifting into lower wavenumbers (right panel of Figure 9), indicating growing strength of H-bonding attractions between BIC and polymer additive. This means that the improved stability of BIC-PVP binary mixtures may be

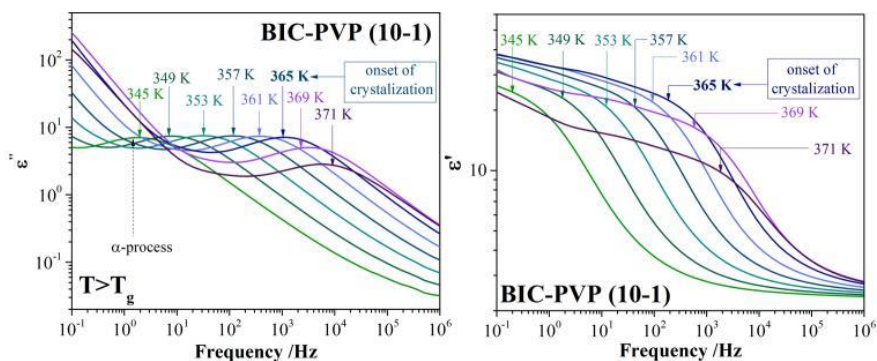


Figure 10. Dielectric absorption (left) and dispersion (right) spectra of a binary BIC-PVP mixture (10–1 weight ratio).

related to both the antiplasticizing effect of the polymer as well as specific attractions between sample components.

To get deeper insight into the molecular mobility of the BIC-PVP binary system, we measured dielectric spectra for the sample mixed in a 10–1 weight ratio. The large conductivity contribution observed for other mixtures covering the structural relaxation peak would hinder data analysis for the rest of the samples. Dielectric spectra obtained for the 10–1 BIC-PVP sample are presented in Figure 10. One can see that crystallization, manifested by the drop of $\Delta\epsilon$, occurs at higher temperature than in the case of neat BIC. As previously, we analyzed dielectric data in terms of the HN equation and described the temperature dependence of the structural relaxation times with the VFTH equation. The obtained temperature dependence of τ_α for a binary mixture is shifted to higher temperatures in comparison to pure BIC, confirming slowing down of molecular dynamics. The higher value of T_g and the lower fragility in comparison to pure drug, i.e. $T_g = 323$ K and $m = 74$, may indicate enhanced stability of the BIC-PVP mixture. To verify this, we predicted the values of α -relaxation times in a glassy state for 10–1 BIC-PVP sample, as was previously done for pure BIC. Indeed, the predicted α -relaxation time at room temperature was definitely longer (see Figure 11) and indicated that the stability of the material should be maintained for almost 2 months.

The question is what will be the predicted stability of material containing more polymer additive for which no recrystallization was observed in DSC studies. Unfortunately, because of a very large contribution of dc-conductivity after mixing BIC with PVP in the ratio 2–1, we were unable to determine the values of τ_α from standard analysis of dielectric spectra. Despite this, we put some effort into predicting the temperature dependence of the α -relaxation time for this mixture. First, we determined the value of τ_α at room temperature from DSC measurements (see the green star point in Figure 11). Next we shifted horizontally the experimental $\tau_\alpha(T)$ curve for BIC-PVP 10–1 to superimpose it into this single data point obtained from DSC measurements. Obviously our procedure provides only a very rough estimation of τ_α at room temperature of BIC-PVP 2–1 but it can be seen that the stability time is found to be extremely long; on the order of a hundred years. As already mentioned in the literature, one can find several examples demonstrating the existence of a correlation between the characteristic recrystallization time and the predicted time-scales of global relaxations below T_g . Grzybowska et al. found that the maximal rate of celecoxib recrystallization, determined from the X-ray diffrac-

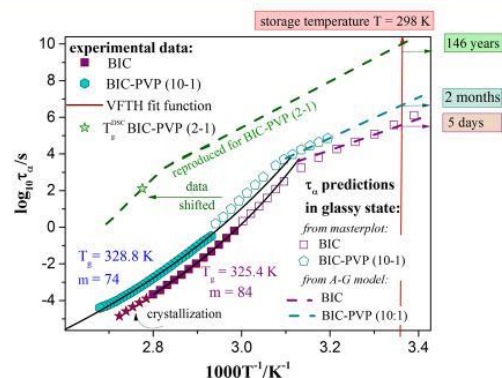


Figure 11. Comparison of the temperature dependence of the structural relaxation times (τ_α) determined from dielectric spectra for pure BIC and a BIC-PVP (10–1) mixture. The filled symbols correspond to experimental data, open symbols represent τ_α values obtained from master plot predictions, while dashed lines indicate τ_α values predicted from the AG model. To approximate the time scale of the molecular mobility for samples with higher polymer content, the data for the BIC-PVP (2–1) sample were reproduced (green symbol, green dashed line).

tion analysis of crystallization degree as a function of storage time, corresponds well with the structural relaxation time at $T = 293$ K found from master plot predictions.⁷ The insightful study performed by Mehta et al. for celecoxib and indomethacin samples indicates the parallel relationship between crystallization and α -relaxation times in the super-cooled liquid state. In the glassy state the crystallization time-scale was found to correlate better with secondary JG-relaxations.⁸⁰

Apparent solubility and dissolution rate of BIC-PVP mixtures. We determined the apparent water solubility for pure BIC in crystalline and amorphous form as well as for BIC-PVP mixtures prepared in different ratios, i.e. 10–1 and 2–1. Our results are presented in Figure 12 (bottom panel). As can be seen, the addition of PVP significantly improved the apparent solubility of the BIC sample, which becomes higher with increasing polymer content. The determined water solubility changed from ~ 5 mg/L for amorphous BIC to even ~ 140 mg/L for the BIC-PVP 2–1 sample. Furthermore, we investigated the influence of PVP on the dissolution rate profiles of BIC (upper panel in Figure 12). The dissolution profiles revealed that the fastest dissolution rate can be observed for the BIC-PVP sample mixed in a 2–1 ratio. After

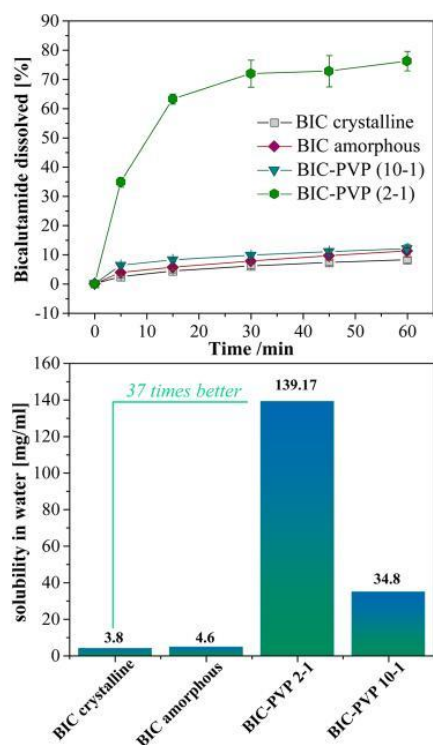


Figure 12. Dissolution rate profiles (upper panel) and apparent water solubility (bottom panel) determined for BIC in crystalline and amorphous form as well as for BIC-PVP samples prepared at various weight ratios (i.e., 2–1 and 10–1).

60 min the amount of dissolved drug was approximately 8-times greater than in the case of drug alone, irrespective of its crystalline or amorphous form. In the case of BIC-PVP samples containing only 10% of PVP carrier, its influence on the dissolution process was not identified.

CONCLUSIONS

In this paper we analyzed the molecular mobility and physical stability of supercooled BIC using the BDS technique. Based on obtained dielectric spectra, we estimated sample T_g , fragility, and β_{KWW} values. The low stability of amorphous BIC and its large ability to recrystallize were confirmed in performed BDS and DSC studies. The stability of the drug in the amorphous form is crucial from a pharmaceutical point of view because it affects the drug formulation and storage process. To improve the stability of BIC, we prepared mixtures of BIC and polymer—polyvinylpyrrolidone. Based on the DSC results, we concluded that 30% addition of PVP efficiently stabilized the BIC drug in the amorphous form. We observed the downturn of molecular dynamics in binary mixtures, which is manifested by a higher glass transition temperature of the BIC-PVP samples. This effect was most likely responsible for improved stability of amorphous BIC-PVP mixtures. Furthermore, the FTIR revealed the existence of specific interactions between both components, which may also affect the recrystallization behavior of BIC-PVP mixtures. We applied the BDS technique to predict how long pure BIC and BIC-PVP mixtures will be stable during storage at room temperature. From the performed analysis we obtained that amorphous BIC remains stable for 5

days, while for a BIC-PVP 10–1 mixture the stability is prolonged to 2 months. We approximate that for BIC-PVP 2–1 such time will be extended to 145 years. DSC results indicate that such a mixture will not have a tendency to recrystallize during heating above T_g . This clearly shows that addition of PVP drastically improved the physical stability of BIC. Moreover, we determined the apparent water solubilities of pure BIC and BIC-PVP mixtures in the ratios 10–1 and 2–1. We did not observe meaningful differences in solubility of neat amorphous samples while for mixtures a significant increase of apparent solubility was observed. An addition of 30% PVP improved solubility up to approximately 140 mg/L. At the same time the dissolution rate was also significantly enhanced. Our results clearly indicate that PVP can successfully stabilize the BIC sample. Such BIC-PVP mixtures have better solubility and extended storage time, which make them useful in the pharmaceutical industry.

ASSOCIATED CONTENT

Supporting Information

The Supporting Information is available free of charge on the ACS Publications website at DOI: 10.1021/acs.molpharmaceut.6b01007.

Kinetics of crystallization of neat BIC in the supercooled liquid state, isothermal crystallization of BIC at various temperatures, and comparison of calculated parameters characterizing the kinetics of BIC crystallization according to the Avrami and Avramov models (PDF)

AUTHOR INFORMATION

Corresponding Author

*E-mail: marzena.rams-baron@us.edu.pl.

ORCID

Marzena Rams-Baron: 0000-0001-8808-8067

Notes

The authors declare no competing financial interest.

ACKNOWLEDGMENTS

The authors acknowledge Polish National Science Centre for the financial support (grant Symfonia 3 no 2015/16/W/NZ7/00404).

REFERENCES

- (1) Siegel, R.; Naishadham, D.; Jemal, A. *Cancer Statistics*, 2012. *Ca-Cancer J. Clin.* **2012**, *62*, 10–29.
- (2) Furr, B. J. A.; Tucker, H. The preclinical development of bicalutamide: Pharmacodynamics and mechanism of action. *Urology* **1996**, *47* (1 SUPPL. A), 13–25.
- (3) Semenas, J.; Dizely, N.; Persson, J. L. Enzalutamide as a second generation antiandrogen for treatment of advanced prostate cancer. *Drug Des., Dev. Ther.* **2013**, *7*, 875–881.
- (4) Bassetto, M.; Ferla, S.; Pertusati, F.; Kandil, S.; Westwell, A. D.; Brancale, A.; McGuigan, C. Design and synthesis of novel bicalutamide and enzalutamide derivatives as antiproliferative agents for the treatment of prostate cancer. *Eur. J. Med. Chem.* **2016**, *118*, 230–243.
- (5) Cockshott, I. D. *Clin. Pharmacokin.* **2004**, *43* (13), 855–878.
- (6) Kanfer, I. Report on the International Workshop on the Biopharmaceutics Classification System (BCS): Scientific and regulatory aspects in practice. *J. Pharm. Pharm. Sci.* **2002**, *5* (1), 1–4.
- (7) Grzybowska, K.; Paluch, M.; Grzybowski, a; Wojnarowska, Z.; Hawelek, L.; Kolodziejczyk, K.; Ngai, K. L. Molecular dynamics and physical stability of amorphous anti-inflammatory drug: celecoxib. *J. Phys. Chem. B* **2010**, *114* (40), 12792–12801.

- (8) Wojnarowska, Z.; Grzybowska, K.; Hawelek, L.; Dulski, M.; Wrzalik, R.; Gruszka, I.; Paluch, M.; Pienkowska, K.; Sawicki, W.; Bujak, P.; et al. Molecular dynamics, physical stability and solubility advantage from amorphous indapamide drug. *Mol. Pharmaceutics* **2013**, *10* (10), 3612–3627.
- (9) Knapik, J.; Wojnarowska, Z.; Grzybowska, K.; Hawelek, L.; Sawicki, W.; Wlodarski, K.; Markowski, J.; Paluch, M. Physical stability of the amorphous anticholesterol agent (ezetimibe): the role of molecular mobility. *Mol. Pharmaceutics* **2014**, *11* (11), 4280–4290.
- (10) Taylor, M. J.; Tanna, S.; Sahota, T. In vivo study of a polymeric glucose-sensitive insulin delivery system using a rat model. *J. Pharm. Sci.* **2010**, *99* (10), 4215–4227.
- (11) Zhou, D.; Zhang, G. G. Z.; Law, D.; Grant, D. J. W.; Schmitt, E. A. Thermodynamics, molecular mobility and crystallization kinetics of amorphous griseofulvin. *Mol. Pharmaceutics* **2008**, *5* (6), 927–936.
- (12) Descamps, M.; Dudognon, E. Crystallization from the amorphous state: Nucleation-growth decoupling, polymorphism interplay, and the role of interfaces. *J. Pharm. Sci.* **2014**, *103* (9), 2615–2628.
- (13) Wu, T.; Yu, L. Origin of enhanced crystal growth kinetics near T_g probed with indomethacin polymorphs. *J. Phys. Chem. B* **2006**, *110* (32), 15694–15699.
- (14) Ediger, M. D.; Harrowell, P.; Yu, L. Crystal growth kinetics exhibit a fragility-dependent decoupling from viscosity. *J. Chem. Phys.* **2008**, *128* (3), 1–6.
- (15) Grzybowska, K.; Paluch, M.; Wlodarczyk, P.; Grzybowski, A.; Kaminski, K.; Hawelek, L.; Zakowiecki, D.; Kasprzycka, A.; Jankowska-Sumara, I. Enhancement of amorphous celecoxib stability by mixing it with octaacetylmaltose: The molecular dynamics study. *Mol. Pharmaceutics* **2012**, *9* (4), 894–904.
- (16) Kaminska, E.; Adrjanowicz, K.; Tarnacka, M.; Kolodziejczyk, K.; Dulski, M.; Mapesa, E. U.; Zakowiecki, D.; Hawelek, L.; Kaczmarczyk-Sedlak, I.; Kaminski, K. Impact of inter- and intramolecular interactions on the physical stability of indomethacin dispersed in acetylated saccharides. *Mol. Pharmaceutics* **2014**, *11* (8), 2935–2947.
- (17) Backensfeld, T.; Müller, B. W.; Wiese, M.; Seydel, J. K. Effect of Cyclodextrin Derivatives on Indomethacin Stability in Aqueous Solution. *Pharm. Res.* **1990**, *07*, 484–490.
- (18) Knapik, J.; Wojnarowska, Z.; Grzybowska, K.; Jurkiewicz, K.; Tajber, L.; Paluch, M. Molecular Dynamics and Physical Stability of Coamorphous Ezetimib and Indapamide Mixtures. *Mol. Pharmaceutics* **2015**, *12* (10), 3610–3619.
- (19) Yamamura, S.; Gotoh, H.; Sakamoto, Y.; Momose, Y. Physicochemical properties of amorphous salt of cimetidine and diflunisal system. *Int. J. Pharm.* **2002**, *241* (2), 213–221.
- (20) Löbmann, K.; Laitinen, R.; Grohgan, H.; Gordon, K. C.; Strachan, C.; Rades, T. Coamorphous drug systems: Enhanced physical stability and dissolution rate of indomethacin and naproxen. *Mol. Pharmaceutics* **2011**, *8* (5), 1919–1928.
- (21) Knapik, J.; Wojnarowska, Z.; Grzybowska, K.; Jurkiewicz, K.; Stankiewicz, A.; Paluch, M. Stabilization of the Amorphous Ezetimibe Drug by Confining Its Dimension. *Mol. Pharmaceutics* **2016**, *13* (4), 1308–1316.
- (22) Watanabe, T.; Wakiyama, N.; Usui, F.; Ikeda, M.; Isobe, T.; Senna, M. Stability of amorphous indomethacin compounded with silica. *Int. J. Pharm.* **2001**, *226* (1–2), 81–91.
- (23) Bahl, D.; Bogner, R. H. Amorphization of indomethacin by co-grinding with Neusilin US2: Amorphization kinetics, physical stability and mechanism. *Pharm. Res.* **2006**, *23* (10), 2317–2325.
- (24) Kawabata, Y.; Wada, K.; Nakatani, M.; Yamada, S.; Onoue, S. Formulation design for poorly water-soluble drugs based on biopharmaceutics classification system: Basic approaches and practical applications. *Int. J. Pharm.* **2011**, *420* (1), 1–10.
- (25) Palermo, R. N.; Anderson, C. A.; Drennen, J. K. Review: Use of thermal, diffraction, and vibrational analytical methods to determine mechanisms of solid dispersion stability. *J. Pharm. Innov.* **2012**, *7* (1), 2–12.
- (26) Baghel, S.; Cathcart, H.; O'Reilly, N. J. Polymeric Amorphous Solid Dispersions: A Review of Amorphization, Crystallization, Stabilization, Solid-State Characterization, and Aqueous Solubilization of Biopharmaceutical Classification System Class II Drugs. *J. Pharm. Sci.* **2016**, *105* (9), 2527–2544.
- (27) Adrjanowicz, K.; Grzybowska, K.; Kaminski, K.; Hawelek, L.; Paluch, M.; Zakowiecki, D. Comprehensive studies on physical and chemical stability in liquid and glassy states of telmisartan (TEL): solubility advantages given by cryomilled and quenched material. *Philos. Mag.* **2011**, *91* (13), 1926–1948.
- (28) (Cmpmp) Guideline on Stability Testing: Stability Testing of Existing Active Substances and Related Finished Products. *Eur. Med. Agency Insp.* 2004, No. December 2003, 1–18.
- (29) James, K. D.; Ekwuribe, N. N. Syntheses of enantiomerically pure (R)- and (S)-bicalutamide. *Tetrahedron* **2002**, *58* (29), 5905–5908.
- (30) Inui, M.; Ueda, M. Structure Determination of Bicalutamide Polymorphic Forms by Powder X-ray Diffraction: Case Studies Using Density Functional Theory Calculations and Rietveld Refinement **2008**, 1–10.
- (31) Nanduri, V. V. S. S. R.; Adapa, V. S. S. P.; Kura, R. R. Development and validation of stability-indicating HPLC and UPLC methods for the determination of bicalutamide. *J. Chromatogr. Sci.* **2012**, *50* (4), 316–323.
- (32) DSC Calibration, Temperature and Heat Flow. http://www.mt.com/my/en/home/supportive_content/matchar_apps/MatChar_HB805.html.
- (33) DSC Calibration, Heating Rate Independence. http://www.mt.com/in/en/home/supportive_content/matchar_apps/MatChar_HB804.html.
- (34) Zhou, D.; Zhang, G. G. Z.; Law, D.; Grant, D. J. W.; Schmitt, E. A. Physical stability of amorphous pharmaceuticals: Importance of configurational thermodynamic quantities and molecular mobility. *J. Pharm. Sci.* **2002**, *91* (8), 1863–1872.
- (35) Bhattacharya, S.; Suryanarayanan, R. Local Mobility in Amorphous Pharmaceuticals-Characterization and Implications on Stability. *J. Pharm. Sci.* **2009**, *98* (9), 2935–2953.
- (36) Havriliak, S.; Negami, S. A complex plane representation of dielectric and mechanical relaxation processes in some polymers. *Polymer* **1967**, *8*, 161–210.
- (37) Vogel, H. Das temperaturabhängigkeitsgesetz der viskosität von flüssigkeiten. *J. Phys. Z.* **1921**, *22*, 645–646.
- (38) Fulcher, G. S. Analysis of recent measurements of the viscosity of glasses. *J. Am. Ceram. Soc.* **1925**, *8*, 789–794.
- (39) Tammann, G.; Hesse, W.; Die Abhängigkeit. der Viskosität von der Temperatur bei unterkühlten Flüssigkeiten. *Zeitschrift für Anorg. und Allg. Chemie* **1926**, *156* (1), 245–257.
- (40) Rodrigues, A. C.; Viciosa, M. T.; Danede, F.; Affouard, F.; Correia, N. T. Molecular mobility of amorphous S-flurbiprofen: A dielectric relaxation spectroscopy approach. *Mol. Pharmaceutics* **2014**, *11* (1), 112–130.
- (41) Metatla, N.; Soldera, A. The Vogel-Fulcher-Tamman equation investigated by atomistic simulation with regard to the Adam-Gibbs model. *Macromolecules* **2007**, *40* (26), 9680–9685.
- (42) Böhmer, R.; Ngai, K. L.; Angell, C. A.; Plazek, D. J. Nonexponential relaxations in strong and fragile glass formers. *J. Chem. Phys.* **1993**, *99* (5), 4201–4209.
- (43) Angell, C. A. *J. Non-Cryst. Solids* **1991**, *133*, 13–31.
- (44) Hodge, I. M. Strong and fragile liquids — a brief critique. *J. Non-Cryst. Solids* **1996**, *202* (1–2), 164–172.
- (45) Tanaka, H. Relationship among glass-forming ability, fragility, and short-range bond ordering of liquids. *J. Non-Cryst. Solids* **2005**, *351* (8–9), 678–690.
- (46) Rams-Baron, M.; Wojnarowska, Z.; Grzybowska, K.; Dulski, M.; Knapik, J.; Jurkiewicz, K.; Smolka, W.; Sawicki, W.; Ratuszna, A.; Paluch, M. Toward a Better Understanding of the Physical Stability of Amorphous Anti-Inflammatory Agents: The Roles of Molecular Mobility and Molecular Interaction Patterns. *Mol. Pharmaceutics* **2015**, *12* (10), 3628–3638.

- (47) Bhugra, C.; Pikal, M. J. Role of Thermodynamic, Molecular, and Kinetic Factors in Crystallization From the Amorphous State. *J. Pharm. Sci.* **2008**, *97* (4), 1329–1349.
- (48) Yoshioka, M.; Hancock, B. C.; Zografi, G. Crystallization of Indomethacin from the Amorphous State below and above Its Glass Transition Temperature. *J. Pharm. Sci.* **1994**, *83* (12), 1700–1705.
- (49) Gupta, M. K.; Vanwert, A.; Bogner, R. H. Formation of physically stable amorphous drugs by milling with Neusilin. *J. Pharm. Sci.* **2003**, *92* (3), 536–551.
- (50) Surana, R.; Pyne, A.; Suryanarayanan, R. Effect of preparation method on physical properties of amorphous trehalose. *Pharm. Res.* **2004**, *21* (7), 1167–1176.
- (51) Williams, G.; Watts, D. C. Non-symmetrical dielectric relaxation behaviour arising from a simple empirical decay function. *Trans. Faraday Soc.* **1970**, *66* (1), 80–85.
- (52) Grzybowska, K.; Capaccioli, S.; Paluch, M. Recent developments in the experimental investigations of relaxations in pharmaceuticals by dielectric techniques at ambient and elevated pressure. *Adv. Drug Delivery Rev.* **2016**, *100*, 158–182.
- (53) Shamblyn, S. L.; Hancock, B. C.; Dupuis, Y.; Pikal, M. J. Interpretation of relaxation time constants for amorphous pharmaceutical systems. *J. Pharm. Sci.* **2000**, *89* (3), 417–427.
- (54) Tombari, E.; Ferrari, C.; Johari, G. P.; Shanker, R. M. Calorimetric relaxation in pharmaceutical molecular glasses and its utility in understanding their stability against crystallization. *J. Phys. Chem. B* **2008**, *112* (35), 10806–10814.
- (55) Kolodziejczyk, K.; Paluch, M.; Grzybowska, K.; Grzybowski, A.; Wojnarowska, Z.; Hawelek, L.; Ziolo, J. D. Relaxation dynamics and crystallization study of sildenafil in the liquid and glassy states. *Mol. Pharmaceutics* **2013**, *10* (6), 2270–2282.
- (56) Aso, Y.; Yoshioka, S.; Kojima, S. Molecular Mobility-Based Estimation of the Crystallization Rates of Amorphous Nifedipine and Phenobarbital in Poly(vinylpyrrolidone) Solid Dispersions. *J. Pharm. Sci.* **2004**, *93* (2), 384–391.
- (57) Bhugra, C.; Rambhatla, S.; Bakri, A.; Duddu, S. P.; Miller, D. P.; Pikal, M. J.; Lechuga-Ballesteros, D. Prediction of the onset of crystallization of amorphous sucrose below the calorimetric glass transition temperature from correlations with mobility. *J. Pharm. Sci.* **2007**, *96* (5), 1258–1269.
- (58) Bhardwaj, S. P.; Suryanarayanan, R. Molecular mobility as an effective predictor of the physical stability of amorphous trehalose. *Mol. Pharmaceutics* **2012**, *9* (11), 3209–3217.
- (59) Kothari, K.; Ragoonanan, V.; Suryanarayanan, R. Influence of molecular mobility on the physical stability of amorphous pharmaceuticals in the supercooled and glassy states. *Mol. Pharmaceutics* **2014**, *11* (9), 3048–3055.
- (60) Johari, G. P. Intrinsic mobility of molecular glasses. *J. Chem. Phys.* **1973**, *58* (4), 1766–1770.
- (61) Johari, G. P.; Goldstein, M. Viscous Liquids and the Glass Transition. II. Secondary Relaxations in Glasses of Rigid Molecules. *J. Chem. Phys.* **1970**, *53* (6), 2372–2388.
- (62) Bhardwaj, S. P.; Arora, K. K.; Kwong, E.; Templeton, A.; Clas, S.-D.; Suryanarayanan, R. Correlation between molecular mobility and physical stability of amorphous itraconazole. *Mol. Pharmaceutics* **2013**, *10* (2), 694–700.
- (63) Dantuluri, A. K. R.; Amin, A.; Puri, V.; Bansal, A. K. *Mol. Pharmaceutics* **2011**, *8*, 814–822.
- (64) Swallen, S. F.; Ediger, M. D. Self-diffusion of the amorphous pharmaceutical indomethacin near T_g. *Soft Matter* **2011**, *7* (21), 10339–10344.
- (65) Alie, J.; Menegotto, J.; Cardon, P.; Duplaa, H.; Caron, A.; Lacabanne, C.; Bauer, M. Dielectric Study of the Molecular Mobility and the Isothermal Crystallization Kinetics of an Amorphous Pharmaceutical Drug Substance. *J. Pharm. Sci.* **2004**, *93* (1), 218–233.
- (66) Aso, Y.; Yoshioka, S.; Kojima, S. Explanation of the crystallization rate of amorphous nifedipine and phenobarbital from their molecular mobility as measured by ¹³C nuclear magnetic resonance relaxation time and the relaxation time obtained from the heating rate dependence of the glass tr. *J. Pharm. Sci.* **2001**, *90* (6), 798–806.
- (67) Hodge, I. M. Effects of annealing and prior history on enthalpy relaxation in glassy polymers. 6. Adam-Gibbs Formulation of Nonlinearity. *Macromolecules* **1987**, *20*, 2997–2908.
- (68) Tool, A. Q.; Eichlin, C. G. Variations Caused in the Heating Curves of Glass By Heat Treatment I. *J. Am. Ceram. Soc.* **1931**, *14* (4), 276–308.
- (69) Ren, F.; Jing, Q.; Tang, Y.; Shen, Y.; Chen, J.; Gao, F.; Cui, J. Characteristics of bicalutamide solid dispersions and improvement of the dissolution. *Drug Dev. Ind. Pharm.* **2006**, *32* (8), 967–972.
- (70) Baird, J. A.; Taylor, L. S. Evaluation of amorphous solid dispersion properties using thermal analysis techniques. *Adv. Drug Delivery Rev.* **2012**, *64* (5), 396–421.
- (71) Van den Mooter, G.; Wuyts, M.; Blaton, N.; Busson, R.; Grobet, P.; Augustijns, P.; Kinget, R. Physical stabilisation of amorphous ketoconazole in solid dispersions with polyvinylpyrrolidone K25. *Eur. J. Pharm. Sci.* **2001**, *12* (3), 261–269.
- (72) Riggleman, R. A.; Douglas, J. F.; De Pablo, J. J. Characterization of the potential energy landscape of an antiplasticized polymer. *Phys. Rev. E - Stat. Nonlinear, Soft Matter Phys.* **2007**, *76* (1), 1–8.
- (73) Riggleman, R. A.; Yoshimoto, K.; Douglas, J. F.; De Pablo, J. J. Influence of confinement on the fragility of antiplasticized and pure polymer films. *Phys. Rev. Lett.* **2006**, *97* (4), 1–4.
- (74) Kelley, F. N.; Bueche, F. Viscosity and glass temperature relations for polymer-diluent systems. *J. Polym. Sci.* **1961**, *50*, 549–556.
- (75) Gordon, M.; Taylor, J. S. Ideal copolymers and the second-order transitions of synthetic rubbers. i. non-crystalline copolymers. *J. Appl. Chem.* **1952**, *2* (9), 493–500.
- (76) Couchman, P. R.; Karasz, F. E. A Classical Thermodynamic Discussion of the Effect of Composition on Glass-Transition Temperatures. *Macromolecules* **1978**, *11* (1), 117–119.
- (77) Lu, X.; Weiss, A. R. Relationship between the Glass Transition Temperature and the Interaction Parameter of Miscible Binary Polymer Blends. *Macromolecules* **1992**, *25*, 3242–3246.
- (78) Marsac, P. J.; Konno, H.; Taylor, L. S. A comparison of the physical stability of amorphous felodipine and nifedipine systems. *Pharm. Res.* **2006**, *23* (10), 2306–2316.
- (79) Taylor, L. S.; Zografi, G. Spectroscopic characterization of interactions between PVP and indomethacin in amorphous molecular dispersions. *Pharm. Res.* **1997**, *14*, 1691–1698.
- (80) Mehta, M.; Ragoonanan, V.; McKenna, G. B.; Suryanarayanan, R. Correlation between Molecular Mobility and Physical Stability in Pharmaceutical Glasses. *Mol. Pharmaceutics* **2016**, *13* (4), 1267–1277.

A2. J. Pacułt (Szczurek), M. Rams-Baron, B. Chrzęszcz, R. Jachowicz, M. Paluch, *Effect of Polymer Chain Length on the Physical Stability of Amorphous Drug–Polymer Blends at Ambient Pressure*, Mol. Pharmaceutics, 15, (2018), 2807–2815.

Impact Factor czasopisma z roku opublikowania pracy: 4.396

Liczba punktów ministerialnych MNiSW czasopisma z roku opublikowania pracy: 40

DOI: 10.1016/j.ejps.2019.06.001

Mój wkład w wyżej wymienionym artykule polegał na wykonaniu pomiarów dielektrycznych i kalorymetrycznych, analizie wszystkich otrzymanych wyników (za wyjątkiem wyników PALS) oraz przygotowaniu manuskryptu. Wkład pozostałych współautorów, w formie oświadczeń, zamieszczono na końcu artykułu.

dr Marzena Rams-Baron

Katowice, 16. września 2020 r.

Zakład Biofizyki i Fizyki Molekularnej

Wydział Nauk Ścisłych i Technicznych

Uniwersytet Śląski

ul. Bankowa 12, 40-007 Katowice

OŚWIADCZENIE

Oświadczam, że w pracy:

J. Pacult (Szczurek), M. Rams-Baron, B. Chrząszcz, R. Jachowicz, M. Paluch, *Effect of Polymer Chain Length on the Physical Stability of Amorphous Drug-Polymer Blends at Ambient Pressure*, Mol. Pharmaceutics, 15, (2018), 2807–2815.

Mój udział polegał na nadzorowaniu przeprowadzonych analiz, dyskusji otrzymanych wyników oraz korekcie manuskryptu.

Marzena Rams-Baron

Podpis

Mgr inż. Beata Chrzęszcz

Katowice, ..18.09.2020

Instytut Inżynierii Materiałowej

Wydział Nauk Ścisłych i Technicznych

Uniwersytet Śląski

ul. Bankowa 12, 40-007 Katowice

OŚWIADCZENIE

Oświadczam, że w pracy:

J. Pacułt (Szcurek), M. Rams-Baron, B. Chrzęszcz, R. Jachowicz, M. Paluch, *Effect of Polymer Chain Length on the Physical Stability of Amorphous Drug-Polymer Blends at Ambient Pressure*, Mol. Pharmaceutics, 15, (2018), 2807–2815.

Mój udział polegał na wykonaniu pomiarów PALS i analizie otrzymanych wyników.



Podpis

Prof. dr hab. Renata Jachowicz

Kraków 16.09.2020

Katedra Technologii Postaci Leku i Biofarmacji

Wydział Farmaceutyczny

Uniwersytet Jagielloński

ul. Medyczna 9, 30-688 Kraków

OŚWIADCZENIE

Oświadczam, że w pracy:

J. Pacułt (Szczurek), M. Rams-Baron, B. Chrzęszcz, R. Jachowicz, M. Paluch, *Effect of Polymer Chain Length on the Physical Stability of Amorphous Drug-Polymer Blends at Ambient Pressure*, Mol. Pharmaceutics, 15, (2018), 2807–2815.

Mój udział polegał na udziale w dyskusji otrzymanych wyników.

Kierownik
Katedry i Zakładu Technologii
Postaci Leku i Biofarmacji CM U.
Renata Jachowicz
prof. dr hab. Renata Jachowicz

Prof. zw. dr hab. Marian Paluch

Chorzów,

Instytut Fizyki

Uniwersytet Śląski

ul. 75 Pułku Piechoty 1A, 41-500 Chorzów

OŚWIADCZENIE

Oświadczam, że w pracy:

J. Pacult (Szczurek), M. Rams-Baron, B. Chrząszcz, R. Jachowicz, M. Paluch, *Effect of Polymer Chain Length on the Physical Stability of Amorphous Drug–Polymer Blends at Ambient Pressure*, Mol. Pharmaceutics, 15, (2018), 2807–2815.

Mój udział polegał na udziale w dyskusji otrzymanych wyników oraz korekcji manuskryptu.

.....

Podpis

Effect of Polymer Chain Length on the Physical Stability of Amorphous Drug–Polymer Blends at Ambient Pressure

Justyna Pacuły,^{†,‡,§} Marzena Rams-Baron,^{*,†,‡,§} Beata Chrzęszcz,[§] Renata Jachowicz,^{||} and Marian Paluch^{†,‡}

[†]Institute of Physics, University of Silesia, 75 Pulku Piechoty 1A, 41-500 Chorzow, Poland

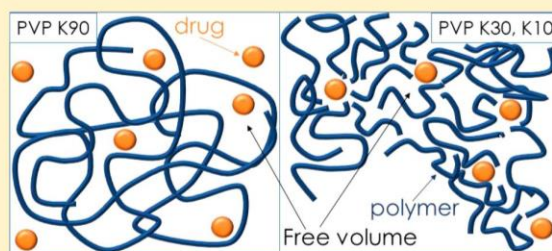
[‡]Silesian Center for Education and Interdisciplinary Research, 75 Pulku Piechoty 1A, 41-500 Chorzow, Poland

[§]Institute of Material Science, University of Silesia 75 Pulku Piechoty 1A, 41-500 Chorzow, Poland

^{||}Faculty of Pharmacy, Department of Pharmaceutical Technology and Biopharmaceutics, Jagiellonian University, Medyczna 9, 30-688 Kraków, Poland

ABSTRACT: Rational selection of polymers for amorphous drug stabilization is necessary for further successful development of solid dispersion technology. In this paper, we investigate the effect of polymer chain length on the inhibition of amorphous drug recrystallization. To consider this problem, we prepared a drug–polymer blend (in 10:1 drug to polymer ratio) containing bicalutamide (BIC) and polyvinylpyrrolidone (PVP) with different chain lengths K10, K30, and K90. We applied broadband dielectric spectroscopy to compare the molecular dynamics of investigated samples and thoroughly recognize their crystallization tendencies from supercooled liquid state. Despite the lack of differences in molecular dynamics, we noticed significant changes in their crystallization rates. To rationalize such behavior, we performed positron annihilation lifetime spectroscopy measurements. The results showed that the value of free volume was the highest for blend with PVP K90, which at the same time was characterized by the greatest tendency to crystallize. We postulate that the polymer chain, depending on its length, can have different configurations in the space, leading to better or worse sample stabilization. Our results highlight how important is detailed understanding of physical properties of polymers for judicious selection of the best stabilization approach.

KEYWORDS: bicalutamide, polyvinylpyrrolidone, crystallization, free volume, polymer chain length



INTRODUCTION

Nowadays, the pharmaceutical industry has been struggling with a major problem of limited solubility of orally administered drugs. This issue is related to about 40% of drugs currently available on the market and about 70% of those in the pipeline.⁵ Therefore, it is a great challenge to develop an appropriate method of drug formulation that would overcome these bioavailability difficulties. One of the solutions is to prepare amorphous solid dispersions (ADS) containing active pharmaceutical ingredients (APIs) dispersed in a polymer matrix. The polymeric excipients may enhance the biopharmaceutical properties, extend shelf time, inhibit crystallization from amorphous state, and increase solubility of the drug. The mechanisms responsible for beneficial physical stability of such systems are widely discussed and attributed to the numerous effects.^{6–9}

First mechanism is commonly described as an antiplasticizing effect. The addition of polymer decreases the free volume of amorphous API hindering its molecular mobility or, equivalently, increasing its viscosity.^{6,7} Consequently, the temperature range in which drug is stable is extended. The higher T_g of a sample upon mixing with polymer is considered as a universal feature of antiplasticization. The observed change in the glass

transition temperature depends on polymer concentration and can be estimated using various models like Gordon–Taylor¹⁰ equation or Couchman–Karasz¹¹ etc. However, in using these equations we should be aware of their limitation, like nonideal mixing of two components, which can reveal the discrepancies between theoretical and experimental value of T_g .

Apart from the polymer impact on the molecular dynamics of API, the presence of specific drug–polymer interactions can improve stability of drug dispersed in polymer carrier. Various drug–polymer interactions, like hydrogen bonds or van der Waals forces, can be responsible for hindered crystallization of amorphous APIs.^{8,12} Moreover, the addition of polymer can prevent interactions between drug molecules which may be responsible for inferior physical stability of the sample. For instance, Taylor and Zografi¹³ reported that the addition of PVP prevents H-bonding formation between indomethacin molecules, improving hereby the physical stability of a drug.

Received: March 23, 2018

Revised: May 22, 2018

Accepted: May 23, 2018

Published: May 23, 2018

To make the right choice during establishing the composition of drug–polymer formulations, the geometry and structure of polymer additive have to be taken into account. The importance of these molecular factors can be recognized during studies performed at elevated pressure.⁹ Lee and Ediger¹⁴ reported that mechanical stress can modify polymer chain conformation leading to the changes in the strength of drug–polymer interactions. Without doubts the geometry and spatial arrangement of polymer chains are relevant for the stabilization outcome. Schram¹⁵ et al. investigated impact of polymer conformation on the crystal growth inhibition in aqueous solution with various pH values. They observed that in the solution at pH = 3 polymer chains take on a coiled shape which leaves many growth sites free for crystal to growth. However, when the pH of the solution is 6.8, the polymer chains are elongated, which makes more growth sites blocked and causes more effective inhibition of crystallization. Moreover, Mosquera-Giraldo¹⁶ et al. investigated the effect of chemically diverse cellulose-based polymers on the nucleation induction time. They observed that polymers with carboxylate groups in combination with the optimal length of the hydrocarbon chain, inhibit nucleation most effectively. Nevertheless, this aspect seems to be insufficiently investigated and actually little is known how conformation of polymer impacts crystallization tendency of drug dispersed in polymer matrix. Thus, we decided to shed more light on this problem and check if spatial arrangement of polymer can affect crystallization rates of amorphous APIs. This goal can be realized when polymers with increasing molecular weight will be applied. Thus, in our study we used PVP with various molecular weights assigned later in discussion as $K \approx 10, 30, 90$. We assumed that depending on the length chain, the arrangement of the polymer in space will be different due to various flexibility and entanglement ability. Recently, similar experiments were conducted by Mohapatra¹⁷ et al. for solid dispersions containing indomethacin and PVP with increasing molecular weight. However, the mentioned issues related to the chain arrangement were not discussed there. The observed increase in the effectiveness of crystallization inhibition as the polymer length increases was attributed to the growing viscosity and slower molecular mobility of investigated ASDs. In our study as a model compound, we have chosen the anticancer drug BIC with a very strong tendency to crystallize from amorphous state. To improve its physical stability, the sample was mixed with polymer PVP. In our previous study, we observed that in solid dispersions containing bicalutamide and 30% of PVP K30 (w/w) the drug recrystallization was completely inhibited.¹⁸ In current study, we used mixtures with 10% of PVP (w/w), where crystallization was slowed down but not inhibited entirely. We performed BDS measurements to analyze molecular dynamic of prepared samples and compare their crystallization tendencies. Finally, we determined the value of free volumes for investigated blends using PALS technique.

MATERIALS AND METHODS

Materials. The crystalline form of bicalutamide (BIC) ($M_w = 430.37$ g/mol) of 99.8% purity was purchased from Hangzhou Hyper Chemicals Limited. Systematic name of BIC is *N*-[4-cyano-3-(trifluoromethyl)phenyl]-3-[4-(4-fluorophenyl)sulfonyl]-2-hydroxy-2-methylpropanamide. Polyvinylpyrrolidone (PVP), PVP K10 grade: $K = 12–18$, $M_w = 10$ 000 g/mol; PVP K30 grade: $K = 29–32$, $M_w = 40$ 000 g/mol;

PVP K90 grade: $K = 80–100$, $M_w = 360$ 000 g/mol; was supplied from Sigma-Aldrich. The amount of water in polymer was determined as 4% (Carl-Fisher method).

Preparation of Binary System. The investigated BIC–PVP systems were prepared at fixed drug to polymer ratio, i.e., 10:1, corresponding to the weight percentage concentration of BIC equal 90% w/w. To obtain homogeneous mixtures, the appropriate amount of crystalline BIC and PVP were mixed in a mortar for a few minutes. Then the physical mixtures were spread on a capacitor plate and kept for 15 min on hot plate at $T = 373$ K in order to remove water. Subsequently, the temperature was increased to the melting temperature being the same for all investigated blends, i.e., $T_m = 463$ K. After melting, the sample was vitrified by fast transfer to a previously chilled copper plate.

Differential Scanning Calorimetry (DSC). Calorimetric measurements for BIC–PVP blends were carried out by Mettler-Toledo DSC 1 STAre system equipped with an HSS8 ceramic sensor having 120 thermocouples and liquid nitrogen cooling station. Temperature and enthalpy calibration were applied using zinc and indium standards. Measurements were performed using aluminum crucibles (40 μ L) with pin–ME-27331 with heating rate of 10 K/min. Melting points were determined as the onset of the peak, while the glass transition temperature was obtained from the midpoint of the heat capacity increment.

Broadband Dielectric Spectroscopy Measurements (BDS). Dielectric studies were performed using Novo-Control Alpha spectrometer, in the frequency range from 10^{-1} Hz to 10^6 Hz and at temperature range from 173 to 385 K (for pure PVP from 323 K to 453 K). Temperature control was provided by the Quatro controller with accuracy up to 0.1 K. All measurements were carried out for samples placed between stainless capacitor plates (diameter equals 15 mm or 10 mm with gap 0.1 mm provided by glassy spacers). In a typical dielectric experiment, we measure a complex impedance $Z^*(\omega)$ defined as a quotient of the voltage $U^*(\omega)$ and current $I^*(\omega)$ magnitudes. The complex dielectric permittivity $\epsilon^*(\omega)$ can be then calculated using the following formula:

$$\epsilon^*(\omega) = \epsilon'(\omega) - i\epsilon''(\omega) = \frac{1}{i\omega Z^*(\omega)C_0} \quad (1)$$

where ω is an angular frequency and C_0 denotes the geometry-dependent capacitance of an empty capacitor. To determine the relaxation times, the dielectric spectra were parametrized using two Havriliak–Negami functions:¹

$$\epsilon''(\omega) = \text{Im} \sum_{i=1}^2 \left(\epsilon_\infty + \frac{\Delta\epsilon}{(1 + (i\omega\tau_{\text{HN}})^\alpha)^\beta} \right) + \frac{\sigma}{\epsilon_0 i\omega} \quad (2)$$

where ϵ_∞ is the high frequency limit permittivity, $\Delta\epsilon$ is the dielectric strength, ϵ_0 signify permittivity of vacuum, τ_{HN} is the HN relaxation time, the exponents α and β denote the shape of relaxation peak, and σ means dc conductivity. Then, structural relaxation times were calculated according to the following equation:

$$\tau = \tau_{\text{HN}} \left[\sin\left(\frac{\alpha\pi}{2\beta + 2}\right) \right]^{-1/\alpha} \left[\sin\left(\frac{\beta\pi}{2\beta + 2}\right) \right]^{1/\alpha} \quad (3)$$

We applied BDS technique to recognize the crystallization tendencies of investigated BIC–PVP blends. For this purpose, we performed isothermal dielectric measurements at $T = 367$ K.

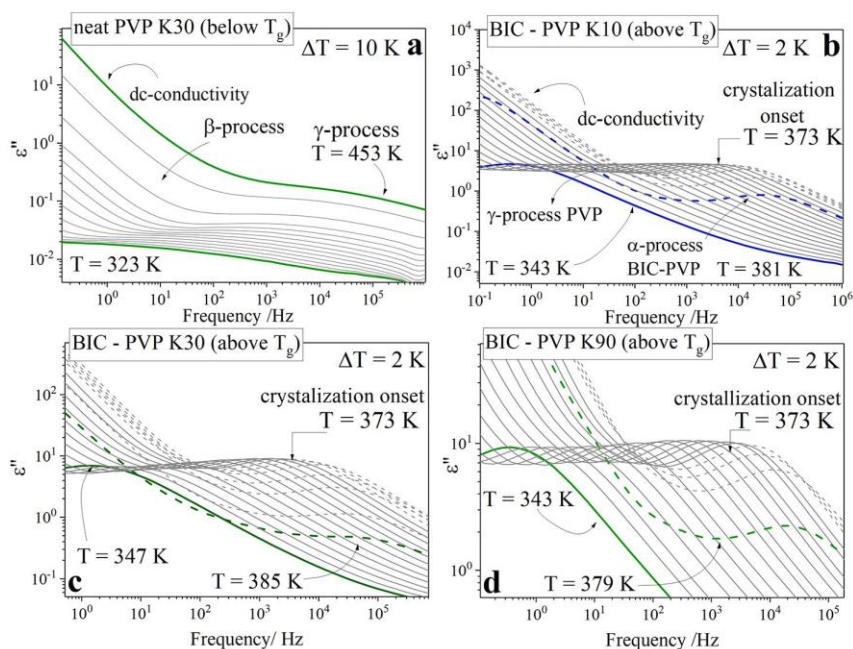


Figure 1. Dielectric loss spectra for binary mixtures of BIC and of PVPs K10 (b), K30 (c), K90 (d) and pure PVP K30 (a).

The dielectric spectra were measured in a frequency range from 10^{-1} to 10^6 Hz in a time-dependent manner with time intervals of 10 min.

Positron Annihilation Lifetime Spectroscopy (PALS).

The positron annihilation lifetime spectrometry studies were performed at room temperature in sandwich geometry with a “fast–fast” coincidence spectrometer equipped with plastic scintillators. A positron source consisted of ~ 500 kBq of ^{22}Na embedded between two $7.6 \mu\text{m}$ Kapton foils. The correction from the positron source self-annihilations was estimated using previous calibration and chemical composition of a mixture of BIC and PVP. The contribution was accepted to be equal to 19%. Measurements were taken every hour for 24 h. One characteristic spectrum containing about 1.1×10^7 counts were obtained by summing up the results of 24 cycles of measurements. All these spectra for a given BIC–PVP were analyzed together using LT10 software (next version of LT9 software²). The lifetime resolution of the spectrometer approximated by the Gaussian function fwhm was found to be equal to 279 ps. The PALS spectra were fitted using the least-squares fitting procedure to free volume model. This model consists of three lifetime components: τ_{free} is a lifetime characteristic for the material, τ_{trap} is a lifetime assigned the defect, and τ_{po} is the longest lifetime component o-Ps captured in the free volumes (holes, nano voids, and other empty volumes), and σ parameter which shows the distribution of τ_{po} . This lifetime τ_{po} strongly depends on the size of the nano voids where the o-Ps is trapped.³ In addition, the procedure first proposed by Dlubek⁴ et al. opens the possibility to obtain radius distribution as well, which results from the localization of the positronium in the free volume with varying sizes. In our model, the free volumes were assumed to have spherical geometry and that the radius distribution can be described by the log-normal distribution

RESULTS AND DISCUSSION

1. Molecular Dynamics of BIC Dispersed in Polymer Matrix Formed by PVP of Various Molecular Weight.

Figure 1b–d shows dielectric loss spectra of amorphous BIC–PVP mixtures prepared using polymers with different molecular weights. Obtained spectra show dc contribution at lower frequencies (left side of graph) and a well-resolved peak attributed to the structural α -relaxation process. As can be seen, the maximum of the α -process moves to the higher frequencies with higher temperature, which indicates the intensified molecular mobility of a sample. At $T = 373$ K, the amplitude of the α -process drastically decreases, which is connected to the decreasing number of relaxing dipoles and progressive crystallization.

One can notice that registered dielectric spectra, presented in Figure 1, demonstrate substantial contribution from dc conductivity. This is a common problem that occurs during dielectric measurements of samples containing conductive additives, such as some polymers, silica etc. At the same time, a large conductivity contribution makes impossible to analyze the dielectric data for samples with higher polymer content. To subtract the conductivity contribution, we applied the derivative formalism according to the following formula:^{19–21}

$$\varepsilon_{\text{der}} = -\frac{\pi}{2} \frac{d\varepsilon'(f)}{d \ln f} \quad (4)$$

The comparison of spectra registered at $T = 371$ K for BIC–PVP K90 before and after derivative analysis is presented in Figure 2. The implemented model revealed the presence of additional relaxation process, slower than the α -process that was previously obscured by the dc conductivity. At registered spectra, before derivative analysis, this process is practically undetectable. The only guideline is a change of dc conductivity slope at higher temperatures, more visible on partially recrystallized spectra (see indication in Figure 1b).

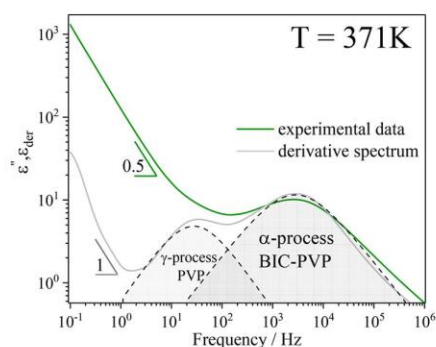


Figure 2. Dielectric spectrum of binary mixture BIC–PVP K90 analyzed with (gray line) and without derivative method (green line).

The additional process slower than α -relaxation was observed for each mixture, which we found interesting, and thus we decided to investigate more thoroughly. We suspected that its presence may be due to the motions of side chains of PVP. To shed more light on this problem we measured dielectric spectra for neat PVP.

The dielectric loss spectra of PVP K30 measured in the temperature range from $T = 323$ K to $T = 453$ K, corresponding to its glassy state, are presented in Figure 3a. The segmental relaxation of pure PVP is visible at temperatures above T_g (for PVP K30 $T_g^{\text{DSC}} = 443$ K), so we could not observe this process during our BDS experiment, which was performed in range from 273 to 453 K. As can be seen in Figure 3b on most spectra, we observed a single process assigned as γ -process. At higher temperatures additionally slower secondary relaxation, assigned as the β -process, was observed. Acquired results are convergent with data from Cerveny et al.,²² who characterized dry PVP and its water mixtures using dielectric spectroscopy. One can see that our results are in good agreement with those reported for dry samples (see data points depicted as gray squares in Figure 3a corresponding to digitalized data). In general, the secondary relaxations depending on their origin can be divided into two groups. First is the Johari–Goldstein (JG) type, which has intermolecular origin and mimics the α -process through the

motion of the whole molecule. We can observe such motions in polymers which have no side groups like 1,4-polybutadiene or poly(vinyl chloride).²³ Another type is considerably decoupled from the entire particle motions and is called non-JG. Such processes are connected to the local motions of molecular subunits such as rocking movements of chain parts in poly(*n*-methyl methacrylates)²⁴ or 180° flips of the side groups in poly(*n*-ethyl methacrylates).²⁵ Because JG processes are sensitive to the applied pressure, in contrast to the non-JG, high-pressure measurements^{22,23} can shed more light on their origin. Cerveny²² performed dielectric measurements under elevated pressure for pure PVP K30, and on the basis of the mentioned criteria, he assigned the γ -process as non-JG relaxation while the β -process was attributed to JG-type relaxation.

Now we would like to return to the discussion about the origin of the additional process in analyzed binary mixtures, which is slower than structural relaxation similar to the Debye-like process (see Figure 2). However, until now, Debye-like response has been mainly discussed in the context of liquid substances that form hydrogen bonds such as water, monohydroxy alcohols, etc.²⁶ Moreover, such additional process may be associated with Maxwell–Wagner polarization, which is observed in heterogeneous materials.²⁷ Cohen et al. proposed that this process may come from spatial inhomogeneity in the sample.²⁸ In our case, we observe an additional process in every blend containing PVP, regardless of used API or preparation method. Therefore, we are inclined to think that this process may come from the secondary relaxation of the polymer. As one can see in Figure 3a, the temperature dependence of relaxation times determined for this additional process for BIC–PVP mixtures corresponds in some extent with temperature dependence of γ -relaxation times determined for pure polymer. The observed differences in the slopes of the temperature dependence of τ_γ can be caused by the applied analysis method.

To compare the molecular dynamics of BIC–PVP samples containing polymers with different molecular weights, we determined the values of τ_α and τ_γ from the derivative spectra. The temperature evolution of both relaxation times for all samples is presented in Figure 4. To describe the temperature

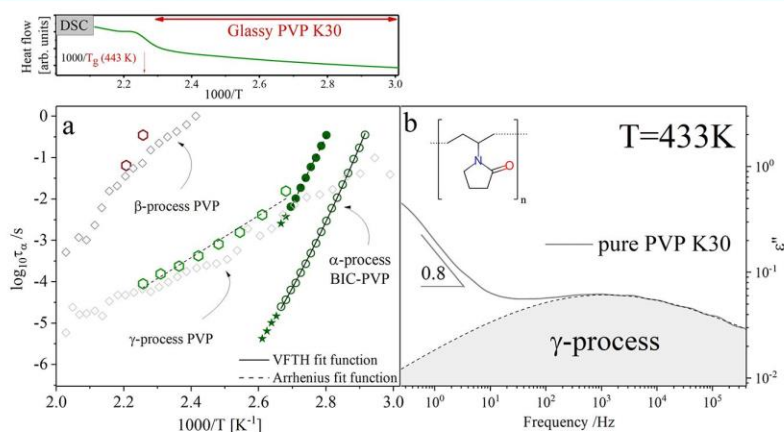


Figure 3. (a) Relaxation map of experimental data of neat PVPK30 (red and green hexagons), digitalized data (gray diamonds), and binary mixture BIC–PVP K30 (open and closed green circles). Green stars indicate structural relaxation times determined after beginning of crystallization process during heating the sample. (b) Exemplary dielectric spectrum of neat PVP K30 (gray line). Upper panel shows thermogram of pure PVP K30.

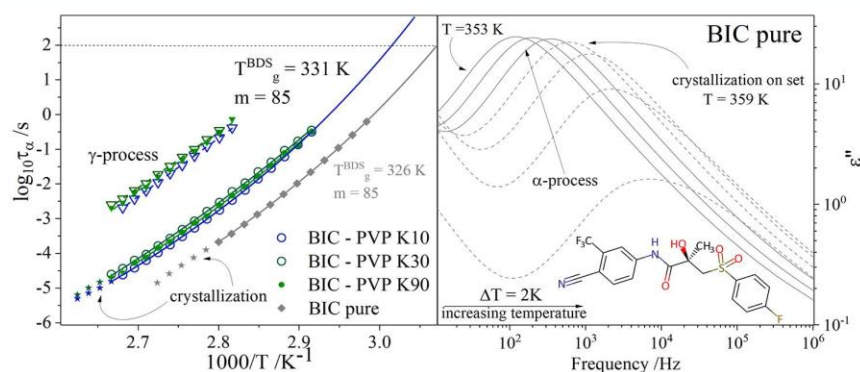


Figure 4. Relaxation map of binary mixtures of BIC PVP K10, K30, and K90 and pure BIC. Solid and dashed lines indicate VFTH and Arrhenius fitting functions, respectively. The right panel presents selected dielectric loss spectra for pure BIC. Data for pure BIC reprinted with permission from ref 18. Copyright 2017 American Chemical Society.

dependence of the α -process, the Vogel–Fulcher–Tammann–Hesse (VFTH) equation^{29–31} was used:

$$\tau_{\alpha} = \tau_{\infty} \exp\left(\frac{DT_0}{T - T_0}\right) \quad (5)$$

where τ_{∞} , T_0 , and D are fitting parameters. Parameter τ_{∞} is a pre-exponential factor denoting the upper limit of temperature for τ_{α} , which is correlated to vibrational frequency ($\sim 10^{-11}$ to 10^{-14} s),³² T_0 is the Vogel temperature, which correspond to the state with infinite relaxation time, and D denotes deviation from the Arrhenius model.³³ One can see that the temperature dependence of τ_{α} for all investigated BIC–PVP samples is similar. The VFTH fitting parameters were only slightly different, i.e., $\log \tau_0 = -15.90 \pm 0.06$, $D = 11.57 \pm 0.09$. From extrapolation of VFTH fit to $\log_{10} \tau_{\alpha} = 2$ ($\tau_{\alpha} = 100$ s), the values of glass transition temperatures were determined. These values for all analyzed systems were almost identical, i.e., $T_g = 331 \pm 0.3$ K.

Obtained glass transition temperature is in good agreement with T_g values determined from DSC measurements, which are shown in Figure 5. Amorphous samples were then heated with the 10 K/min rate. All thermograms show an endothermic event corresponding to glass transition temperature at $T_g = 331$ K. The observed similarity in T_g values is consistent with our

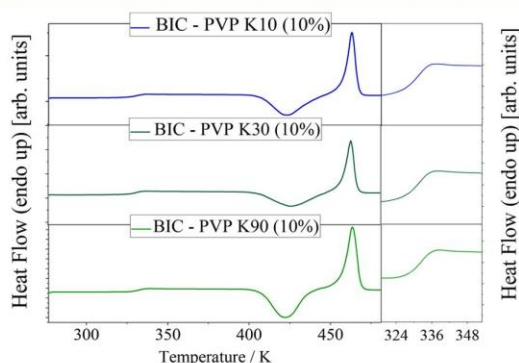


Figure 5. DSC thermograms for binary mixtures of BIC and additive of PVPs K10, K30, and K90. Right panel contains zoom at glass transition for each mixture.

dielectric results. Besides T_g we can also compare the value of the m parameter, which describes deviation of temperature dependence of relaxation times from Arrhenius behavior, expressed with the following formula:³⁴

$$m = \left. \frac{d \log \tau_{\alpha}}{d(T_g/T)} \right|_{T=T_g} = \frac{D(T_0 - T_g)}{(1 - (T_0 - T_g))^2 \ln(10)} \quad (6)$$

The acquired value of parameter m for all of samples was $m = 85 \pm 1$, which classified them as intermediate glass formers.³⁵ Readers interested in a more detailed description of the effect of PVP K30 on stabilization of BIC are encouraged to get acquainted with our earlier article where we investigated molecular dynamics of BIC–PVP K30 (10%) (w/w) blends.³⁶

Our BDS and DSC results clearly indicate the lack of differences in the supercooled molecular dynamics of BIC–PVP samples containing polymers with different molecular weight. In general, the relationship between the polymer length chain and molecular mobility can be expected, however, in analyzed mixtures, the polymer content was very small (10% w/w). In such a case, the lack of differences in molecular dynamics is possible. This is consistent with results reported by Mohapatra³⁷ for indomethacin–PVP mixtures. No significant effect on molecular dynamics has been observed for 5% polymer addition to the mixtures, but for the 30% additive the change was apparent. Li et al.⁷ analyzed a mixture of indomethacin and ketoconazole with 75% addition of different polymers. Only such high polymer concentration allowed observation and examination of the differences in the molecular mobility of investigated samples.

2. Isothermal Dielectric Measurements. To verify if there is a difference in crystallization behavior of samples containing BIC and PVP with increasing length chains, we performed isothermal BDS measurements. The dielectric spectra were collected at $T = 367$ K in a time-dependent manner. Measurement were done with a predefined time step, which in our experiment was set to 10 min. To analyze the kinetics of the process, the obtained dielectric data were normalized using the following formula:

$$\varepsilon_n'(t) = \frac{\varepsilon'(0) - \varepsilon'(t)}{\varepsilon'(0) - \varepsilon'(\infty)} \quad (7)$$

where $\varepsilon_n'(t)$ is normalized dielectric permittivity, $\varepsilon'(0)$ is the static dielectric permittivity connected with onset of crystal-

lization, $\varepsilon'(t)$ is the value in exact point in time, and $\varepsilon'(\infty)$ is the long-time limiting value.

The obtained $\varepsilon'_n(t)$ dependencies for all investigated BIC–PVP mixtures are presented in Figure 6. As can be seen, the

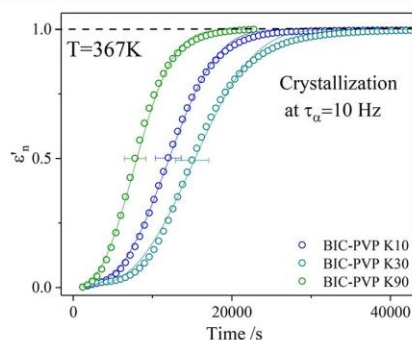


Figure 6. Isothermal kinetics of crystallization measured at $T = 367$ K for mixtures of BIC and PVPs K10, K30, and K90. Solid lines denote the best fits to Avrami equation.^{38,39} Error bars are calculated as standard deviation of triplicate analysis.

BIC–PVP K90 has the biggest tendency to crystallization. The beginning of sample crystallization was almost immediately after temperature stabilization, while other mixtures, i.e., BIC–PVP K10 and BIC–PVP K30, start crystallizing after about 80 and 120 min, respectively. In the case of shorter polymers, their flexibility allows for their denser molecular packing, which may increase the stability of the mixture by hindering the crystal nuclei formation. Contrary, for PVP K90, the more loose chain arrangement may facilitate crystallization process. Furthermore, on the basis of results shown in Figure 6, it can be noted that there is a certain length of polymeric chain that is optimal for stabilizing effect of the drug.

3. The Analysis of Free Volume Using Positron Annihilation Lifetime Spectroscopy. To understand the faster crystallization of BIC dispersed in PVP K90, we performed a series of PALS measurements. This technique is often used to measure the free volume of polymers and their mixtures.^{40–44} Using PALS, one can estimate the size of free spaces determined by spatial arrangement of polymer chains by the investigation of the lifetime of positron implanted into the sample. In the simplest situation, the positron can interact with a sample in three ways. In the first case, positrons may interact with an electron and thus annihilate with lifetime specific to the investigated material (free annihilation). Other cases involve formation of the bounded positron–electron pair so-called positronium. This bond can exist in two states: *para*-

positronium (*p*-Ps), which contains an electron and a positron with the antiparallel spin arrangement and annihilates by intrinsic short lifetime, while the another possibility is related to the creation of the *ortho*-positronium (*o*-Ps), with parallel spin orientation. The *o*-Ps can be trapped inside the free volumes created by polymer chains, and its annihilation time depends on the free volume radius. Consequently, the lifetime of *o*-Ps gives information about the size of free volumes of the material^{40,41,45,46} on the basis of an extended Tao-Eldrup.⁴⁷

The results obtained from the PALS measurements are summarized in Table 1. As can be seen for neat BIC, the mean free volume (V_f) was 94.4 \AA^3 , while for pure polymers the value was lower, i.e., 64.0 \AA^3 and 75.1 \AA^3 for PVP K30 and PVP K90, respectively. A similar value of free volume for PVP K30 was published by Li⁷ and equals 64.1 \AA^3 . Li also studied the free volume of several drugs, polymers, and their mixtures, and among others, he showed that the free volume for indomethacin and ketoconazole was equal 42.0 \AA^3 and 44.7 \AA^3 , respectively.⁷ In our measurements, we observed that the value of free volume for pure API is larger than for the polymer. This may be due to the fact that BIC is a very polar molecule and its functional groups such as phenyl rings can increase its free volume by incorporating large steric hindrance. As a similar example, two polymers, tetramethyl bisphenol-a polycarbonate (TMPC) and bisphenol-a polycarbonate (PC), described by Liu⁴⁶ can be given. PALS measurements have shown that the TMPC has larger free volume than PC. Liu attributed this effect to the presence of methyl groups in TMPC. Back to our data, we observed that mixtures with polymers with a shorter chain like PVP K10 and PVP K30 have similar values of $V_f = 88.1 \text{ \AA}^3$ and $V_f = 87.1 \text{ \AA}^3$ whereas BIC–PVP K90 is characterized by a higher free volume value equal to $V_f = 92.1 \text{ \AA}^3$. These results can be now correlated with data obtained from BDS measurements. The highest value of free volume was obtained for pure BIC, which is the least stable, and the crystallization process starts very quickly. The high value of free volume was also noted for BIC–PVP K90 mixture. Compared to the other polymer blends, the BDS measurements showed that its crystallization begins faster than the others. For the remaining samples, the BIC–PVP K10 mixture has a higher free volume value than BIC–PVP K30. These results are also reflected in the data obtained from dielectric measurements. The mixture with PVP K10 crystallized faster than the blend with PVP K30. In addition, small differences in the free volume values obtained between the BIC–PVP K10 and BIC–PVP K30 mixtures may be due to the slight difference in the molecular weights of used polymers. Among the tested polymer blends, the highest value of free volume was obtained for the BIC–PVP K90 mixture, indicating that the polymer with the longest chain reduces the

Table 1. Results from PALS Measurements^a

	τ_{free} [ns]	τ_{trapp} [ns]	τ_{po} [ns]	σ_{po1} [nm]	R_{mean} [nm]	$\sigma_{R_{\text{mean}}}$ [nm]	V_f [\AA^3]	σ_{V_f} [nm]
BIC–PVP K10	0.221 ± 0.001	0.399 ± 0.004	1.799 ± 0.019	0.332	0.269	0.042	88.1	0.043
BIC–PVP K30	0.232 ± 0.001	0.406 ± 0.003	1.774 ± 0.022	0.359	0.267	0.045	87.1	0.047
BIC–PVP K90	0.226 ± 0.001	0.403 ± 0.002	1.903 ± 0.017	0.203	0.278	0.027	92.1	0.027
BIC	0.235 ± 0.002	0.411 ± 0.004	1.927 ± 0.015	0.204	0.280	0.027	94.4	0.028
PVP30	0.230 ± 0.002	0.389 ± 0.005	1.576 ± 0.013	0.256	0.245	0.030	64.0	0.024
PVP90	0.234 ± 0.001	0.401 ± 0.001	1.700 ± 0.020	0.247	0.258	0.030	75.1	0.024

^a τ_{free} is a lifetime of free positron, τ_{trapp} is a lifetime of trapped positron, and τ_{po} is a mean lifetime of *ortho*-positronium; obtained values are presented with standard deviations determined using LT software. The calculated values of mean radius of cavity R_{mean} and mean volume of cavity V_f are presented. σ_{po1} , $\sigma_{R_{\text{mean}}}$, σ_{V_f} denote the width of distribution of *ortho*-positronium lifetime, mean radius, and mean volume, respectively.

free volume of the drug but not as effectively as the other polymers. It means that the crystallization process may depend on spatial arrangement of polymer chains in a drug–polymer mixture. Moreover, the best crystallization inhibitor was PVP K30, what may suggest that there is an optimal length of polymer chain that allows satisfactory stabilization of the drug. Nowadays, the value of free volume is more often correlated with the stability of amorphous drug mixtures with various excipients. P. Szabo et al.⁴⁸ examined carvedilol and HPMC polymer mixtures and also observed the increase in the unoccupied volume during sample storage. This effect may correspond to the partial crystallization of the drug. Also, B. Szabo⁴⁹ et al. prepared films containing vitamin B12, sodium alginate, and polymer Carbopol 71 G NF, which were stored for 1 month in relative humidity. They noticed the correlation between increasing free volume value and storage time. The authors point out that examining polymer films using the PALS technique and obtaining information about unoccupied volume allows preparation of the drug formulation process with the required drug release profile and stability.

The impact of molecular architecture on polymer properties is of great scientific and technological interest. The number of possible chain configurations is getting higher with increasing chain length and can be statically estimated as 2^{2n} , where n denotes the number of units.⁵⁰ In the available literature, the different polymer–polymer systems with linear, star, or branched structures are described. Their preferred conformation might be driven by external environment and depends on a multitude of factors, that is, on polymer type (homopolymer or copolymer),⁵¹ its chemistry,^{51,52} molecular weight,⁵¹ geometry,¹⁶ potential to interchain attraction,⁵⁰ etc. In the case of polymer–solvent systems, the interaction between solvent and polymer⁵³ and solvent pH should also be taken into account.¹⁵ Most polymers with linear chains have a tendency to be randomly coiled and when the chain size increases their entanglement occurs.⁵⁴ To observe the entanglement of the polymer, critical chain length is required, which is correlated to shape and polarity of polymer.⁵⁰ Some polymer chains can attain dendrimer configurations as was proposed in the 1990s. In this case, as the molecular weight increases the polymers change their conformation from elongated to spherical.⁵¹ The tangling ability of PVP K90 may rationalize the higher value of the free volume observed for BIC–PVP K90 mixture in our study. Despite the relation of polymer molecular architecture with its properties, there is still little known about the impact of conformation of polymer chains on the stability of drug–polymer mixtures.

CONCLUSIONS

In this paper, we investigated BIC mixtures with various polymers, i.e., PVP K10, PVP K30, and PVP K90 (10% w/w). Performed BDS studies demonstrated that all mixtures were characterized by the same molecular dynamics. This has been also confirmed by the DSC studies that have shown identical glass transition temperatures for all investigated samples. To verify if there are differences in their crystallization tendencies, we performed isothermal crystallization studies using BDS technique. The results showed that mixture containing polymer with the longest chain, i.e., PVP K90, proved to be the least effective as crystallization inhibitor and drug recrystallization was observed as faster than for the rest of investigated samples. To understand such behavior, we took advantage of the PALS technique. We found out that the value of free volume was the

largest for BIC–PVP K90 mixture, while for remaining blends with shorter polymer chains, the obtained free volume values were smaller and similar to each other. This indicates that PVP K90 lowers free volume less effectively than other polymers, leading thereby to worse sample stabilization. The best crystallization inhibitor turned out to be the PVP K30, which may suggest that in order to stabilize the drug we have to choose the polymer with the certain optimal chain length. Our results show that the choice of the appropriate polymer for drug stabilization outcome is crucial and should be thoroughly investigated. Besides the length of the polymer, the impact of molecular features should be deeply investigated, e.g., rigidity, geometry, etc. Further detailed research could allow simplification of the selection of polymer additive in the future, thereby increasing the practical outcome of using amorphous solid dispersion systems.

AUTHOR INFORMATION

Corresponding Author

*E-mail: marzena.rams-baron@us.edu.pl

ORCID

Justyna Pacult: 0000-0002-3923-7852

Marzena Rams-Baron: 0000-0001-8808-8067

Notes

The authors declare no competing financial interest.

ACKNOWLEDGMENTS

Authors J. P., M. R-B., R. J., and M. P acknowledge Polish National Science Centre for the financial support (grant Symfonia 3 no. 2015/16/W/NZ7/00404).

REFERENCES

- (1) Havriliak, S.; Negami, S. A complex plane representation of dielectric and mechanical relaxation processes in some polymers. *Polymer* **1967**, *8*, 161–210.
- (2) Kansy, J. Microcomputer program for analysis of positron annihilation lifetime spectra. *Nucl. Instrum. Methods Phys. Res., Sect. A* **1996**, *374* (2), 235–244.
- (3) Tao, S. J. Positronium annihilation in molecular substances. *J. Chem. Phys.* **1972**, *56* (11), 5499–5510.
- (4) Dlubek, G.; De, U.; Pionteck, J.; Arutyunov, N. Y.; Edelman, M.; Krause-Rehberg, R. Temperature dependence of free volume in pure and silica-filled poly(dimethyl siloxane) from positron lifetime and PVT experiments. *Macromol. Chem. Phys.* **2005**, *206* (8), 827–840.
- (5) Ting, J. M.; Porter, W. W.; Mecca, J. M.; Bates, F. S.; Reineke, T. M. Advances in Polymer Design for Enhancing Oral Drug Solubility and Delivery. *Bioconjugate Chem.* **2018**, *29*, 939–952.
- (6) Baghel, S.; Cathcart, H.; O'Reilly, N. J. Polymeric Amorphous Solid Dispersions: A Review of Amorphization, Crystallization, Stabilization, Solid-State Characterization, and Aqueous Solubilization of Biopharmaceutical Classification System Class II Drugs. *J. Pharm. Sci.* **2016**, *105* (9), 2527–2544.
- (7) Li, J.; Zhao, J.; Tao, L.; Wang, J.; Wanknis, V.; Pan, D.; Hubert, M.; Raghavan, K.; Patel, J. The effect of polymeric excipients on the physical properties and performance of amorphous dispersions: Part I, free volume and glass transition. *Pharm. Res.* **2015**, *32* (2), 500–515.
- (8) Paudel, A.; Worku, Z. A.; Meeus, J.; Guns, S.; Van Den Mooter, G. Manufacturing of solid dispersions of poorly water soluble drugs by spray drying: Formulation and process considerations. *Int. J. Pharm.* **2013**, *453* (1), 253–284.
- (9) Ayenew, Z.; Paudel, A.; Van Den Mooter, G. Can compression induce demixing in amorphous solid dispersions? A case study of naproxen-PVP K25. *Eur. J. Pharm. Biopharm.* **2012**, *81* (1), 207–213.

- (10) Wlodarski, K.; Sawicki, W.; Kozyra, A.; Tajber, L. Physical stability of solid dispersions with respect to thermodynamic solubility of tadalafil in PVP-VA. *Eur. J. Pharm. Biopharm.* **2015**, *96*, 237–246.
- (11) Couchman, P. R.; Karasz, F. E. A Classical Thermodynamic Discussion of the Effect of Composition on Glass-Transition Temperatures. *Macromolecules* **1978**, *11* (1), 117–119.
- (12) Grzybowska, K.; Chmiel, K.; Knapik-Kowalczyk, J.; Grzybowski, A.; Jurkiewicz, K.; Paluch, M. Molecular factors governing the liquid and glassy states recrystallization of celecoxib in binary mixtures with excipients of different molecular weights. *Mol. Pharmaceutics* **2017**, *14* (4), 1154–1168.
- (13) Taylor, L. S.; Zografi, G. Spectroscopic characterization of interactions between PVP and indomethacin in amorphous molecular dispersions. *Pharm. Res.* **1997**, *14*, 1691–1698.
- (14) Lee, H. N.; Ediger, M. D. Mechanical rejuvenation in poly(methyl methacrylate) glasses? Molecular mobility after deformation. *Macromolecules* **2010**, *43* (13), 5863–5873.
- (15) Schram, C. J.; Beaudoin, S. P.; Taylor, L. S. Impact of polymer conformation on the crystal growth inhibition of a poorly water-soluble drug in aqueous solution. *Langmuir* **2015**, *31* (1), 171–179.
- (16) Mosquera-Giraldo, L. I.; Borca, C. H.; Meng, X.; Edgar, K. J.; Slipchenko, L. V.; Taylor, L. S. Mechanistic Design of Chemically Diverse Polymers with Applications in Oral Drug Delivery. *Biomacromolecules* **2016**, *17* (11), 3659–3671.
- (17) Mohapatra, S.; Samanta, S.; Kothari, K.; Mistry, P.; Suryanarayanan, R. Effect of Polymer Molecular Weight on the Crystallization Behavior of Indomethacin Amorphous Solid Dispersions. *Cryst. Growth Des.* **2017**, *17* (6), 3142–3150.
- (18) Szczurek, J.; Rams-Baron, M.; Knapik-Kowalczyk, J.; Antosik, A.; Szafraniec, J.; Jamróz, W.; Dulski, M.; Jachowicz, R.; Paluch, M. Molecular dynamics, recrystallization behavior, and water solubility of the amorphous anticancer agent bicalutamide and its polyvinylpyrrolidone mixtures. *Mol. Pharmaceutics* **2017**, *14* (4), 1071–1081.
- (19) Fragiadakis, D.; Dou, S.; Colby, R. H.; Runt, J. Molecular mobility, ion mobility and mobile ion concentration in polyethylene oxide-based polyurethane ionomers. *Macromolecules* **2008**, *41* (15), 5723–5728.
- (20) Fragiadakis, D.; Dou, S.; Colby, R. H.; Runt, J. Molecular mobility and Li⁺ conduction in polyester copolymer ionomers based on poly(ethylene oxide). *J. Chem. Phys.* **2009**, *130* (6), 064907.
- (21) Knapik, J.; Wojnarowska, Z.; Grzybowska, K.; Jurkiewicz, K.; Stankiewicz, A.; Paluch, M. Stabilization of the Amorphous Ezetimibe Drug by Confining Its Dimension. *Mol. Pharmaceutics* **2016**, *13* (4), 1308–1316.
- (22) Cerveny, S.; Alegria, A.; Colmenero, J. Broadband dielectric investigation on poly(vinyl pyrrolidone) and its water mixtures. *J. Chem. Phys.* **2008**, *128* (4), 044901.
- (23) Ngai, K. L.; Paluch, M. Classification of secondary relaxation in glass-formers based on dynamic properties. *J. Chem. Phys.* **2004**, *120* (2), 857–873.
- (24) Schmidt-Rohr, K.; Kulik, A. S.; Beckham, H. W.; Ohlemacher, A.; Pawelzik, U.; Boeffel, C.; Spiess, H. W. Molecular Nature of the β Relaxation in Poly(methyl methacrylate) Investigated by Multidimensional NMR. *Macromolecules* **1994**, *27*, 4733–4745.
- (25) Kulik, A. S.; Beckham, H. W.; Schmidt-Rohr, K.; Radloff, D.; Pawelzik, U.; Boeffel, C.; Spiess, H. W. Coupling of the α and β Processes in Poly(ethyl methacrylate) Investigated by Multidimensional NMR. *Macromolecules (Washington, DC, U. S.)* **1994**, *27*, 4746–4754.
- (26) Rams-Baron, M.; Wojnarowska, Z.; Dulski, M.; Ratuszna, A.; Paluch, M. Evidence of slow Debye-like relaxation in the anti-inflammatory agent etoricoxib. *Phys. Rev. E - Stat. Nonlinear, Soft Matter Phys.* **2015**, *92*, 022309–5.
- (27) Sjöström, J.; Swenson, J.; Bergman, R.; Kittaka, S. Investigating hydration dependence of dynamics of confined water: Monolayer, hydration water and Maxwell-Wagner processes. *J. Chem. Phys.* **2008**, *128*, 154503.
- (28) Cohen, M. H.; Neaton, J. B.; He, L.; Vanderbilt, D. Extrinsic models for the dielectric response of CaCu₃Ti₄O₁₂. *J. Appl. Phys.* **2003**, *94* (5), 3299–3306.
- (29) Fulcher, G. S. Analysis of recent measurements of the viscosity of glasses. *J. Am. Ceram. Soc.* **1925**, *8*, 789–794.
- (30) Tammann, G.; Hesse, W. Die Abhängigkeit der Viskosität von der Temperatur bei unterkühlten Flüssigkeiten. *Zeitschrift für Anorg. und Allg. Chemie* **1926**, *156* (1), 245–257.
- (31) Vogel, H. Das temperaturabhängigkeitsgesetz der viskosität von flüssigkeiten. *J. Phys. Z.* **1921**, *22*, 645–646.
- (32) Rodrigues, A. C.; Viciosa, M. T.; Danede, F.; Affouard, F.; Correia, N. T. Molecular mobility of amorphous S-flurbiprofen: A dielectric relaxation spectroscopy approach. *Mol. Pharmaceutics* **2014**, *11* (1), 112–130.
- (33) Metatla, N.; Soldera, A. The Vogel-Fulcher-Tamman equation investigated by atomistic simulation with regard to the Adam-Gibbs model. *Macromolecules* **2007**, *40* (26), 9680–9685.
- (34) Böhmer, R.; Ngai, K. L.; Angell, C. A.; Plazek, D. J. Nonexponential relaxations in strong and fragile glass formers. *J. Chem. Phys.* **1993**, *99* (5), 4201–4209.
- (35) Angell, C. A. Relaxation on liquid, polymers and plastic crystal - strong/fragile patterns and problems. *J. Non-Cryst. Solids* **1991**, *131-133*, 13–31.
- (36) Szczurek, J.; Rams-Baron, M.; Knapik-Kowalczyk, J.; Antosik, A.; Szafraniec, J.; Jamróz, W.; Dulski, M.; Jachowicz, R.; Paluch, M. Molecular dynamics, recrystallization behavior, and water solubility of the amorphous anticancer agent bicalutamide and its polyvinylpyrrolidone mixtures. *Mol. Pharmaceutics* **2017**, *14* (4), 1071.
- (37) Mohapatra, S.; Samanta, S.; Kothari, K.; Mistry, P.; Suryanarayanan, R. Effect of Polymer Molecular Weight on the Crystallization Behavior of Indomethacin Amorphous Solid Dispersions. *Cryst. Growth Des.* **2017**, *17*, 3142–3150.
- (38) Avrami, M. Kinetics of Phase Change. II - Transformation-Time Relations for Random Distribution of Nuclei. *J. Chem. Phys.* **1940**, *8* (1940), 212–224.
- (39) Avrami, M. Kinetics of phase change. I general theory. *J. Chem. Phys.* **1939**, *7*, 1103–1112.
- (40) Zelkó, R.; Süvegh, K. Correlation between the release characteristics of theophylline and the free volume of polyvinylpyrrolidone. *Eur. J. Pharm. Sci.* **2005**, *24* (4), 351–354.
- (41) Rowe, B. W.; Pas, S. J.; Hill, A. J.; Suzuki, R.; Freeman, B. D.; Paul, D. R. A variable energy positron annihilation lifetime spectroscopy study of physical aging in thin glassy polymer films. *Polymer* **2009**, *50* (25), 6149–6156.
- (42) Kobayashi, Y.; Zheng, W.; Meyer, E. F.; McGervey, J. D.; Jamieson, A. M.; Simha, R. Free volume and physical aging of poly(vinyl acetate) studied by positron annihilation. *Macromolecules* **1989**, *22* (5), 2302–2306.
- (43) Kobayashi, Y.; Haraya, K.; Hattori, S.; Sasuga, T. Evaluation of polymer free volume by positron annihilation and gas diffusivity measurements. *Polymer* **1994**, *35* (5), 925–928.
- (44) Deng, Q.; Jean, Y. C. Free-Volume Distributions of an epoxy polymer probed by positron annihilation: pressure dependence. *Macromolecules* **1993**, *26*, 30–34.
- (45) Zelkó, R.; Süvegh, K. Comparison of the enthalpy recovery and free volume of polyvinylpyrrolidone during anomalous glassy to rubbery transition. *Eur. J. Pharm. Sci.* **2004**, *21* (4), 519–523.
- (46) Liu, J.; Jean, Y. C.; Yang, H. *Macromolecules* **1995**, *28*, 5774–5779.
- (47) Śniegocka, M.; Jasińska, B.; Wawrzyszczuk, J.; Zaleski, R.; Deryło-Marczewska, A.; Skrzypek, I. Testing the extended tao - Eldrup model. Silica gels produced with polymer template. *Acta Phys. Pol., A* **2005**, *107* (5), 868–873.
- (48) Szabó, P.; Sebe, I.; Stiedl, B.; Kállai-szabó, B.; Zelkó, R. Journal of Pharmaceutical and Biomedical Analysis Tracking of crystalline-amorphous transition of carvedilol in rotary spun microfibers and their formulation to orodispersible tablets in vitro dissolution enhancement. *J. Pharm. Biomed. Anal.* **2015**, *115*, 359–367.

(49) Szabó, B.; Kallái, N.; Tóth, G.; Hetényi, G.; Zelkó, R. Journal of Pharmaceutical and Biomedical Analysis Drug release profiles and microstructural characterization of cast and freeze dried vitamin B 12 buccal films by positron annihilation lifetime spectroscopy. *J. Pharm. Biomed. Anal.* **2014**, *89*, 83–87.

(50) Carraher, C. E., Jr. *Carraher's Polymer Chemistry*, 10th ed.; CRC Press, 2017.

(51) Frechet, J. M. J. Functional Polymers and Dendrimers: Reactivity, Molecular Architecture, and Interfacial Energy. *Science* **1994**, *263*, 1710–1715.

(52) Vacha, M.; Habuchi, S. Conformation and physics of polymer chains: a single-molecule perspective. *NPG Asia Mater.* **2010**, *2*, 134–142.

(53) Zhou, Z.; Davis, P. J. Molecular dynamics study of polymer conformation as a function of concentration and solvent quality. *J. Chem. Phys.* **2009**, *130*, 224904.

(54) Kapnistos, M.; Lang, M.; Vlassopoulos, D.; Pyckhout-Hintzen, W.; Richter, D.; Cho, D.; Chang, T.; Rubinstein, M. Unexpected power-law stress relaxation of entangled ring polymers. *Nat. Mater.* **2008**, *7* (12), 997–1002.

A3. J. Pacułt (Szczurek), M. Rams-Baron, K. Chmiel, K. Jurkiewicz, A. Antosik, J. Szafraniec, M. Kurek, R. Jachowicz, M. Paluch, *How can we improve the physical stability of co-amorphous system containing flutamide and bicalutamide? The case of ternary amorphous solid dispersions*, Eur. J. Pharm. Sci. 136, (2019), 104947.

Impact Factor czasopisma z roku opublikowania pracy: 3.532

Liczba punktów ministerialnych MNiSW czasopisma z roku opublikowania pracy: 100

DOI: 10.1016/j.ejps.2019.06.001

Mój wkład w wyżej wymienionym artykule polegał na wykonaniu części pomiarów dielektrycznych i kalorymetrycznych, analizie wszystkich otrzymanych wyników (za wyjątkiem pomiarów rentgenowskich) oraz przygotowaniu manuskryptu. Wkład pozostałych współautorów, w formie oświadczeń, zamieszczono na końcu artykułu.

dr Marzena Rams-Baron

Katowice, 16 września 2020 r.

Zakład Biofizyki i Fizyki Molekularnej

Wydział Nauk Ścisłych i Technicznych

Uniwersytet Śląski

ul. Bankowa 12, 40-007 Katowice

OŚWIADCZENIE

Oświadczam, że w pracy:

J. Pacułt (Szczurek), M. Rams-Baron, K. Chmiel, K. Jurkiewicz, A. Antosik, J. Szafraniec, M. Kurek, R. Jachowicz, M. Paluch, *How can we improve the physical stability of co-amorphous system containing flutamide and bicalutamide? The case of ternary amorphous solid dispersions*, Eur. J. Pharm. Sci. 136, (2019), 104947.

Mój udział polegał na nadzorowaniu przeprowadzonych analiz, dyskusji otrzymanych wyników oraz korekcji manuskryptu.

Marzena Rams-Baron

Podpis

mgr Krzysztof Chmiel

Katowice, 30.09.2020

Zakład Biofizyki i Fizyki Molekularnej

Wydział Nauk Ścisłych i Technicznych

Uniwersytet Śląski

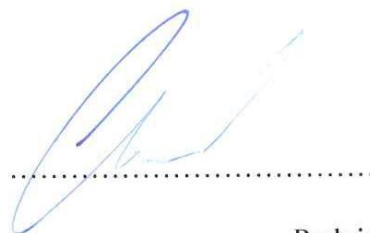
ul. Bankowa 12, 40-007 Katowice

OŚWIADCZENIE

Oświadczam, że w pracy:

J. Pacułt (Szczurek), M. Rams-Baron, K. Chmiel, K. Jurkiewicz, A. Antosik, J. Szafraniec, M. Kurek, R. Jachowicz, M. Paluch, *How can we improve the physical stability of co-amorphous system containing flutamide and bicalutamide? The case of ternary amorphous solid dispersions*, Eur. J. Pharm. Sci. 136, (2019), 104947.

Mój udział polegał na wykonaniu części badań DSC oraz BDS.



Podpis

dr inż. Karolina Jurkiewicz

Katowice, 16.09.2020

Zakład Biofizyki i Fizyki Molekularnej

Wydział Nauk Ścisłych i Technicznych

Uniwersytet Śląski

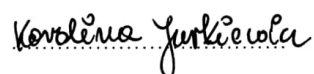
ul. Bankowa 12, 40-007 Katowice

OŚWIADCZENIE

Oświadczam, że w pracy:

J. Pacułt (Szczurek), M. Rams-Baron, K. Chmiel, K. Jurkiewicz, A. Antosik, J. Szafraniec, M. Kurek, R. Jachowicz, M. Paluch, *How can we improve the physical stability of co-amorphous system containing flutamide and bicalutamide? The case of ternary amorphous solid dispersions*, Eur. J. Pharm. Sci. 136, (2019), 104947.

Mój udział polegał na wykonaniu badań XRD oraz analizie i opisie otrzymanych wyników.



Podpis

dr Agata Antosik-Rogóż

Kraków, 16.09.2020.

Katedra Technologii Postaci Leku i Biofarmacji

Wydział Farmaceutyczny

Uniwersytet Jagielloński

ul. Medyczna 9, 30-688 Kraków

OŚWIADCZENIE

Oświadczam, że w pracy:

J. Pacułt (Szczurek), M. Rams-Baron, K. Chmiel, K. Jurkiewicz, A. Antosik, J. Szafraniec, M. Kurek, R. Jachowicz, M. Paluch, *How can we improve the physical stability of co-amorphous system containing flutamide and bicalutamide? The case of ternary amorphous solid dispersions*, Eur. J. Pharm. Sci. 136, (2019), 104947.

Mój udział polegał na wykonaniu badań rozpuszczalności.



Podpis

dr Joanna Szafraniec-Szczęsny

Kraków, 16.09.2020

Katedra Technologii Postaci Leku i Biofarmacji

Wydział Farmaceutyczny

Uniwersytet Jagielloński

ul. Medyczna 9, 30-688 Kraków

OŚWIADCZENIE

Oświadczam, że w pracy:

J. Pacuł (Szczurek), M. Rams-Baron, K. Chmiel, K. Jurkiewicz, A. Antosik, J. Szafraniec, M. Kurek, R. Jachowicz, M. Paluch, *How can we improve the physical stability of co-amorphous system containing flutamide and bicalutamide? The case of ternary amorphous solid dispersions*, Eur. J. Pharm. Sci. 136, (2019), 104947.

Mój udział polegał na wykonaniu badań szybkości rozpuszczania substancji leczniczej.

Joanna Szafraniec-Szczęsny

Podpis

mgr Mateusz Kurek

Kraków, 16.09.2020

Katedra Technologii Postaci Leku i Biofarmacji

Wydział Farmaceutyczny

Uniwersytet Jagielloński

Collegium Medicum

ul. Medyczna 9, 30-688 Kraków

OŚWIADCZENIE

Oświadczam, że w pracy:

J. Pacułt (Szczurek), M. Rams-Baron, K. Chmiel, K. Jurkiewicz, A. Antosik, J. Szafraniec, M. Kurek, R. Jachowicz, M. Paluch, *How can we improve the physical stability of co-amorphous system containing flutamide and bicalutamide? The case of ternary amorphous solid dispersions*, Eur. J. Pharm. Sci. 136, (2019), 104947.

Mój udział polegał na wykonaniu badań HPLC.

mgr farmacji

.....Mateusz Kurek.....

Podpis

Prof. dr hab. Renata Jachowicz

Kraków 16.09.2020

Katedra Technologii Postaci Leku i Biofarmacji

Wydział Farmaceutyczny

Uniwersytet Jagielloński

ul. Medyczna 9, 30-688 Kraków

OŚWIADCZENIE

Oświadczam, że w pracy:

J. Pacułt (Szczurek), M. Rams-Baron, K. Chmiel, K. Jurkiewicz, A. Antosik, J. Szafraniec, M. Kurek, R. Jachowicz, M. Paluch, *How can we improve the physical stability of co-amorphous system containing flutamide and bicalutamide? The case of ternary amorphous solid dispersions*, Eur. J. Pharm. Sci. 136, (2019), 104947.

Mój udział polegał na udziale w dyskusji otrzymanych wyników.

Kierownik
Katedry i Zakładu Technologii
Postaci Leku i Biofarmacji CM U.
Renata Jachowicz
Prof. dr hab. Renata Jachowicz

Prof. zw. dr hab. Marian Paluch

Chorzów,

Instytut Fizyki

Uniwersytet Śląski

ul. 75 Pułku Piechoty 1A, 41-500 Chorzów

OŚWIADCZENIE

Oświadczam, że w pracy:

J. Pacułt (Szczurek), M. Rams-Baron, K. Chmiel, K. Jurkiewicz, A. Antosik, J. Szafranec, M. Kurek, R. Jachowicz, M. Paluch, *How can we improve the physical stability of co-amorphous system containing flutamide and bicalutamide? The case of ternary amorphous solid dispersions*, Eur. J. Pharm. Sci. 136, (2019), 104947.

Mój udział polegał na udziale w dyskusji otrzymanych wyników oraz korekcji manuskryptu.

.....

Podpis



How can we improve the physical stability of co-amorphous system containing flutamide and bicalutamide? The case of ternary amorphous solid dispersions

Justyna Pacult^{a,b}, Marzena Rams-Baron^{a,b,?}, Krzysztof Chmiel^{a,b}, Karolina Jurkiewicz^{a,b}, Agata Antosik^c, Joanna Szafranec^c, Mateusz Kurek^c, Renata Jachowicz^c, Marian Paluch^{a,b}

^a Institute of Physics, University of Silesia, 75 Pulku Piechoty 1A, 41-500 Chorzow, Poland

^b Silesian Center for Education and Interdisciplinary Research, 75 Pulku Piechoty 1A, 41-500 Chorzow, Poland

^c Jagiellonian University Medical College, Faculty of Pharmacy, Department of Pharmaceutical Technology and Biopharmaceutics, Medyczna 9, 30-688 Kraków, Poland

ARTICLE INFO

Keywords:

Co-amorphous
Flutamide
Bicalutamide
Molecular dynamics
Physical stability
Glass transition

ABSTRACT

The article describes the preparation and characterization of binary mixtures of two antiandrogens used in prostate cancer treatment, i.e. flutamide (FL) and bicalutamide (BIC), as well as their ternary mixtures with either poly(methyl methacrylate-co-ethyl acrylate) (MMA/EA) or polyvinylpyrrolidone (PVP). The samples were converted into amorphous form to improve their water solubility and dissolution rate. Broadband dielectric spectroscopy and differential scanning calorimetry revealed that FL-BIC (65%) (w/w) does not tend to crystallize from the supercooled liquid state. We made the assumption that the drug-to-drug weight ratio should be maintained as in the case of monotherapy so we decided to investigate the system containing FL and BIC in 15:1 (w/w) ratio with 30% additive of polymers as stabilizers. Our research has shown that only in the case of the FL-BIC-PVP mixture the crystallization has been completely inhibited, both in glassy and supercooled liquid state, which was confirmed by X-ray diffraction studies. In addition, we performed solubility and dissolution rate tests, which showed a significant improvement in solubility of ternary system as compared to its crystalline counterpart. Enhanced physical stability and water solubility of the amorphous ternary system makes it promising for further studies.

1. Introduction

Treatment of patients with cancer is a very complicated process that has many unknowns, which means that new solutions in applied therapies are still being sought after. In the case of treatment of prostate cancer usually monotherapies are employed with administration of antiandrogens such as flutamide (FL) and bicalutamide (BIC) (Smith et al., 2004; Iversen et al., n.d.; Bañez et al., 2009). Those drugs are also used in combined androgen blockade therapy along with luteinizing hormones (Schellhammer et al., 1997) as well as in the so-called vintage hormonal manipulation therapy (Nagai et al., 2018), in which patients first receive bicalutamide and then, deferred flutamide. Recently, Liu et al. (2017), showed the possibility of application of bicalutamide with niclosamide in combination therapy for the treatment of advanced prostate cancer which is resistant to enzalutamide.

Due to the very low water-solubility and high membrane permeability both of the aforementioned drugs belong to class II of the

Biopharmaceutical Classification System (BCS) (Samy, 2012; Vega et al., 2007). Given the fact that ca. 46% of the drugs registered in the BCS exhibit dissolution rate-limited bioavailability, the issue of solubility enhancement is a matter of many recent research projects. One of the most frequently used strategies is amorphization of Active Pharmaceutical Ingredients (API). Over the last few years, numerous articles have been published which showed that amorphous drugs have better solubility, dissolution rate and therefore it is also possible to improve their bioavailability in comparison to their crystalline counterparts (Baghel et al., 2016; Grzybowska et al., 2010; Bhattacharya and Suryanarayanan, 2009; Bhugra and Pikal, 2008; Yoshioka and Aso, 2007). However, the amorphous state is thermodynamically unstable and characterized by a strong tendency to recrystallization. Therefore, an important aspect is the stabilization of drugs in the amorphous form to preserve the advantages of such a system (Rams-Baron et al., 2018; Knapik-Kowalczyk et al., 2017; Lim et al., 2016).

One of the methods of stabilizing amorphous drugs is to impede the

[?] Corresponding author.

E-mail address: marzena.rams-baron@us.edu.pl (M. Rams-Baron).

<https://doi.org/10.1016/j.ejps.2019.06.001>

Received 5 January 2019; Received in revised form 24 April 2019; Accepted 2 June 2019

Available online 04 June 2019

0928-0987/ © 2019 Elsevier B.V. All rights reserved.

molecular dynamics by creating binary mixtures with polymers (Pacult et al., 2018; Mohapatra et al., 2017; Mistry et al., 2015; Bhardwaj et al., 2014), sugars (Backensfeld et al., 1990; Grzybowska et al., 2012), silicones (Knapik et al., 2016; Watanabe et al., 2001; Bahl and Bogner, 2006), etc. Moreover, in recent years, the drug-drug systems elicited great interest in the field of drug stabilization. For the first time, a system composed of two drugs in an amorphous form was proposed by Yamamura et al. (2000), who mixed indomethacin with cimetidine. He observed that the addition of 20–80% of cimetidine to the binary mixture efficiently stabilized the sample and inhibited crystallization of indomethacin. Those mixtures were called co-amorphous systems and are characterized by improved stability of the drugs in glassy state as well as enhanced solubility and dissolution rate (Lim et al., 2016; Löbmann et al., 2011; Löbmann et al., 2012). Furthermore, the use of such a binary system is beneficial for the synergic effect in therapy and reducing tablet weight compared to amorphous drug-polymer co-administered systems (Knapik et al., 2015; Ueda et al., 2017). In the last years, several papers have been published on co-amorphous systems, in which, among others, naproxen was mixed with indomethacin (Löbmann et al., 2013), atorvastatin with glipizide (Renuka et al., 2017) or tranilast with diphenhydramine hydrochloride (Ueda et al., 2017).

In this paper, we focus on improving the stability of amorphous forms of flutamide and bicalutamide by formation of co-amorphous systems. Both of these drugs are characterized by very poor solubility in water. For this reason, we transformed them into an amorphous form to overcome these limitations. For this purpose, we used the vitrification method. The samples were heated to the melting point and then quickly chilled which allowed to convert the crystalline form of drugs to an amorphous form. The structure and physicochemical properties of the prepared samples were investigated using X-ray diffraction (XRD) and differential scanning calorimetry (DSC) techniques. In addition, we examined their molecular dynamics, which is considered one of the key factors controlling the stability of drugs in amorphous form (Yoshioka and Aso, 2007; Shamblin and Tang, 1999; Hancock et al., 1995). For this purpose we used the broadband dielectric spectroscopy (BDS) technique. In the second part of the manuscript, we discuss ternary drug-drug-polymer mixtures intended to stabilize the drugs mixed in a 15:1 (w/w) ratio (corresponding to FL and BIC daily doses, i.e. 750?mg and 50?mg, respectively (Andrews et al., 2010; Murphy et al., 2004)) and to increase their solubility and dissolution rate. To analyze the ternary systems we also used XRD, DSC and BDS techniques and performed solubility and dissolution tests according to pharmacopoeial recommendations.

2. Materials and methods

2.1. Materials

The crystalline form of bicalutamide (BIC, N-[4-Cyano-3-(trifluoromethyl)phenyl]-3-[(4-fluorophenyl)sulfonyl]-2-hydroxy-2-methylpropanamide) ($M_w = 430.37$ g/mol, $T_m = 467$ K, $pK_a = 12$, water solubility ~ 5 mg/L (Kumbhar and Pokharkar, 2013)) of 99.8% purity was purchased from Hangzhou Hyper Chemicals Limited (Hangzhou, Zhejiang, China). Flutamide (FL, 2-Methyl-N-[4-nitro-3-(trifluoromethyl)phenyl]propanamide) ($M_w = 276.2$ g/mol, $T_m = 384$ K, $pK_a = 13.1$, water solubility 50 mg/L (Brittain, 2001)) was obtained from Cayman Chemical company (Ann Arbor, Michigan, USA). Polyvinylpyrrolidone (PVP) K30 grade: $K = 29-32$, $M_w = 40,000$ g/mol was supplied from Sigma-Aldrich (Saint Louis, Missouri, USA). Poly(methyl methacrylate-co-ethyl acrylate) (MMA/EA) was purchased from Sigma Aldrich, $M_w \sim 101,000$ g/mol, $M_n \sim 39,500$ g/mol, ethyl acrylate < 5 wt% (Saint Louis, Missouri, USA). Potassium dihydrogen phosphate (KH_2PO_4 , pure p.a., POCH Gliwice, Poland), sodium hydroxide microgranular (NaOH, pure, POCH Gliwice, Poland) and TweenTM80 (Croda INC NJ, USA) were used to prepare the dissolution medium. Acetonitrile (HPLC isocratic grade, J.T. Baker[®],

New Jersey, USA) and water (HPLC gradient grade, J.T. Baker[®], NJ, USA) were used as mobile phase for high-performance liquid chromatography (HPLC) measurements. Distilled water was used to prepare all of the aqueous solutions.

2.2. Methods

2.2.1. Preparation of binary and ternary systems

The investigated FL-BIC systems were prepared in various drug-to-drug ratios, where the addition of BIC was 10%, 30%, 50% and 65% (w/w). To obtain homogeneous mixtures the appropriate amount of crystalline BIC and FL were mixed in a mortar for several minutes. Then, the physical mixtures were spread on a capacitor plate and melted on a hot plate at $T = 403$ K. After melting, the sample was vitrified by fast transfer to a previously chilled copper plate. Ternary mixtures were prepared by mixing 70% of the co-amorphous mixture (FL-BIC 15:1 (w/w)) with 30% of polymer excipient (MMA/EA or PVP). As before, they were melted on a hot plate at $T = 403$ K and converted to an amorphous form by vitrification.

2.2.2. Differential scanning calorimetry (DSC)

Calorimetric measurements for FL-BIC and FL-BIC-polymer blends were carried out using a Mettler-Toledo DSC 1 STARe System (Columbus, Ohio, USA) equipped with an HSS8 ceramic sensor with 120 thermocouples and liquid nitrogen cooling station. For temperature and enthalpy calibration, zinc and indium standards were applied. Measurements were performed using aluminum crucibles (40 μ L) with pin – ME - 27.331. In the first run, we heated the crystalline form up to about 20 K above melting point with a heating rate of 10 K/min; then samples were quickly cooled (cooling rate 20 K/min) and reheated. Ternary mixtures were heated to $T = 413$ K with a heating rate 10 K/min, cooled down (cooling rate 30 K/min) and reheated. Melting points were determined as the onset of the peak while the glass transition temperature was determined from the midpoint of the heat capacity increment.

2.2.3. Physical stability studies

The physical stability studies were performed using X-ray diffraction technique. Measurements were carried out with a Rigaku-Denki D/MAX RAPID II-R diffractometer (Wilmington, Massachusetts, USA) equipped with a rotating Ag anode, an incident beam graphite (002) monochromator, and an image plate in the Debye-Scherrer geometry as a detector. The wavelength of the incident beam was 0.5608 Å. The pixel size was 100 μ m \times 100 μ m. The studied samples were closed inside glass capillaries (1.5 mm in diameter) and stored at 295 K. Measurements were performed for sample-filled and empty capillaries, to allow subtraction of the background intensity. The beam width at the sample was 0.3 mm. The obtained two dimensional diffraction patterns were converted into one dimensional intensity functions versus the scattering angle.

2.2.4. Broadband dielectric spectroscopy measurements (BDS)

Dielectric measurements of prepared blends at ambient pressure were carried out using a Novocontrol GMBH Alpha spectrometer (Montabaur, Germany), in the frequency range from 10^{-1} Hz to 10^6 Hz and at temperature range from 173 K to 473 K. The temperature was controlled by a Quatro temperature controller providing an accuracy of temperature stabilization up to 0.1 K. The analyzed samples were placed between stainless capacitor plates (diameter equals 15 mm or 10 mm with a 0.1 mm gap obtained by glass fibre spacers). All spectra were fitted with Havriliak and Negami (1967) (HN) equation using the following formula:

$$\epsilon^*(\omega) = \epsilon_8 + \frac{\epsilon_e}{(1 + (i\omega T_{HN})^\alpha)^\beta} i^\beta \epsilon_0 \quad (1)$$

where ϵ_8 is the high frequency limit permittivity, ϵ_e is the dielectric

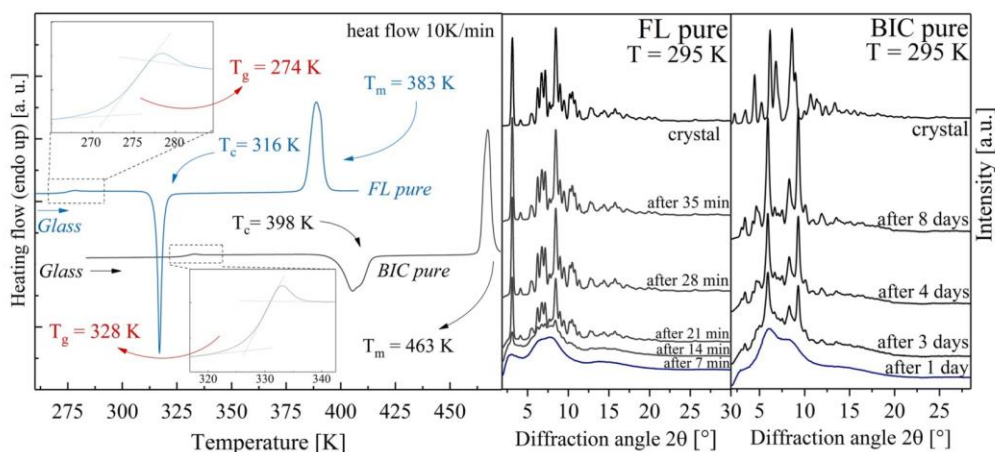


Fig. 1. The left panel shows DSC thermograms for pure FL (blue solid line) and BIC (black solid line). The right panels represent X-ray diffraction patterns for FL and BIC at $T = 295\text{ K}$. The appearance of sharp Bragg peaks indicate the crystallization process. (For interpretation of the references to colour in this figure legend, the reader is referred to the web version of this article.)

strength, t_{HN} is the HN relaxation time and the exponents α and β denote the shape of a relaxation peak. Based on the determined fitting parameters we calculated the structural relaxation times according to the equation:

$$t = t_{HN} \left[\sin\left(\frac{\alpha p}{2\beta + 2}\right) \right]^{-\frac{1}{\alpha}} \left[\sin\left(\frac{\alpha \beta p}{2\beta + 2}\right) \right]^{\frac{1}{\alpha}} \quad (2)$$

The temperature dependence of relaxation times in the supercooled liquid state for binary mixtures was described by the Vogel-Fulcher-Tammann-Hesse (VFTH) formula (Fulcher, 1925; Tammann and Hesse, 1926; Vogel, 1921):

$$t_a = t_g \exp\left(\frac{DT_0}{T - T_0}\right) \quad (3)$$

where t_g , T_0 , D are fitting parameters. The parameter t_g is a pre-exponential factor describing the limiting high-temperature value of t_a related to vibrational frequency ($\sim 10^{-11}$ to 10^{-14} s) (Rodrigues et al., 2014), the parameter D determines the deviation from the Arrhenius behavior and T_0 is the Vogel temperature connected to the state with infinite relaxation time (Metatla and Soldara, 2007).

2.2.5. Saturation solubility determination

The equilibrium apparent solubility of FL and BIC was determined using the shake-flask method. An excess amount of powder was added to 10 mL of distilled water. The Erlenmeyer flasks were shaken for 24 h at room temperature using a KS 130 Basic orbital shaker (IKA, Germany). In order to determine the amount of active substances in the samples by HPLC, the samples were filtered and transferred into HPLC vials. All measurements were performed in triplicate. Crystalline BIC and FL as well as FL-BIC-PVP (30%) were dissolved as received. Glasses obtained by melting at 130°C (or 200°C in case of pure BIC) were crushed prior to performing the tests.

2.2.6. Dissolution studies

The dissolution of active substances, i.e. BIC and FL from solid dispersions, physical mixtures as well as amorphous active substances, were performed in the pharmacopoeial paddle dissolution apparatus. Glasses were gently grounded in the mortar prior to the dissolution tests carried out in a small volume kit using a Vision G2 Elite 8 dissolution test station (Hanson Research, CA, USA) connected to AutoPlus auto-sampler. An appropriate amount of powder (equivalent to 25 mg of FL and 1.6 mg of BIC) was introduced into the dissolution beakers filled with 100 mL of phosphate buffer of pH = 6.8 containing 0.2% of

Tween™ 80. The paddle speed was set to 75 rpm and the temperature to $37^\circ\text{C} \pm 0.5^\circ\text{C}$. The samples were withdrawn from dissolution medium at predetermined time intervals, filtered and transferred into the HPLC vials. The amount of dissolved active substances was determined using HPLC.

2.2.7. HPLC method

An automated HPLC system (Agilent 1260 Infinity, Agilent Technologies, California, United States) with UV-diode-array detector was used. The stationary phase was a core-shell RP-18 column (Kinetex® 2.6 μm C18 100 Å, LC Column 100 \times 4.6 mm, Phenomenex, CA, USA) and the oven temperature was 25°C . The mobile phase containing acetonitrile and water (50:50 v/v) was delivered isocratically at 1.0 mL/min. The injection volume was 5 μL and the peaks were evaluated at 272 nm and 306 nm for BIC and FL, respectively. The retention times were 3.033 min and 4.326 min for bicalutamide and flutamide, respectively. The linearity was confirmed between 10% and 140% of the tested doses of BIC and FL ($R_2 > 0.99995$).

3. Results and discussion

3.1. Crystallization tendencies of flutamide and bicalutamide and their binary mixtures

In order to determine the crystallization tendency of pure drugs both from the glassy and supercooled liquid state, we performed calorimetric and X-ray measurements.

In the first step, we characterized pure drugs using the DSC technique. The samples were melted in situ and then quickly cooled to obtain a glassy state (melting point for crystalline forms of FL and BIC are $T_m = 384\text{ K}$ (Chmiel et al., 2017), $T_m = 467\text{ K}$ (Szczyrek et al., 2017), respectively). Fig. 1 shows thermograms obtained during heating of the amorphous form of APIs. The heating rate applied in experiments was equal 10 K/min. Both materials are characterized by the glass transition at $T_g = 274\text{ K}$ and $T_g = 328\text{ K}$ for FL and BIC, respectively. As can be seen, both investigated samples have strong tendency to crystallize from the supercooled liquid state. The crystallization process is manifested by an exothermic event from $T = 310\text{ K}$ to $T = 325\text{ K}$ for FL and from $T = 390\text{ K}$ to $T = 417\text{ K}$ for BIC. Further heating leads to melting of the samples, which can be observed by the occurrence of an endothermic peak at $T = 383\text{ K}$ and $T = 463\text{ K}$ for FL and BIC, respectively.

To analyze the stability of amorphous FL at room temperature, XRD studies were performed at $T = 295\text{ K}$. The obtained results show

whether the drug has a tendency to crystallize during a storage period. It is an important aspect to examine, because on that basis we can conclude about the shelf life of prepared sample. The obtained XRD patterns of glassy FL and BIC, presented in Fig. 1, show their common structural feature that is the appearance of a “pre-peak” at diffraction angle 2θ of around 2.9° (scattering vector Q of 0.57\AA^{-1}) before main diffraction peak at around 6.2° ($Q = 1.22\text{\AA}^{-1}$) with a shoulder at around 8.0° (1.56\AA^{-1}), which can be mainly attributed to the short-range order between neighbouring molecules. The broad, diffuse nature of these peaks is characteristic of the disordered, amorphous phase. However, the clear evidence of the pre-peak in the glassy FL and BIC is highly suggestive of the formation of an intermediate range ordering (Elliott, 1991). The distance $d = \frac{2\pi}{Q} \approx 11.0\text{\AA}$ calculated from the pre-peak position corresponds the spatial period of the intermolecular organization. Similar structural feature in diffraction patterns were observed for other glass formers exhibiting a tendency to form hydrogen bonds (Morineau and Alba-Simionesco, 1998; Descamps et al., 2007; Hédoux et al., 2013). Therefore, the observed pre-peak may be a signature of formation of small clusters of hydrogen-bonded FL and BIC molecules.

The presence of hydrogen bonding groups may favor the recrystallization of FL and BIC from glassy state. The time-dependent XRD measurements clearly showed that FL near glass transition crystallize around 14 min after preparation (right panel of Fig. 1). It is manifested by the appearance of sharp Bragg peaks. The polymorphic form of FL in the recrystallized sample is the same as for reference crystalline sample before melting (orthorhombic symmetry, space group $Pn2_1$, cell: a 11.856(2) Å, b 20.477(3) Å, c 4.9590(9) Å, α 90° , β 90° , γ 90° , as reported in The Cambridge Crystallography Data Centre no. 1292938). In turn, the BIC glass at 295 K was found to be more stable in comparison to FL. The beginning of BIC crystallization was observed 3 days after the sample preparation. However, it should be noted that after 8 days the sample was fully converted to a mixture of two polymorphic forms: form I - as for the crystalline reference (monoclinic symmetry, space group $P2_1/c$, cell: a 14.882(5) Å, b 12.213(3) Å, c 10.461(3) Å, α 90° , β $104.680(13)^\circ$, γ 90° , as reported in The Cambridge Crystallography Data Centre no. 289635), and form II (triclinic symmetry, space group $P-1$, cell: a 7.8220(16) Å, b 11.060(2) Å, c 11.324(2) Å, α $88.19(3)^\circ$, β $77.03(3)^\circ$, γ $77.96(3)^\circ$, as reported in The Cambridge Crystallography Data Centre no. 602633). The obtained results confirmed a strong tendency to recrystallization of both FL and BIC drugs at room temperature. Because of the quick conversion to their crystalline counterparts, it is not possible to apply pure FL and BIC in amorphous form in the pharmaceutical industry. For this reason, we were looking for approaches to stabilize analyzed drugs in the glassy and supercooled liquid state. The solution to this problem may be the preparation of binary systems consisting of both drugs.

For this purpose, we have prepared the FL-BIC mixtures with various drug-drug ratios. Fig. 2 shows thermograms for the mixtures vitrified in DSC and measured with heating rate of 10 K/min. As can be seen, a FL-BIC sample with a 10% addition of BIC has a higher T_g value than pure FL. However, above T_g one can observe an exothermic peak indicating sample recrystallization which mean that the addition of 10% of BIC is not sufficient to prevent crystallization of FL from supercooled liquid state. For this reason, we also analyzed mixtures with a higher BIC concentration, i.e. FL-BIC (30%) and FL-BIC (50%). The obtained thermograms are also shown in Fig. 2. In these case, the crystallization process is not observed within the investigated range of temperatures. In addition, we also performed DSC measurements for the FL-BIC mixture (65%), which showed no tendency to crystallize (see green line in Fig. 2). However, we will come back for a detailed discussion of this sample later in the manuscript.

3.2. Molecular dynamics of FL-BIC mixtures

To study the molecular dynamics of the examined systems, we

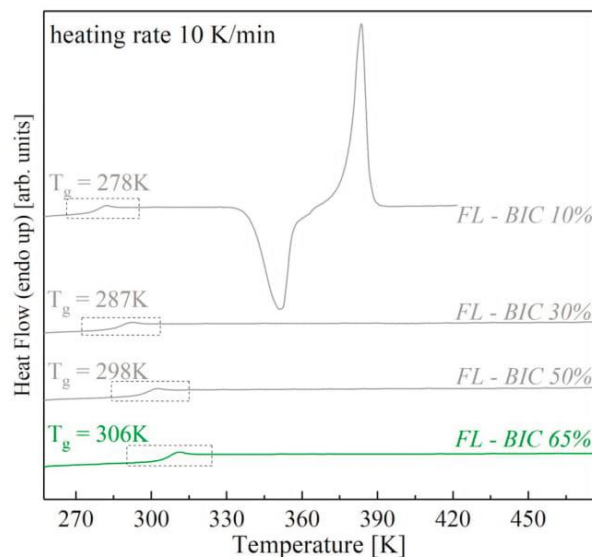


Fig. 2. DSC thermograms of amorphous FL-BIC blends mixed at various ratios.

performed BDS measurements. The representative dielectric loss spectra for the FL-BIC mixture (30%) are shown in the right panel of Fig. 3. The data for the pure APIs were acquired elsewhere (Chmiel et al., 2017; Szczurek et al., 2017). In the spectrum, one can observe the loss-peak attributed to the α -relaxation process. It originates from a cooperative intramolecular reorientation of molecules. As the temperature increases, the maximum of the α -process shifts towards higher frequencies, resulting from the intensified molecular dynamics of the system. At $T = 331\text{K}$, a drastic change in the intensity of the α -relaxation peak is visible. Since the dielectric strength (ϵ'') is correlated to the number of dipoles participating in the reorientation (N) and the average electric dipole moment of the analyzed sample (μ) (according to equation $\epsilon'' = \epsilon_s - \epsilon_\infty - N\mu^2$), such a decrease in peak height indicates the beginning of crystallization. However, in the DSC measurement we do not observe a crystallization process. The difference between the DSC and BDS results from the fact that during the dielectric tests the heating rate is much slower (Knapik et al., 2014). The same behavior was observed for the FL-BIC (50%) mixture. In the case of the DSC study, we did not notice any tendency to crystallize when heating above T_g , while during the BDS measurements we observed a decreasing intensity of α -peak indicating the crystallization process. To thoroughly analyze the effect of sample composition on molecular dynamics, we have plotted the temperature dependence of the α -relaxation times for the studied binary systems, which are shown in the left panel of the Fig. 3. To obtain the presented data, the dielectric spectra were fitted using the Havriliak-Negami equation (Eq. (1)) and α -relaxation times were calculated according to Eq. (2). To describe the non-Arrhenius behavior of the α -process in supercooled liquid state we used a VFTH function. In Fig. 3 we show a relaxation map for all prepared drug-drug mixtures as well as for pure components. For each measured sample, the T_g is determined as the temperature where $\tau_a = 100\text{s}$. It can be seen that with increasing addition of BIC, the molecular mobility of the system is slowed down. In consequence, the value of T_g increases with higher concentration of BIC in the binary mixture. In the case of FL-BIC (10%), the T_g value was determined as $T_g = 275\text{K}$, which is slightly higher than T_g obtained for pure FL. The prepared mixture has a tendency to crystallize. The relaxation times determined for partially recrystallized samples have been marked in Fig. 3 as closed stars. For the next two drug-drug samples FL-BIC (30%) and FL-BIC (50%), the T_g values were determined as $T_g = 286\text{K}$ and $T_g = 298\text{K}$, respectively. The tested sample with the most inhibited molecular dynamics and thus characterized by the highest value of $T_g = 304\text{K}$ was FL-BIC (65%).

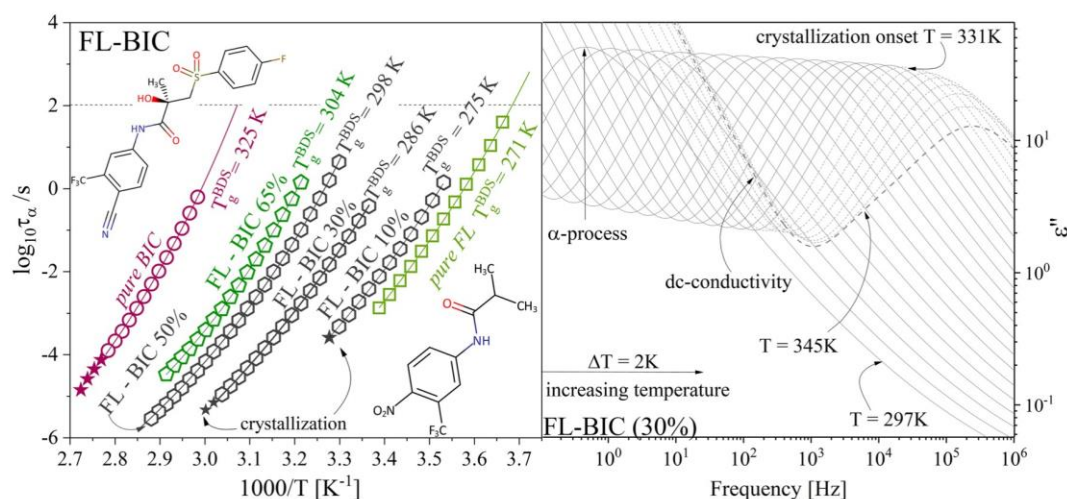


Fig. 3. The left panel displays the relaxation map of pure FL and BIC and mixtures of FL and (10%), (30%), (50%) and (65%) addition of BIC, where relaxation times determined for partially recrystallized samples are marked as closed stars. The solid lines indicate VFTH fits. The right panel shows dielectric loss spectra for FL-BIC (30%).

Unfortunately, our dielectric results revealed that almost all prepared mixtures show a tendency to recrystallize from supercooled liquid state (crystallization of FL-BIC (50%) was observed in isothermal experiment – data not included in manuscript). The only exception was FL-BIC (65%), which did not crystallize both during DSC and BDS studies. This concentration, appearing at this moment as optimal to stabilize the investigated drug-drug system, was found using a strategy recently proposed by Chmiel et al. (2017).

The authors studied mixtures with 1:1 and 5:1:M concentrations of FL and PVP/VA. Within the course of the BDS study, they noticed that during crystallization the structural relaxation peak does not disappear completely as in most cases, but some residual peak with lower amplitude is still visible in the experimental window. It was found that this process originates from the relaxation of a residual amount of API in supercooled liquid state remaining in the sample after the recrystallization process. To determine the exact concentration of this new mixture, its T_g value as determined from dielectric spectra was compared to the Gordon-Taylor (GT) prediction. To confirm their observation Chmiel et al. (Chmiel et al., 2017) performed measurements for various drug-polymer concentrations. In each of the investigated cases, the mixture after crystallization corresponds to the same concentration reported as a stable one which was confirmed during long-term room-temperature XRD studies. We decided to take advantage of this method and carried out a series of BDS and DSC tests to find a potentially stable concentration of the FL-BIC mixture. For this purpose, we have performed a BDS experiment for FL-BIC (30%) in the temperature range from $T = 309K$ to $T = 365K$. As can be seen in the right panel of Fig. 4 above $T = 331K$, the beginning of crystallization is visible as a decrease of the intensity of the α -process. Usually, this process completely declines during the progression of crystallization process. However, in this case, after complete conversion to the crystalline phase, a peak of smaller intensity than the α -process (spectrum marked with green dots) is still visible. To study the observed residual relaxation, we applied the method proposed by Chmiel et al. and cooled the sample to $T = 309K$ before reheating it to $T = 365K$ (data marked as green spectra). The obtained spectra were fitted using the Havriliak-Negami equation (Eq. (1)). Next, the acquired fitting parameters were used to calculate the structural relaxation times and plot the relaxation map. From the temperature dependence of the relaxation times for the new mixture, the temperature $T = 304K$ corresponding to the glass transition was obtained and compared to the GT predictions. To determine the theoretical T_g values for BIC-FL samples we

used the following equation (Gordon and Taylor, 1952; Couchman and Karasz, 1978):

$$T_g = \frac{w_1 T_{g1} + K w_2 T_{g2}}{w_1 + K w_2} \quad (4)$$

where w_1 and w_2 are the weight of components, T_{g1} and T_{g2} are the glass transition temperatures of pure APIs determined from DSC measurements, and K is defined as:

$$K = \frac{\Delta C_p}{\Delta C_{p1}} \quad (5)$$

where ΔC_p is the change in heat capacity at T_g and is equal $\Delta C_p^{BIC} = 0.48 J/gK$ and $\Delta C_p^{FL} = 0.43 J/gK$ for the BIC and FL, respectively. The calculated values of T_g as well as experimental data acquired from the DSC measurements are shown in the left panel in Fig. 4. To identify the concentration of the FL-BIC mixture obtained after crystallization, the value of T_g determined from dielectric data was compared with the predicted ones. The obtained T_g was marked as green star in Fig. 4 and corresponds to 65% addition of BIC in FL-BIC. The obtained results are in good agreement with the data acquired using DSC and BDS techniques, which did not show crystallization of the tested sample.

Improvement of stability in binary systems is often considered in the context of interactions between molecules or an antiplasticizing effect as in the case of mixtures with polymers. To analyze the interaction between the two components it can be used the Gordon-Taylor prediction given by Eq. (4). The theoretical value of T_g is calculated from data obtained from DSC experiment and then compared to experimental ones. In literature, the lack of interactions between components is described as behavior according to the prediction of GT (Lu and Weiss, 1992; Teja et al., 2015). In the case of our research, we can observe a negative deviation of experimental from theoretical values, which may result in moderate interactions. There are many examples of binary systems where authors also attribute this phenomenon to the presence of specific interactions between the components, as in the case of tranilast and diphenhydramine hydrochloride mixtures as well as talinolol and naringin (Ueda et al., 2017; Teja et al., 2015). Considering the architecture of the investigated drug molecules, we can see that BIC and FL have hydrogen atom donating groups such as OH and NH and proton acceptors such as amino, nitro, sulfonyl and carbonyl groups. In our previous article (Szczurek et al., 2017), we reported that BIC tends to form hydrogen bonds with PVP. We tested BIC and PVP mixtures with different concentrations using the FT-IR method and confirmed

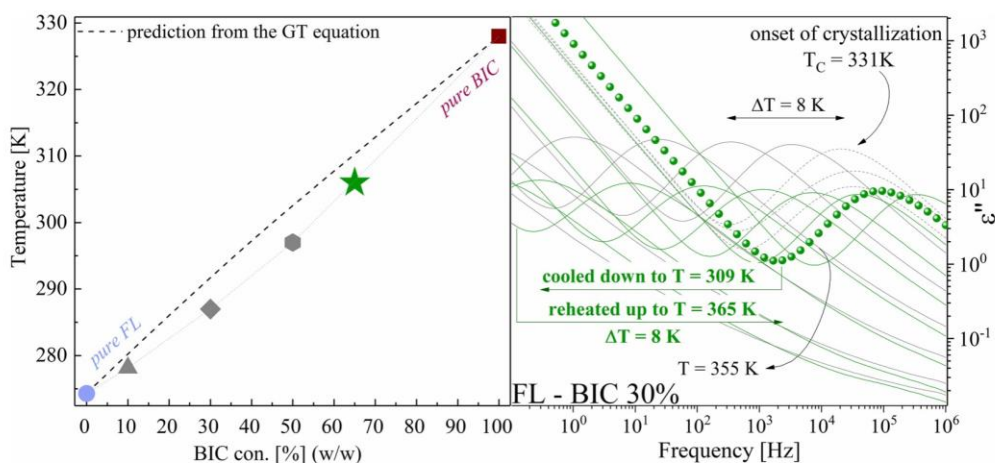


Fig. 4. The left panel represents the comparison of experimental T_g values (closed symbols) and those predicted from GT equation (dashed line) for FL-BIC mixtures. Blue solid line is guide for the eyes. Right panel shows dielectric spectra obtained for FL-BIC (30%) (grey lines). The decrease in signal amplitude visible at higher temperatures denotes crystallization. The dielectric spectra registered after crystallization for partially crystalline sample are marked on green. The remaining amorphous fraction was identified as so-called stable concentration using approach proposed by Chmiel et al. (For interpretation of the references to colour in this figure legend, the reader is referred to the web version of this article.)

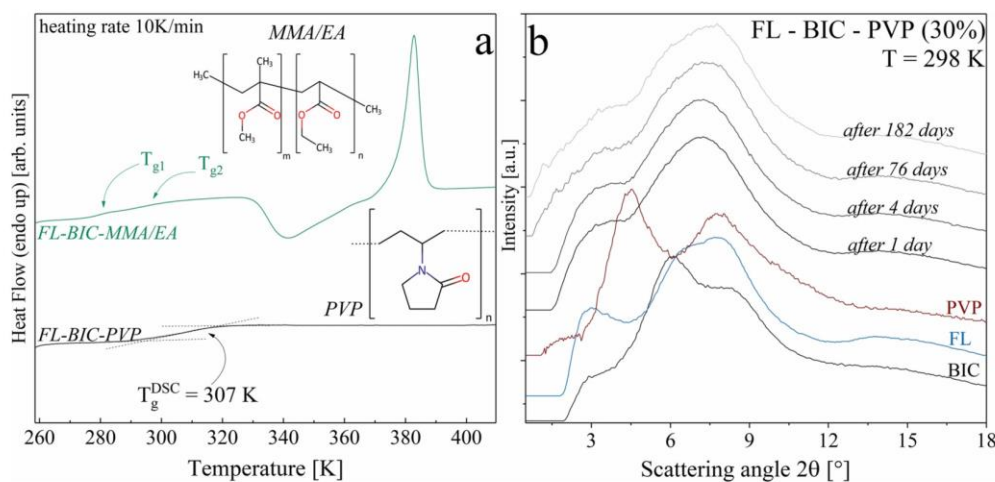


Fig. 5. Panel a shows DSC thermograms obtained for FL-BIC-MMA/EA (green solid line) and FL-BIC-PVP (black solid line). Panel b represents X-ray diffraction patterns for amorphous BIC, FL, PVP and FL-BIC-PVP measured at $T = 298$ K as a function of storage time. (For interpretation of the references to colour in this figure legend, the reader is referred to the web version of this article.)

the presence of specific interactions.

3.3. Characterization, solubility and stability studies of ternary mixtures with polymers

In the case of co-amorphous systems, the most commonly chosen concentration, which ensures stability and improvement of solubility, is the molar ratio 1:1. This is due to the fact that the strongest interactions are observed in that concentration, inhibiting the tendency to crystallize (Löbmann et al., 2011; Löbmann et al., 2012; Löbmann et al., 2013). In 2016, Lim et al. (2016) investigated indomethacin-cimetidine and naproxen-cimetidine mixtures in a concentration 1:1. To prepare these systems the authors used various methods such as quench cooling, co-evaporation and ball milling. For the prepared blends stability tests were performed at 40°C and no crystallization was observed. In our case, the preparation of the mixture FL-BIC with a molar ratio of 1:1 corresponds to the concentration FL-BIC (61%) (w/w). The stability of such a system has not been studied in this manuscript, however, according to the approach by Chmiel et al. we can speculate that such

mixture FL-BIC (61%) might have the tendency to recrystallize. Regardless of the result, neither the sample FL-BIC (61%) nor FL-BIC (65%) investigated herein correspond to the therapeutic dose of FL and BIC. To obtain a therapeutic concentration of FL and BIC, we have to prepare a drug-drug mixture with the ratio of FL-BIC 15:1 (w/w) (which is equal to FL-BIC (6%)), corresponding to the daily dose of both drugs (750 mg for FL and 50 mg for BIC). Our previous results allow us to assume that the mixture with the mentioned concentration will not be characterized by sufficient stability. For this reason, it was necessary to use a third component such as a polymer. Nowadays, polymers are frequently selected excipients to stabilize amorphous drugs. The mechanism of stabilization of the drug-polymer mixture is widely discussed in the literature. Many factors have been described to have an impact on inhibiting the crystallization of such a system. One of them is the downturn of molecular dynamics through the so-called anti-plasticizing effect (Riggleman et al., 2007; Riggleman et al., 2006) or presence of specific interactions between drug and polymer molecules (Rams-Baron et al., 2015). In addition, the mixture may be thermodynamically stable if the drug remains below the solubility limit in the

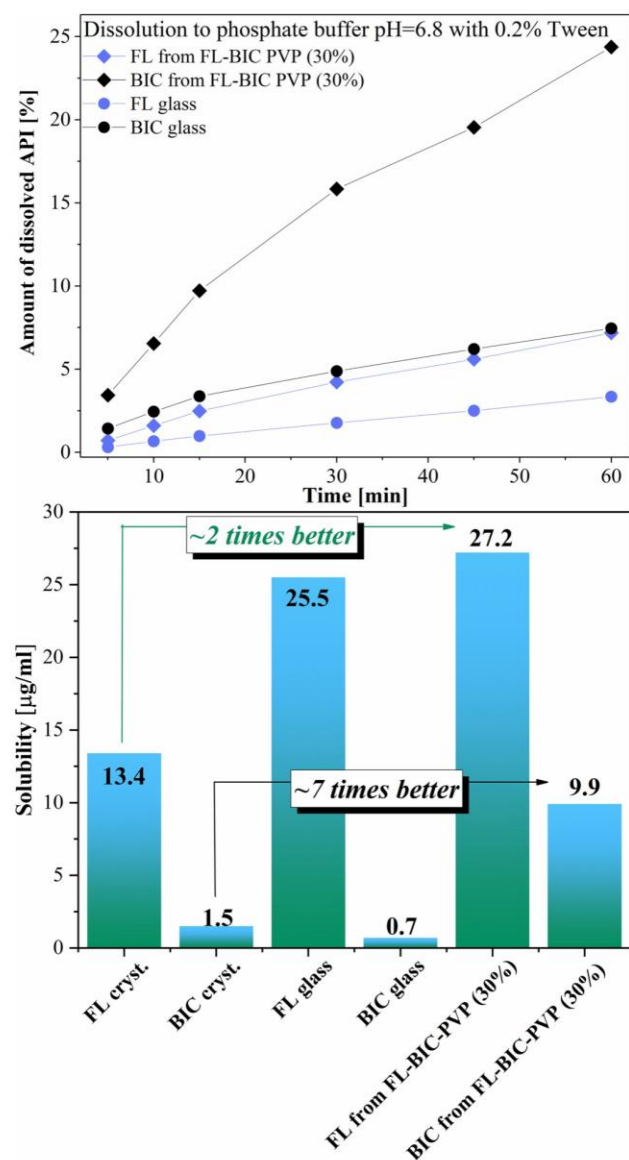


Fig. 6. Dissolution profiles (upper panel) and apparent water solubility (bottom panel) determined for FL and BIC and FL-BIC-PVP (30%) mixture.

polymer matrix. For this reason, an important aspect is to find out the solubility of the drug and the miscibility of the drug in the polymer carrier (Tian et al., 2013; Lehmkomper et al., 2017). In recent years, it has also been shown that the key elements affecting the stability of the mixture may be the polymer structure, i.e. the backbone chain structure or chain length. Mosquera-Giraldo et al. (Mosquera-Giraldo et al., 2016) found that a polymer with a carboxylate group in combination with an optimal hydrocarbon chain length can hinder nucleation. In turn, Frank and Matzger (2018) also confirmed that the stabilization of drug-polymer systems should be considered in the context of the interaction between the drug and the polymer. Our previous studies (Pacult et al., 2018) have also shown that the length of the polymer chain is a very important aspect that needs to be taken into account. Depending on the molecular weight of the polymer and thus the chain length, we can distinguish a different arrangement of the polymer in space, which determines the crystallization behavior of the system. For this reason, the selection of the appropriate polymer to stabilize the

drug in amorphous form should be careful and meticulous.

To prepare ternary samples, we chose two polymers which molecular structures are shown in the left panel of Fig. 5. First is MMA/EA, a derivative of Eudragits, which is widely used in pharmaceutical formulation, while the second polymer is PVP. It is an excipient commonly used due to its positive effect on the solubility and dissolution rate of the systems in which it is applied. The glass transition temperatures of the applied polymers are $T_g = 383\text{K}$ and $T_g = 438\text{K}$ for MMA/EA and PVP, respectively. The mixtures were prepared at a ratio corresponding to daily doses of the APIs used in monotherapy, i.e. 15:1 (w/w) FL-BIC, where 70% of the mixture was constituted by the drug-drug system, and the remaining 30% by a polymeric additive. For each ternary mixture we performed DSC measurements to observe phase transitions. In the first run we heated the crystalline samples up to $T = 420\text{K}$ to completely melt the mixture. Next, we cooled the samples and reheated them to determine the glass transition temperatures. Panel a of Fig. 5 shows the obtained thermograms for the vitrified samples. In the case of mixture with MMA/EA, two glass transitions can be observed, indicating inhomogeneity of the sample (Andrews et al., 2010; Gupta et al., 2004). In addition, in supercooled liquid state we observe an exothermic event from $T = 328\text{K}$ to $T = 368\text{K}$ which indicates the tendency of the sample to crystallize. On the thermogram obtained for the FL-BIC-PVP mixture, a singular glass transition is observed at $T_g = 306\text{K}$ indicating sample homogeneity. Observed differences in polymer miscibility may result from polymer geometry. The polymers used significantly differ in architecture, and hence the present substituents and electron factors. It may affect the arrangement of polymers in space, the presence of steric hindrance or the possibility of creating specific interactions. It was previously reported that PVP forms homogeneous mixtures with drugs such as BIC (Szczyrek et al., 2017) or indomethacin (Mohapatra et al., 2017). In addition, the PVP K30 which was used to prepare ternary sample was proposed as a polymer with an optimal polymer chain length to stabilize the drug (Pacult et al., 2018). In the case of polymer MMA/EA, we suggest that the inhomogeneity of the mixture may be due to the spatial orientation of the polymer that may result in the formation of heterogeneous domains in the sample. As was mentioned previously in the case of amorphous samples it is necessary to recognize their tendency to crystallization both from glassy and supercooled liquid state. The eventual drug crystallization at higher temperatures is a significant factor that must be taken into account during the formulation of the dosage forms using technique such as for example hot-melt extrusion. Our DSC results indicate the stability of the FL-BIC-PVP system during heating above T_g . In the case of the amorphous phase, it is important that the drug remains unchanged throughout the storage period, which is referred to shelf life and is equal to about 2–3 years. Thus we performed XRD studies to check the long-term stability of the ternary mixture. As can be seen, in Fig. 5b, the obtained X-ray diffraction patterns of FL-BIC-PVP system do not exhibit Bragg peaks and long-range order even after 182 days of storage. It means that the sample has no tendency to crystallize and remains amorphous during our experiment. The observed diffractogram for the FL-BIC-PVP seems not to be a linear combination of the diffraction patterns of individual components. The presence of a pronounced pre-peak at around 3° in the diffraction pattern of the FL-BIC-PVP may be a signature of formation of aggregates of hydrogen-bonded molecules in this triple system. Our FL-BIC-PVP mixture does not show any tendency to crystallize both in the glassy state and in the supercooled liquid state, what might indicate the possibility of applying this ternary system for further investigations.

In the formulation of the orally administered dosage forms, high solubility and dissolution rate of the API is of crucial importance as these factors affect the bioavailability of the drug (Ting et al., 2018). This is a key aspect, because improving bioavailability may result in a reduction of the therapeutic dose and in consequence, a decline in the invasiveness of the therapy for the patient. For this reason, we examined the solubility and dissolution of the crystalline and amorphous

forms of FL and BIC as well as for the FL-BIC-PVP mixture. As can be seen in Fig. 6, the ternary system has an improved solubility of the FL and BIC. The studied water solubility increased about 2 times for FL and about 7 times for BIC in comparison to the crystalline counterparts. We also investigated the effect of using a ternary mixture on dissolution of a drug substance. The experiment was carried out in a phosphate buffer of pH = 7.8 with the addition of 0.2% Tween™80 (Samy, 2012). The results are presented in the upper panel of Fig. 6. The FL-BIC-PVP sample has a significantly improved dissolution relative to the amorphous forms of the drugs tested separately. After 60 min, the amount of dissolved drugs was about 2 and 3 times greater for FL and BIC, respectively, than in the case of drugs dissolved alone.

4. Conclusions

In this article, we studied a co-amorphous mixture of FL and BIC in various concentrations using DSC, BDS and XRD techniques. We examined the molecular dynamics of binary mixtures by performing BDS measurements. Both drugs are characterized by different T_g values, therefore their concentration in the FL-BIC mixture affects the parameters defining the molecular dynamics. With the increasing addition of BIC in the FL-BIC mixture, the molecular dynamics of the system slowed down and in consequence the observed value of T_g increased. However, the inhibition of the mobility was not sufficient and for most of the tested samples, crystallization while heating above T_g was observed during BDS and DSC tests. Only for a concentration of FL-BIC (65%) the crystallization was completely inhibited, which was confirmed by dielectric and calorimetric measurements. The addition of polymeric excipient, i.e. 30% of PVP, inhibited the recrystallization of the FL-BIC system from the supercooled liquid state as confirmed by DSC measurements. In addition, the X-ray diffraction results indicated that the ternary mixture is stable at room temperature for at least 182 days. The ternary system exhibited improvement in water-solubility and dissolution which might indicate its advantageous features in terms of bioavailability improvement.

Acknowledgements

The authors acknowledge Polish National Science Centre for the financial support (grant Symfonia 3 no 2015/16/W/NZ7/00404).

References

- Andrews, G.P., AbuDiak, O.A., Jones, D.S., 2010. Physicochemical characterization of hot melt extruded bicalutamide-polyvinylpyrrolidone solid dispersions. *J. Pharm. Sci.* 99 (3), 1322–1335.
- Backensfeld, T.; Müller, B. W.; Wiese, M.; Seydel, J. K. Effect of Cyclodextrin Derivatives on Indomethacin Stability in Aqueous Solution. *Pharmaceutical Research: An Official Journal of the American Association of Pharmaceutical Scientists*. 1990, pp 484–490.
- Baghel, S., Cathcart, H., O'Reilly, N.J., 2016. Polymeric Amorphous Solid Dispersions: A Review of Amorphization, Crystallization, Stabilization, Solid-State Characterization, and Aqueous Solubilization of Biopharmaceutical Classification System Class II Drugs. *J. Pharm. Sci.* 105 (9), 2527–2544.
- Bahl, D., Bogner, R.H., 2006. Amorphization of indomethacin by co-grinding with Neusilin US2: Amorphization kinetics, physical stability and mechanism. *Pharm. Res.* 23 (10), 2317–2325.
- Bañez, L.L., Blake, G.W., McLeod, D.G., Crawford, E.D., Moul, J.W., 2009. Combined low-dose flutamide plus finasteride vs low-dose flutamide monotherapy for recurrent prostate cancer: A comparative analysis of two phase II trials with a long-term follow-up. *BJU Int.* 104 (3), 310–314.
- Bhardwaj, S.P., Arora, K.K., Kwong, E., Templeton, A., Clas, S.D., Suryanarayanan, R., 2014. Mechanism of amorphous itraconazole stabilization in polymer solid dispersions: Role of molecular mobility. *Mol. Pharm.* 11 (11), 4228–4237.
- Bhattacharya, S., Suryanarayanan, R., 2009. Local mobility in amorphous pharmaceuticals—characterization and implications on stability. *J. Pharm. Sci.* 98 (9), 2935–2953.
- Bhugra, C., Pikal, M.J., 2008. Role of thermodynamic, molecular, and kinetic factors in crystallization from the amorphous state. *J. Pharm. Sci.* 97 (4), 1329–1349.
- Brittain, H. G. *Analytical Profiles of Drug Substances and Excipients*, Vol. 27; Academic Press, 2001.
- Chmiel, K., Knapik-Kowalczyk, J., Jurkiewicz, K., Sawicki, W., Jachowicz, R., Paluch, M., 2017. A new method to identify physically stable concentration of amorphous solid dispersions (i): case of flutamide + kollidon VA64. *Mol. Pharm.* 14 (10), 3370–3380.
- Couchman, P.R., Karasz, F.E., 1978. A classical thermodynamic discussion of the effect of composition on glass-transition temperatures. *Macromolecules* 11 (1), 117–119.
- Descamps, M., Legrand, V., Guinet, Y., Amazzal, A., Alba, C., Dore, J., 2007. "Pre-Peak" in the structure factor of simple molecular glass formers. *Prog. Theor. Phys. Suppl.* 126 (January), 207–212.
- Elliott, S.R., 1991. Medium-range structural order in covalent amorphous solids. *Nature* 354, 445–452.
- Frank, D., Matzger, S., A., J., 2018. Probing the interplay between amorphous solid dispersion stability and polymer functionality. *Mol. Pharm.* 15, 2714–2720.
- Fulcher, G.S., 1925. Analysis of recent measurements of the viscosity of glasses. *J. Am. Ceram. Soc.* 8, 789–794.
- Gordon, M., Taylor, J.S., 1952. Ideal copolymers and the second-order transitions of synthetic rubbers. i. non-crystalline copolymers. *J. Appl. Chem.* (9), 493–500.
- Grzybowska, K., Paluch, M., Grzybowski, A., Wojnarowska, Z., Wojnarowska, L., Kolodziejczyk, K., Ngai, K.L., 2010. Molecular dynamics and physical stability of amorphous anti-inflammatory drug: celecoxib. *J. Phys. Chem.* 114 (40), 12792–12801.
- Grzybowska, K., Paluch, M., Włodarczyk, P., Grzybowski, A., Kaminski, K., Hawelek, L., Zakowiecki, D., Kasprzycka, A., Jankowska-Sumara, I., 2012. Enhancement of amorphous celecoxib stability by mixing it with octaacetylmaltose: the molecular dynamics study. *Mol. Pharm.* 9 (4), 894–904.
- Gupta, P., Kakumanu, V.K., Bansal, A.K., 2004. Stability and solubility of celecoxib-PVP amorphous dispersions: a molecular perspective. *Pharm. Res.* 21 (10), 1762–1769.
- Hancock, B. C.; Shamblin, S. L.; Zografi, G. 1995. Molecular mobility of amorphous pharmaceutical solids below their glass transition temperatures. *Pharmaceutical Research: An Official Journal of the American Association of Pharmaceutical Scientists*, 799–806.
- Havriliak, S., Negami, S., 1967. A complex plane representation of dielectric and mechanical relaxation processes in some polymers. *Polymer (Guildf.)* 8, 161–210.
- Hédoux, A., Guinet, Y., Paccou, L., Derollez, P., Dané, F., 2013. Vibrational and structural properties of amorphous n-butanol: a complementary Raman spectroscopy and X-ray diffraction study. *J. Chem. Phys.* 138 (21), 214506.
- Iversen, P., Kaisary, A.V., Andersen, J.B., Baert, L., Tammela, T., Chamberlain, M., Carroll, K., Gotting-Smith, K., Blackledge, G.R.P., T. C. J., 1998. Casodex (bicalutamide) 150 mg monotherapy compared with castration in patients with previously untreated prostate cancer. results from two multi - centre randomized trials at a median follow - up of 4 years 51 (3), 389–396.
- Knapik, J., Wojnarowska, Z., Grzybowska, K., Hawelek, L., Sawicki, W., Włodarski, K., Markowski, J., Paluch, M., 2014. Physical stability of the amorphous anticholesterol agent (ezetimibe): the role of molecular mobility. *Mol. Pharm.* 11 (11), 4280–4290.
- Knapik, J., Wojnarowska, Z., Grzybowska, K., Jurkiewicz, K., Tajber, L., Paluch, M., 2015. Molecular dynamics and physical stability of coamorphous ezetimibe and indapamide mixtures. *Mol. Pharm.* 12 (10), 3610–3619.
- Knapik, J., Wojnarowska, Z., Grzybowska, K., Jurkiewicz, K., Stankiewicz, A., Paluch, M., 2016. Stabilization of the amorphous ezetimibe drug by confining its dimension. *Mol. Pharm.* 13 (4), 1308–1316.
- Knapik-Kowalczyk, J., Wojnarowska, Z., Rams-Baron, M., Jurkiewicz, K., Cielecka-Piontek, J., Ngai, K.L., Paluch, M., 2017. Atorvastatin as a promising crystallization inhibitor of amorphous probucol: dielectric studies at ambient and elevated pressure. *Mol. Pharm.* 14 (8), 2670–2680.
- Kumbhar, D.D., Pokharkar, V.B., 2013. Engineering of a nanostructured lipid carrier for the poorly water-soluble drug, bicalutamide: physicochemical investigations. *Colloids Surfaces A Physicochem. Eng. Asp.* 416 (1), 32–42.
- Lehmkeper, K., Kyeremateng, S.O., Bartels, M., Degenhardt, M., Sadowski, G., 2018. Physical stability of API/polymer-blend amorphous solid dispersions. *Eur. J. Pharm. Biopharm.* (124), 147–157.
- Lim, A.W., Löbmann, K., Grohgan, H., Rades, T., Chieng, N., 2016. Investigation of physical properties and stability of indomethacin-cimetidine and naproxen-cimetidine co-amorphous systems prepared by quench cooling, coprecipitation and ball milling. *J. Pharm. Pharmacol.* 68 (1), 36–45.
- Liu, C., Armstrong, C.M., Lou, W., Lombard, A.P., Cucchiara, V., Gu, X., Yang, J.C., Nadiminty, N., Pan, C., Evans, C.P., 2017. Niclosamide and Bicalutamide Combination Treatment Overcomes Enzalutamide- and Bicalutamide-Resistant Prostate Cancer. *Mol. Cancer Ther.* 16 (8), 1521–1530.
- Löbmann, K., Laitinen, R., Grohgan, H., Gordon, K.C., Strachan, C., Rades, T., 2011. Coamorphous drug systems: Enhanced physical stability and dissolution rate of indomethacin and naproxen. *Mol. Pharm.* 8 (5), 1919–1928.
- Löbmann, K., Strachan, C., Grohgan, H., Rades, T., Korhonen, O., Laitinen, R., 2012. Coamorphous simvastatin and glipizide combinations show improved physical stability without evidence of intermolecular interactions. *Eur. J. Pharm. Biopharm.* 81 (1), 159–169.
- Löbmann, K., Laitinen, R., Grohgan, H., Strachan, C., Rades, T., Gordon, K.C., 2013. A theoretical and spectroscopic study of co-amorphous naproxen and indomethacin. *Int. J. Pharm.* 453 (1), 80–87.
- Lu, X., Weiss, A.R., 1992. Relationship between the Glass Transition Temperature and the Interaction Parameter of Miscible Binary Polymer Blends. *Macromolecules* 25, 3242–3246.
- Metatla, N., Soldara, A., 2007. The Vogel-Fulcher-Tamman equation investigated by atomistic simulation with regard to the Adam-Gibbs model. *Macromolecules* 40 (26), 9680–9685.
- Mistry, P., Mohapatra, S., Gopinath, T., Vogt, F.G., Suryanarayanan, R., 2015. Role of the strength of drug-polymer interactions on the molecular mobility and crystallization inhibition in ketoconazole solid dispersions. *Mol. Pharm.* 12 (9), 3339–3350.
- Mohapatra, S., Samanta, S., Kothari, K., Mistry, P., Suryanarayanan, R., 2017. Effect of polymer molecular weight on the crystallization behavior of indomethacin

- amorphous solid dispersions. *Cryst. Growth Des.* 17 (6), 3142–3150.
- Morineau, D., Alba-Simionesco, C., 1998. Hydrogen-bond-induced clustering in the fragile glass-forming liquid *m*-toluidine: Experiments and simulations. *J. Chem. Phys.* 109 (19), 8494–8503.
- Mosquera-Giraldo, L.I., Borca, C.H., Meng, X., Edgar, K.J., Slipchenko, L.V., Taylor, L.S., 2016. Mechanistic design of chemically diverse polymers with applications in oral drug delivery. *Biomacromolecules* 17 (11), 3659–3671.
- Murphy, J.C., Srinivas, S., Terris, M.K., 2004. Flutamide administration at 500 mg daily has similar effects on serum testosterone to 750 mg daily. *J. Androl.* 25 (4), 630–634.
- Nagai, T., Naiki, T., Iida, K., Etani, T., Ando, R., Hamamoto, S., Sugiyama, Y., Akita, H., Kubota, H., Hashimoto, Y., et al., 2018. Early abiraterone acetate treatment is beneficial in Japanese castration-resistant prostate cancer after failure of primary combined androgen blockade. *Prostate Int.* 6 (1), 18–23.
- Pacult, J., Rams-Baron, M., Chrzaszcz, B., Jachowicz, R., Paluch, M., 2018. Effect of polymer chain length on the physical stability of amorphous drug-polymer blends at ambient pressure. *Mol. Pharm.* 15, 2807–2815.
- Rams-Baron, M., Wojnarowska, Z., Grzybowska, K., Dulski, M., Knapik, J., Jurkiewicz, K., Smolka, W., Sawicki, W., Ratuszna, A., Paluch, M., 2015. Toward a better understanding of the physical stability of amorphous anti-inflammatory agents: the roles of molecular mobility and molecular interaction patterns. *Mol. Pharm.* 12 (10), 3628–3638.
- Rams-Baron, M., Pacult, J., Jedrzejowska, A., Knapik-Kowalczyk, J., Paluch, M., 2018. Changes in physical stability of supercooled etoricoxib after compression. *Mol. Pharm.* 15 (9), 3969–3978.
- Renuka, Singh, S.K., Gulati, M., Narang, R., 2017. Stable amorphous binary systems of glipizide and atorvastatin powders with enhanced dissolution profiles: formulation and characterization. *Pharm. Dev. Technol.* 22 (1), 13–25.
- Riggleman, R.A., Yoshimoto, K., Douglas, J.F., De Pablo, J.J., 2006. Influence of confinement on the fragility of antiplasticized and pure polymer films. *Phys. Rev. Lett.* 97 (4), 1–4.
- Riggleman, R.A., Douglas, J.F., De Pablo, J.J., 2007. Characterization of the potential energy landscape of an antiplasticized polymer. *Phys. Rev. E - Stat. Nonlinear, Soft Matter Phys.* 76 (1), 1–8.
- Rodrigues, A.C., Viciosa, M.T., Danede, F., Affouard, F., Correia, N.T., 2014. Molecular mobility of amorphous *S*-flurbiprofen: A dielectric relaxation spectroscopy approach. *Mol. Pharm.* 11 (1), 112–130.
- Samy, W.M., 2012. Class II drugs; a dissolution / bioavailability challenge: Flutamide-loaded spray dried lactose for dissolution control. *Int. J. Drug Dev. Res.* 4 (2), 195–204.
- Schellhammer, P.F., Sharifi, R., Block, N.L., Soloway, M.S., Venner, P.M., Patterson, A.L., Sarosdy, M.F., Vogelzang, N.J., Schellenger, J.J., Kolvenbag, G.J.C.M., 1997. Clinical benefits of bicalutamide compared with flutamide in combined androgen blockade for patients with advanced prostatic carcinoma: Final report of a double-blind, randomized, multicenter trial. *Urology* 50 (3), 330–336.
- Shamblin, S., Tang, X., 1999. Characterization of the time scales of molecular motion in pharmaceutically important glasses. *J. Phys. Chem. B* 103 (20), 4113–4121.
- Smith, M.R., Goode, M., Zietman, A.L., McGovern, F.J., Lee, H., Finkelstein, J.S., 2004. Bicalutamide monotherapy versus leuprolide monotherapy for prostate cancer: Effects on bone mineral density and body composition. *J. Clin. Oncol.* 22 (13), 2546–2553.
- Szczurek, J., Rams-Baron, M., Knapik-Kowalczyk, J., Antosik, A., Szafraniec, J., Jamróz, W., Dulski, M., Jachowicz, R., Paluch, M., 2017. Molecular dynamics, recrystallization behavior, and water solubility of the amorphous anticancer agent bicalutamide and its polyvinylpyrrolidone mixtures. *Mol. Pharm.* 14 (4), 1071–1081.
- Tammann, G., Hesse, W., 1926. Die Abhängigkeit der Viskosität von der Temperatur bei unterkühlten Flüssigkeiten. *Zeitschrift für Anorg. und Allg. Chemie* 156 (1), 245–257.
- Teja, A., Musmade, P.B., Khade, A.B., Dengale, S.J., 2015. Simultaneous improvement of solubility and permeability by fabricating binary glassy materials of Talinolol with Naringin: Solid state characterization, in-vivo in-situ evaluation. *Eur. J. Pharm. Sci.* 78, 234–244.
- Tian, Y., Booth, J., Meehan, E., Jones, D.S., Li, S., Andrews, G.P., 2013. Construction of drug-polymer thermodynamic phase diagrams using Flory-Huggins interaction theory: Identifying the relevance of temperature and drug weight fraction to phase separation within solid dispersions. *Mol. Pharm.* 10 (1), 236–248.
- Ting, J., Porter, W.W., Mecca, J.M., Bates, F.S., Reineke, T.M., 2018. Advances in polymer design for enhancing oral drug solubility and delivery. *Bioconjug. Chem.* 29 (4), 939–952.
- Ueda, H., Kadota, K., Imono, M., Ito, T., Kunita, A., Tozuka, Y., 2017. Co-amorphous formation induced by combination of tranilast and diphenhydramine hydrochloride. *J. Pharm. Sci.* 106 (1), 123–128.
- Vega, D.R., Polla, G., Martinez, A., Mendioroz, E., Reinoso, M., 2007. Conformational polymorphism in bicalutamide. *Int. J. Pharm.* 328 (2), 112–118.
- Vogel, H., 1921. Das temperaturabhängigkeitsgesetz der viskosität von flüssigkeiten. *J. Phys. Z.* 22, 645–646.
- Watanabe, T., Wakiyama, N., Usui, F., Ikeda, M., Isobe, T., Senna, M., 2001. Stability of amorphous indomethacin compounded with silica. *Int. J. Pharm.* 226 (1–2), 81–91.
- Yamamura, S., Gotoh, H., Sakamoto, Y., Momose, Y., 2000. Physicochemical properties of amorphous precipitates of cimetidine-indomethacin binary system. *Eur. J. Pharm. Biopharm.* 49 (3), 259–265.
- Yoshioka, S., Aso, Y., 2007. Correlations between molecular mobility and chemical stability during storage of amorphous pharmaceuticals. *J. Pharm. Sci.* 96 (5), 960–981.

4. Podsumowanie

Niniejszą rozprawę doktorską stanowi seria trzech publikacji opisujących badania dynamiki molekularnej oraz fizycznej stabilności stałych rozprożeń bikalutamidu w formie amorficznej w matrycach polimerowych. Główną motywacją była chęć polepszenia rozpuszczalności leku przeciwnowotworowego bikalutamidu ze względu na jego bardzo ograniczoną rozpuszczalność w wodzie oraz duże znaczenie na rynku farmaceutycznym. Do tego celu wybrano metodę konwersji farmaceutyku do formy amorficznej. Niestety otrzymana w ten sposób forma szklista leku wykazała silną tendencję do krystalizacji zarówno poniżej jak i powyżej temperatury zeszklenia. Z tego względu utworzono amorficzne stałe rozproszenia bikalutamidu w polimerze poliwinylpirolidonie aby poprawić stabilność fizyczną układu. Wykonane analizy wykazały, iż zastosowanie polimeru pozwoliło z powodzeniem zahamować proces krystalizacji mieszaniny. Ponadto dokonano przybliżonej estymacji czasu, w którym badana mieszanina pozostanie stabilna. Jest to istotny aspekt, ponieważ przyjmuje się, iż lek, który został dopuszczony do obrotu handlowego powinien pozostać w niezmienniej formie, w określonych warunkach temperatury i wilgotności, przez okres około 2-3 lat. Szacowany czas stabilności fizycznej analizowanego układu BIC-PVP (30%) wyniósł ponad sto lat, co stanowi dużo dłuższy okres niż wcześniej wspomniany okres trwałości, nawet biorąc pod uwagę duży margines błędu estymacji. Co więcej badania uwalniania oraz rozpuszczalności również potwierdziły, iż mieszanina BIC-PVP charakteryzuje się lepszą rozpuszczalnością w wodzie niż bikalutamid w formie krystalicznej.

Na podstawie otrzymanych wyników zaczęto rozważać wpływ długości łańcucha polimerowego na stabilność fizyczną układów lek-polimer. Z tego względu w pracy [A2] skupiono się na tym aspekcie. Otrzymane wyniki eksperymentów dielektrycznych przeprowadzonych w warunkach izotermicznych jasno wskazują, iż istnieje zależność pomiędzy długością łańcucha polimeru i zahamowaniem procesu krystalizacji badanych mieszanin. Jest to bardzo interesujący i istotny aspekt wymagający pochylenia się nad tym tematem, ponieważ polimery są często wybieranym dodatkiem mającym na celu stabilizację farmaceutyków w formie amorficznej. Dodatkowo stworzenie amorficznych stałych rozprożeń wpływa znacząco na poprawę rozpuszczalności w wodzie analizowanych API. Jednakowoż obecnie na rynku dostępne są bardzo różnorodne polimery różniące się np. długością łańcucha polimerowego. Dlatego badanie wpływu właściwości fizycznych polimeru na stabilizację układów lek-polimer jest tak istotne. W pracy [A2] wykazano, iż

istnieje optymalna długość łańcucha polimerowego, która pozwala najskuteczniej zahamować proces krystalizacji układu lek-polimer.

W ostatnim etapie badań poszukiwano alternatywnej drogi prowadzącej do ustabilizowania bikalutamidu. W tym celu sporządzono układ binarny zawierający BIC oraz flutamid, który również jest lekiem stosowanym w leczeniu nowotworu gruczołu krokowego. Zastosowanie takiej mieszaniny niesie za sobą możliwość uzyskania efektu synergicznego działań leczniczych obu leków, co jest niezaprzeczalnym atutem w stosunku do stosowania farmaceutyków pojedynczo. W artykule [A3] zbadano dynamikę molekularną oraz stabilność fizyczną mieszaniny FL-BIC w formie amorficznej. Zahamowany proces krystalizacji uzyskano dla stężenia FL-BIC (65%), który jednak nie znajdował odzwierciedlenia w dawkach terapeutycznych farmaceutyków. Z tego względu wykonano stałe rozproszenia układu FL-BIC, o stężeniu odpowiadającym dawce dziennej leków, w matrycach polimerowych. Do tego celu wykorzystano polimery często stosowane w przemyśle farmaceutycznym: MMA/EA oraz PVP. Otrzymane wyniki wykazały, iż próbka FL-BIC-PVP charakteryzuje się zwiększoną rozpuszczalnością w wodzie oraz przedłużoną stabilnością fizyczną..

5. Bibliografia

1. Fradet Y. Bicalutamide (Casodex®) in the treatment of prostate cancer. *Expert Rev Anticancer Ther.* 2004;4(1):37-48. doi:10.1586/14737140.4.1.37
2. James KD, Ekwuribe NN. Syntheses of enantiomerically pure (R)- and (S)- bicalutamide. *Tetrahedron.* 2002;58(29):5905-5908. doi:10.1016/S0040-4020(02)00560-4
3. Cockshott ID. Clinical Pharmacokinetics and Metabolism. 2004;43(13):855-878.
4. Craig DQM, Royall PG, Kett VL, Hopton ML. The relevance of the amorphous state to pharmaceutical dosage forms: Glassy drugs and freeze dried systems. *Int J Pharm.* 1999;179(2):179-207. doi:10.1016/S0378-5173(98)00338-X
5. Wojnarowska Z, Grzybowska K, Hawelek L, et al. Molecular dynamics, physical stability and solubility advantage from amorphous indapamide drug. *Mol Pharm.* 2013;10(10):3612-3627. doi:10.1021/mp400116q
6. Hancock BC, Parks M. <Solubility advantage of amorphous materials_Hancock & Parks.pdf>. 2000;17(4).
7. Williams HD, Trevaskis NL, Charman SA, et al. Strategies to address low drug solubility in discovery and development. *Pharmacological Reviews*, v. 65, n. 1, p. 315–499, 2013. Williams HD, Hywel D.; TREVASKIS, Natalie L.; CHARMAN, Susan A.; et al. Strategies to address low drug solubility in discovery and development. *Pharmacol Rev.* 2013;65(1):315-499. doi:10.1124/pr.112.005660
8. Knapik J, Wojnarowska Z, Grzybowska K, et al. Physical stability of the amorphous anticholesterol agent (ezetimibe): the role of molecular mobility. *Mol Pharm.* 2014;11(11):4280-4290. doi:10.1021/mp500498e
9. Zallen R. *Fizyka Ciał Amorficznych.*; 1994.
10. EMA. Note For Guidance On Evaluation Of Stability Data (CPMP/ICH/420/02). *EMA.* 2003;(August 2002):1-17. <http://www.ema.europa.eu/ema/>.
11. European Medicines Agency. *Definitions.* 2020;(August):1-20. doi:10.32388/yokp53
12. Grzybowska K, Paluch M, Włodarczyk P, et al. Enhancement of amorphous celecoxib

- stability by mixing it with octaacetylmaltose: The molecular dynamics study. *Mol Pharm.* 2012;9(4):894-904. doi:10.1021/mp200436q
13. Kaminska E, Adrjanowicz K, Tarnacka M, et al. Impact of inter- and intramolecular interactions on the physical stability of indomethacin dispersed in acetylated saccharides. *Mol Pharm.* 2014;11(8):2935-2947. doi:10.1021/mp500286b
 14. Backensfeld T, Müller BW, Wiese M, Seydel JK. Effect of Cyclodextrin Derivatives on Indomethacin Stability in Aqueous Solution. *Pharm Res An Off J Am Assoc Pharm Sci.* 1990;7(5):484-490. doi:10.1023/A:1015860531565
 15. Knapik J, Wojnarowska Z, Grzybowska K, Jurkiewicz K, Stankiewicz A, Paluch M. Stabilization of the Amorphous Ezetimibe Drug by Confining Its Dimension. *Mol Pharm.* 2016;13(4):1308-1316. doi:10.1021/acs.molpharmaceut.5b00903
 16. Watanabe T, Wakiyama N, Usui F, Ikeda M, Isobe T, Senna M. Stability of amorphous indomethacin compounded with silica. *Int J Pharm.* 2001;226(1-2):81-91. doi:10.1016/S0378-5173(01)00776-1
 17. Bahl D, Bogner RH. Amorphization of indomethacin by co-grinding with Neusilin US2: Amorphization kinetics, physical stability and mechanism. *Pharm Res.* 2006;23(10):2317-2325. doi:10.1007/s11095-006-9062-x
 18. Beyer A, Radi L, Grohganz H, Löbmann K, Rades T, Leopold CS. Preparation and recrystallization behavior of spray-dried co-amorphous naproxen-indomethacin. *Eur J Pharm Biopharm.* 2016;104:72-81. doi:10.1016/j.ejpb.2016.04.019
 19. Wairkar S, Gaud R. Co-Amorphous Combination of Nateglinide-Metformin Hydrochloride for Dissolution Enhancement. *AAPS PharmSciTech.* 2016;17(3):673-681. doi:10.1208/s12249-015-0371-4
 20. Löbmann K, Laitinen R, Grohganz H, Strachan C, Rades T, Gordon KC. A theoretical and spectroscopic study of co-amorphous naproxen and indomethacin. *Int J Pharm.* 2013;453(1):80-87. doi:10.1016/j.ijpharm.2012.05.016
 21. Löbmann K, Laitinen R, Grohganz H, Gordon KC, Strachan C, Rades T. Coamorphous drug systems: Enhanced physical stability and dissolution rate of indomethacin and naproxen. *Mol Pharm.* 2011;8(5):1919-1928. doi:10.1021/mp2002973
 22. Knapik J, Wojnarowska Z, Grzybowska K, Jurkiewicz K, Tajber L, Paluch M.

- Molecular Dynamics and Physical Stability of Coamorphous Ezetimib and Indapamide Mixtures. *Mol Pharm.* 2015;12(10):3610-3619.
doi:10.1021/acs.molpharmaceut.5b00334
23. Yamamura S, Gotoh H, Sakamoto Y, Momose Y. Physicochemical properties of amorphous salt of cimetidine and diflunisal system. *Int J Pharm.* 2002;241(2):213-221.
doi:10.1016/S0378-5173(02)00195-3
 24. Lehmkemper K, Kyeremateng SO, Heinzerling O, Degenhardt M, Sadowski G. Long-Term Physical Stability of PVP- and PVPVA-Amorphous Solid Dispersions. *Mol Pharm.* 2017;14(1):157-171. doi:10.1021/acs.molpharmaceut.6b00763
 25. Baghel S, Cathcart H, O'Reilly NJ. Polymeric Amorphous Solid Dispersions: A Review of Amorphization, Crystallization, Stabilization, Solid-State Characterization, and Aqueous Solubilization of Biopharmaceutical Classification System Class II Drugs. *J Pharm Sci.* 2016;105(9):2527-2544. doi:10.1016/j.xphs.2015.10.008
 26. Feng Q, Huang J, Hussain MA. Drug-Polymer Solubility and Miscibility: Stability Consideration and Practical Challenges in Amorphous Solid Dispersion Development. *Int J Drug Dev Res.* 2011;3(2):26-33. doi:10.1002/jps
 27. Konno H, Handa T, Alonzo DE, Taylor LS. Effect of polymer type on the dissolution profile of amorphous solid dispersions containing felodipine. *Eur J Pharm Biopharm.* 2008;70(2):493-499. doi:10.1016/j.ejpb.2008.05.023
 28. Paudel A, Worku ZA, Meeus J, Guns S, Van Den Mooter G. Manufacturing of solid dispersions of poorly water soluble drugs by spray drying: Formulation and process considerations. *Int J Pharm.* 2013;453(1):253-284. doi:10.1016/j.ijpharm.2012.07.015
 29. Grzybowska K, Chmiel K, Knapik-Kowalczyk J, Grzybowski A, Jurkiewicz K, Paluch M. Molecular factors governing the liquid and glassy states recrystallization of celecoxib in binary mixtures with excipients of different molecular weights. *Mol Pharm.* 2017;14(4):1154-1168. doi:10.1021/acs.molpharmaceut.6b01056
 30. Hodge IM. Strong and fragile liquids — a brief critique. *J Non Cryst Solids.* 1996;202(1-2):164-172. doi:10.1016/0022-3093(96)00151-2
 31. Tanaka H. Relationship among glass-forming ability, fragility, and short-range bond ordering of liquids. *J Non Cryst Solids.* 2005;351(8-9):678-690.

doi:10.1016/j.jnoncrysol.2005.01.070

32. Bhugra C, Pikal MJ. Role of Thermodynamic, Molecular, and Kinetic Factors in Crystallization From the Amorphous State. *J Pharm Sci.* 2008;97(4):1329-1349. doi:10.1002/jps
33. Yoshioka M, Hancock BC, Zografi G. Crystallization of Indomethacin from the Amorphous State below and above Its Glass Transition Temperature. *J Pharm Sci.* 1994;83(12):1700-1705.
34. Gupta MK, Vanwert A, Bogner RH. Formation of physically stable amorphous drugs by milling with neusilin. *J Pharm Sci.* 2003;92(3):536-551. doi:10.1002/jps.10308
35. Surana R, Pyne A, Suryanarayanan R. Effect of preparation method on physical properties of amorphous trehalose. *Pharm Res.* 2004;21(7):1167-1176.
36. Joyce R, Fenton MA, Rode P, et al. High dose bicalutamide for androgen independent prostate cancer: effect of prior hormonal therapy. *J Urol.* 1998;159(1):149-153.